

**Modulating Prolyl Hydroxylase (PHD₂) activity to
alter Glycolytic Pathway and Fatty acid Synthase
Expression in Tumor Cells**

THESIS

**SUBMITTED IN FULFILMENT FOR THE AWARD OF THE
DEGREE OF**

DOCTOR OF PHILOSOPHY

In

PHARMACEUTICAL SCIENCES

**BABASAHEB
BHIMRAO
AMBEDKAR
UNIVERSITY**



LUCKNOW

**प्रज्ञा शील करुणा
ESTABLISHED 1996**

SUBMITTED BY

Manjari Singh

Enrollment No. – 177/11

SUPERVISOR

Dr. Gaurav Kaithwas

Associate Professor

**DEPARTMENT OF PHARMACEUTICAL SCIENCES
SCHOOL OF BIOMEDICAL AND PHARMACEUTICAL SCIENCES
BABASAHEB BHIMRAO AMBEDKAR UNIVERSITY
(A CENTRAL UNIVERSITY)**

VIDYA VIHAR, RAIBARELI ROAD, LUCKNOW-226025 (U.P.), INDIA

2018

This attempt is dedicated to

My

Respected Parents & Friend



*Whose inimitable love and affection stand before me as a
constant source of inspiration in every walk of my life.*

DECLARATION

I hereby declare that the thesis entitled “**Modulating Prolyl Hydroxylase (PHD₂) activity to alter Glycolytic Pathway and Fatty acid Synthase Expression in Tumor Cells**” has been prepared by me under the supervision of **Dr. Gaurav Kaithwas** at Department of Pharmaceutical Sciences, School of Biomedical and Pharmaceutical Sciences, Babasaheb Bhimrao Ambedkar University, Lucknow (U.P.).

No part of this thesis has formed the basis for the award of my degree, diploma or fellowship previously. I further declare that the material embodied in the present work is based on original research work and indebtedness to others has been duly acknowledged at relevant places. I hereby also declare that the thesis is essentially free from all kind of plagiarism.

Manjari
Manjari Singh
Candidate

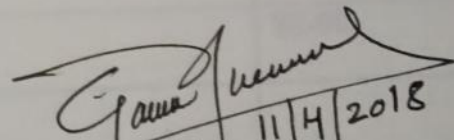
Gaurav Kaithwas
11/4/2018
Dr. Gaurav Kaithwas
Supervisor

CERTIFICATE

This is to certify that the thesis titled “**Modulating Prolyl Hydroxylase (PHD₂) activity to alter Glycolytic Pathway and Fatty acid Synthase Expression in Tumor Cells**” submitted by **Ms. Manjari Singh (Enrollment no. 177/11)** is an original work and has not been previously submitted in part or full for the award of any other degree or diploma to this or any other university.

The thesis submitted to Babasaheb Bhimrao Ambedkar University Lucknow satisfies all the requirements as stipulated in the Doctor of Philosophy (Ph.D.) regulations -1999 as amended in 2008/2010/2013 and it is fit for submission and evaluation for the award of the degree of Doctor of Philosophy of the University.

Date: 11/4/2018


Supervisor 11/4/2018

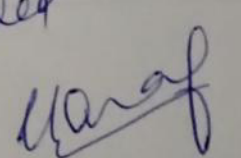
forwarded

Head of the Department

TABLE OF CONTENTS

S.No.	Title	Page No.
1.	Acknowledgment	i-ii
2.	List of Tables	iii
3.	List of Figures	iv
4.	List of symbols and abbreviations	v-vi

S.No.	Chapters	Page No.
1.	Introduction	1-27
2.	Screening of compounds	28-30
3.	Materials and Methods	31-44
4.	Results and Discussion	45-76
5.	Summary and Conclusion	77-79
6.	References	80-90
	Appendix I	
	Appendix-II	
	Appendix-III	

ACKNOWLEDGEMENT

*I consider myself most lucky to work under the guidance of **Dr. Gaurav Kaithwas**, Associate Professor, Babasaheb Bhimrao Ambedkar University, Lucknow (U.P) for his valuable support. His discipline, principles, simplicity, caring attitude and provision of fearless work environment will be cherished in all walks of my life. I am very much grateful for his invaluable guidance and everlasting encouragement throughout my course.*

*I express my hearty and humble thanks to **Prof. Shubhini A. Saraf**, Professor and Head of the Department, Babasaheb Bhimrao Ambedkar University, Lucknow (U.P) for making all facilities available, her timely help, encouragement, boosting my confidence in the progress of my dissertation work.*

*I wish to offer my sincere thanks to **Prof. R.C. Sobti**, Honourable Vice Chancellor of Babasaheb Bhimrao Ambedkar University, Lucknow for providing infrastructure facilities for carrying the project advices throughout my academic carrier.*

*Besides my advisor, I would like to thank the rest of DRC committee members: **Dr. V. Elangovan**, **Dr. N.K.S. More** and **Dr. Sudipta Saha** for their encouragement, insightful comments and meaningful quires.*

*My sincere thanks also go out to **Prof. Shailendra K Saraf**, Director (Pharmacy), BBDNITM, Lucknow for providing me approval for using software named Maestro (version 9.3, Schrödinger, LLC New York, NY, 2012).*

*I also want to acknowledge the **University Grant Commission, Government of India** for providing me fellowship to pursue the research work.*

*I would like to express my sincere thanks to **Dr. Sunil Gorla** (Librarian), **Mr. O.P. Saini** (Assistant Librarian) BBAU for their kind support.*

*I must place on record very special thanks to my batchmates and friends, **Mr. Subhadeep Roy**, **Mr. Rajnish Kumar Yadav**, **Mr. Lakhveer Singh**, **Mr. Jitendra Kumar Rawat**, **Ms. Swetlana** and **Ms. Rashmi Singh** for their charming company, kind co-operation and encouragement throughout my doctoral study.*

I am also grateful to my juniors Anurag, Azad and Chanchal for their kind support and help.

*I wish to thank the staff members, **Mr. Ramesh, Mr. Anand Pandey, Mr. Amar and Mr. Bhandari** for providing all the needful official accessories.*

Finally, I acknowledge the people who mean a lot to me, my parents and my friends for showing faith in me and giving me liberty to choose what I desired. I wish to thank almighty God who keep his blessings on me every second and giving me the strength and patience to work through all these years so that today I can stand proudly with completion of my research work.

Manjari
MANJARI SINGH

List of Tables

Table No.	Table Caption	Page No.
1.	Lists of Equipments Used	32-33
2.	Sequence of forward and reverse primers used for qRT PCR	44
3.	Effect of BBAP-1 on electrocardiographic changes in mammary gland carcinoma	61
4.	Effect of BBAP-1 on HRV changes in MNU induced mammary gland carcinogenesis	62
5.	Effect of MNU and BBAP-1 on differentiation of mammary gland	64
6.	Effect of BBAP-1 and MNU on oxidative stress markers	67

List of Figures

Figure No.	Table Caption	Page No.
1.	Energy requirement for normal cell and for cancer cell	2
2.	Effect of normoxic and hypoxic condition on cellular proliferation	4
3.	Regulatory pathway for FASN and its modulation by HIF-1 α and PHD-2	10
4.	Hypothesized outcomes of PHD-2 activation	11
5.	Principle of <i>in vitro</i> PHD-2 assay	35
6.	<i>In silico</i> binding efficacy and toxicity profiling of BBAP-1 and BBAP-2	47-48
7.	Metabolic profiling of BBAP-1 and BBAP-2	49
8.	Effect of BBAP-1 and BBAP-2 and cobalt upon <i>in vitro</i> PHD-2 activity	50-51
9.	Effect of BBAP-1 and BBAP-2 upon MTT assay	52
10.	Effect of BBAP-1 and BBAP-2 upon morphological symptoms of apoptosis	53-54
11.	Effect of BBAP-1 and BBAP-2 upon mitochondria membrane potential	55-56
12.	Effect of BBAP-1 and BBAP-2 upon cell cycle arrest and apoptotic cell burden	58-59
13.	Effect of BBAP-1 upon cellular, morphological and surface architecture of mammary gland tissue	65
14.	Effect of BBAP-1 treatment on mitochondrial mediated apoptosis	69
15.	Effect of BBAP-1 treatment on hypoxic pathway in mammary gland cancer	70

List of Abbreviations

- Acridine orange (AO)
- Alveolar buds (AB)
- Adenosine triphosphate (ATP)
- Bovine serum albumin (BSA)
- Cancer associated fibroblasts (CAFs)
- Cuboidal epithelial cells (CEC)
- Dithiothreitol (DTT)
- Dimethyl sulphoxide (DMSO)
- Differentiation score (DF score)
- 7,12-Dimethylbenz[a]anthracene (DMBA)
- Dense connective tissue (DCT)
- Ethidium bromide (EtBr)
- Eagle's based salt solution (EBSS)
- Electrocardiogram (ECG)
- Epigallocatechin-3-gallate (EGCG)
- Fatty acid synthase (FASN)
- Fetal bovine serum (FBS)
- Fluorescence activated cell sorter (FACS)
- Glutathione (GSH)
- Hypoxia-inducible factor (HIF)
- Hypoxia response element (HRE)
- Heart rate variability (HRV)
- Heart rate (HR)
- Hematoxylin and eosin (H&E)
- Hank's balanced salt solution (HBSS)
- High frequency (HF)
- Low frequency (LF)
- Loose connective tissue (LCT)
- Nicotinamide adenine dinucleotide phosphate (NADPH)
- N-methyl-n-nitrosourea (MNU)
- Myoepithelial cells (MC)

- 3-(4,5-dimethylthiazol-2-yl)-2,5-diphenyltetrazolium bromide (MTT)
- 2-oxoglutarate (2-OG)
- o-phenylenediamine (OPD)
- Phosphate buffer saline (PBS)
- Prolyl hydroxylase-2 (PHD-2)
- Propidium iodide (PI)
- Protein carbonyl (PC)
- Reactive oxygen species (ROS)
- Scanning electron microscope (SEM)
- Sterol regulatory element-binding protein (SREBP)
- Superoxide dismutase (SOD)
- Toxicity estimation software tool (TEST)
- Turbidity reduction unit (TRU)
- Thiobarbituric acid reactive substances (TBARs)
- Vascular endothelial growth factor (VEGF)
- von Hippel-Lindau (pVHL).

CHAPTER 1

INTRODUCTION

1. Cancer cells and normal cells

The animal/human body is made up of many living cells and these cells have the tendency to grow, multiply and generate new cells and die after some time. This cell death phenomenon is known as cell apoptosis [1]. During cancer, the cells start growing in uncontrolled manner, they cannot die and grow deliberately to form new cells and form their own blood vessels through angiogenesis [2]. Afterwards, cancer cells metastasize into the nearby organs and their growth is not arrested [3]. There are eight major characteristics of cancer cells:

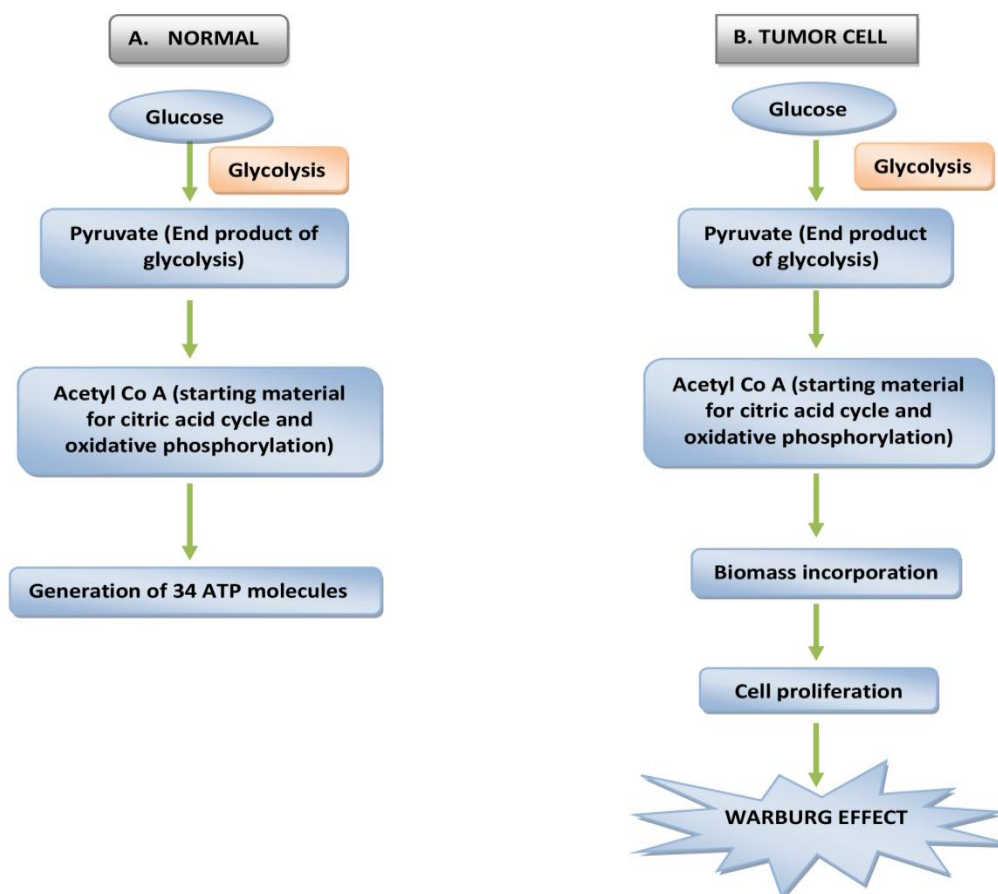
- I. Self sufficient pro growth signalling
- II. Loss of sensitivity to antigrowth signals
- III. Resistance to cell death
- IV. Replicating without limit
- V. Angiogenesis
- VI. Invasion and metastasis
- VII. Reprogrammed metabolism
- VIII. Evading immune surveillance

Cells required energy for the proper functioning. Sugar molecule plays a very important role in this process as they are oxidized in small steps to carbon dioxide and water [4]. A large array of mechanisms is involved in the breakdown/catabolism of sugars to produce adenosine tri phosphate (ATP), nicotinamide adenine di phosphate (NADPH) and other molecules [5].

The normal cells and cancer cells are peculiar from each other in their intermediary metabolism, which helps the cancerous cells to survive in hypoxic microenvironment.

Cancer cells get energy from the process of glycolysis rather than any other process, as more ATP is generated via glycolysis (Warburg effect) [6]. During glycolysis, two molecules of pyruvate with a net gain of two molecules of ATP are generated from the metabolism of one molecule of glucose [7]. Under normoxic conditions, the end product of glycolysis i.e. pyruvate gets converted into acetyl CoA which works as the starting material for the citric acid cycle and oxidative phosphorylation, yielding about 34 ATP molecules [8]. In tumor hypoxia (low oxygen level), cells go through a shift to the glycolytic pathway for the stipulation of energy [9] (Figure 1).

Figure 1: Energy requirement for normal cell and for cancer cell



Hypoxic microenvironment in cancerous cell is a result of high oxygen consumption within the tumor vasculature by rapidly procreating tumor cells [10]. To support the unceasing growth in the hypoxic microenvironment, cancer cells are known to stimulate alternate metabolic pathways including anaerobic metabolism, increased signalling of growth factors, diversified regulation of cell cycle, cellular proliferation and protein catabolism [11]. Hypoxia inducible factor (HIF) activation also vitiates mitochondrial respiration by making HIF-1 α key regulator of cancer cell metabolism along with stimulation of glycolysis [12]. It was previously reported that in cancer cells, there are alterations in lipid metabolism and de novo fatty acid biosynthesis [13]. Fatty acid synthase (FASN) is identified as the breast tumor associated protein and there are diversified studies to show that FASN is overexpressed in cancer cells including mammary gland carcinomas [14]. According to various clinical and preclinical studies, it is clear that human cancer have the capacity to synthesize their own fatty acid which is autonomous of the regulatory signals. The mechanism which is culpable for FASN up regulation in cancer is unknown [15, 16].

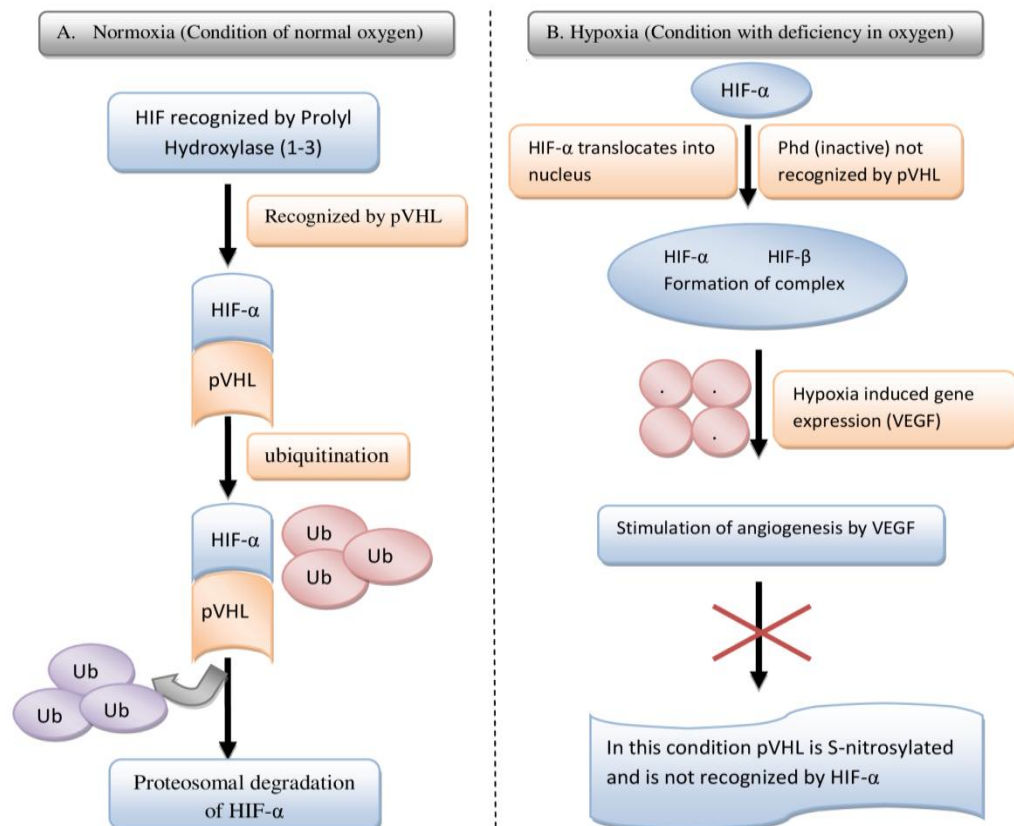
1.1 Tumor hypoxia

In tumor hypoxic condition, the level of oxygen is decreased. Oxygen is the primary requirement for a cell to grow [17] and most of the solid tumors are hypoxic in nature due to the limited amount of vasculature, poor tumor vessels with chaotic architecture [18]. HIF is the main effector of oxygen homeostasis, allocating various genes involved in biological processes like angiogenesis [19]. HIF also regulate the genes associated with vascular endothelial growth factor (VEGF) which is requisite for transactivation of VEGF mediated angiogenesis [20]. This type of binding promotes the proliferation which

accompany to the formation of blood vessels. HIF-1 α plays a very imperative role in metabolic angiogenesis and is proclaimed to be highly expressed in a wide variety of human cancers [21].

Under normoxic condition, prolyl hydroxylation (PHD) allows the interplay of HIF-1 α to von Hippel Lindau (pVHL) and acts as recognition component of E3 ubiquitin ligase and subsequently HIF-1 α goes through proteasomal degradation [22]. In hypoxic condition, HIF-1 α fails to interact with pVHL mediated degradation and translocates into the nucleus to form a complex with HIF-1 β [23] (Figure 2).

Figure 2: Effect of normoxic and hypoxic condition on cellular proliferation



This complex can actuate the transcription of target genes with the help of core hypoxia response element (HRE) [24]. HIF-1 α also interacts with p300/CBP co-activator complex which is regulated by oxygen and Asn 803(human HIF-1 α) [25].

1.2 PHDs

PHDs domain proteins are the group of enzymes, which hydroxylate HIF-1 α and supervise its activity. PHDs belong to a 2-oxoglutarate (2-OG) dependent dioxygenase superfamily [26]. Along with 2-OG, these enzymes require Fe²⁺, oxygen and ascorbate to modify the functions of HIF-1/2 α . There are four isoforms of this enzyme, named as PHD-1, PHD-2, PHD-3 and PHD-4 [27]. In relation to HIF-1 α , PHD-1 and PHD-2 are found to be very comparable (407 and 426 amino acid residue proportionately) while PHD-3 is found to be short (only 236 amino acid residues). PHD-4 is recorded to be the larger one with 502 amino acids [28]. PHD-4 has been found to be appended with membrane and its active site is located to the lumen of endoplasmic reticulum [29]. PHDs possess a double stranded β -helix core fold in which Fe²⁺ is bound with catalytic centre [30]. PHD-2 is ubiquitously expressed, while PHD-1 is expressed in placenta and PHD-3 in the heart. Role of PHD-2 in tumor angiogenesis is controversial [31]. Some reports suggested that, tumor vasculature is regulated by PHD-2 whereas others observed that PHD-2 expression is reduced and lead to the normalization of blood vessels with reduced tumor metastasis [32, 33]. A modest set of researchers have also divulged that PHD-2 deficiency is associated with cell invasion and metastasis in pancreatic tumor cells, thereby suggesting its tumor promoting nature [33, 34]. By and large, PHD-2 is perceived to reduce tumor metastasis and few of the activators of PHD-2 have been reported to manifest anticancer activity [35-37].

1.3 FASN

FASN is a major enzyme for lipogenesis. It is a complex multienzyme protein that contains seven catalytic domains [38]. The major function of FASN is to catalyze the condensation of acetyl CoA and malonyl CoA to produce palmitic acid in the presence of NADPH [39]. FASN is allocated into two classes: type I and type II. FASN I is a multifunctional polypeptide and very common in mammals and fungi. FASN I produces palmitic acid and cooperate with FASN II for the production of lipid products [40]. FASN II is commonly found in archaea and bacteria and it is symbolized to be multifunctional enzymes [41]. In highly lipogenic tissues like liver, lactating breast and adipose tissues, FASN have three major functions:

- I. Storage of profound excess energy in the form of fat.
- II. If the diet is low in fat then the synthesis of fat from carbohydrate or protein.
- III. Synthesis of fat for lactation.

Analogues to normal cells, the majority of fatty acid in cancer cells are derived from *de novo* synthesis rather than dietary fats [13]. Upsurge in lipogenesis is reflected as an inflated activity of lipogenic enzymes such as ATP citrate lyase and FASN [42]. The FASN level is overexpressed in lipoidal tumor cells and is one of the most common molecular changes which occur in cancerous cell [43]. Generally, glycolysis increases the uptake of oxygen in cancer cells away from blood vessels and consumes glucose which results in accumulation of pyruvate and lactate. This exhaustion of glucose and agglomeration of lactate is the main cause of hypoxia induced apoptosis [10]. A decent set of FASN inhibitors like cerulenin, C75 and orlistat are reported to urge cell death in a variety of tumors mainly lipoidal tumors [44]. FASN inhibitors can cause cell death and

considered to be a particularised target for the treatment of cancer. It has been proclaimed that the essential part of FASN act as energy substrates for the cells. Thereby inhibition of FASN induces decrease in the production of lipids in the tumor cells by which the tumor cells cannot get the energy for their propagation [45].

1.4 FASN and mammary gland carcinoma

A unique pathophysiological microenvironment including hypoxia, low pH and nutrient starvation implicates in the mammary gland tumors [46]. This type of environment triggers several intracellular signalling pathways and induce the level of FASN [47]. It was reported that hypoxic microenvironment can upregulates sterol regulatory element-binding protein (SREBP), which is a major transcriptional regulator of FASN gene through Akt phosphorylation [48]. FASN overexpression is a well reported phenomenon in the preclinical and clinical cases of mammary gland carcinoma [49, 50].

Researchers have reported increased expression of FASN in n-methyl-n-nitrosourea (MNU) and 7, 12-Dimethylbenz (a) anthracene (DMBA) induced mammary gland carcinoma in mouse models and thereby considered it as a viable target for chemoprevention [51, 52]. Inhibition of FASN has been reported to be associated with reduced synthesis of some essential fatty acids requisite for the cell growth [45]. In line to the animal studies, FASN is reported to be highly expressed in hormone independent SKBR3 and hormone dependent MCF-7 and ZR-75-1 cells lines as well [53]. Over expression of FASN has been linked with poor prognosis and reduced disease free survival in many cancer types including mammary gland carcinoma [54]. Infact, several cohort studies have linked the FASN overexpression with poor patient's survival and chemoresistance [55, 56]. It was previously reported that chemoresistance in cancer

patients have been linked with FASN overexpression mediated palmitate overproduction [57]. Clinical studies revealed that the stage 1 of breast cancer patients with high levels of FASN expression have fourfold increased risk for death [51]. Together with previous findings for FASN as a poor prognostic marker for breast cancer patients, we suggest FASN has a key role to play in drug resistance and can be considered as an ideal target for chemosensitization in breast cancer chemotherapy.

1.5 HIF and tumor microenvironment

Hypoxia plays a paramount role in the embryonic development and human physiology [58]. Almost all cancerous cells are reported to be hypoxic in nature and their proliferation is resolved through HIF-1 activation [59]. Henceforth, HIF-1 α plays a momentous role in tumor proliferation. Energy is implemented to the cells with the help of angiogenesis which fulfil the oxygen supply [60]. This energetic shift in cancerous cell coordinates with the variety of enzymes, which are diversified in the process of glycolysis for example glucose transporters (aldolase A and pyruvate kinase) [61]. These transporters help the cells to produce energy in the hypoxic micrenvironment. This constitutive activation of anaerobic metabolism in tumor cells provides a relationship of cell response to the oxygen deficiency [62]. Thus, HIF-1 α function in hypoxic environment involves in VEGF arbitrated angiogenesis, increased glycolysis and other steps in tumor progression [23].

1.6 Regulating PHD-2 to counteract tumor hypoxia and FASN over expression

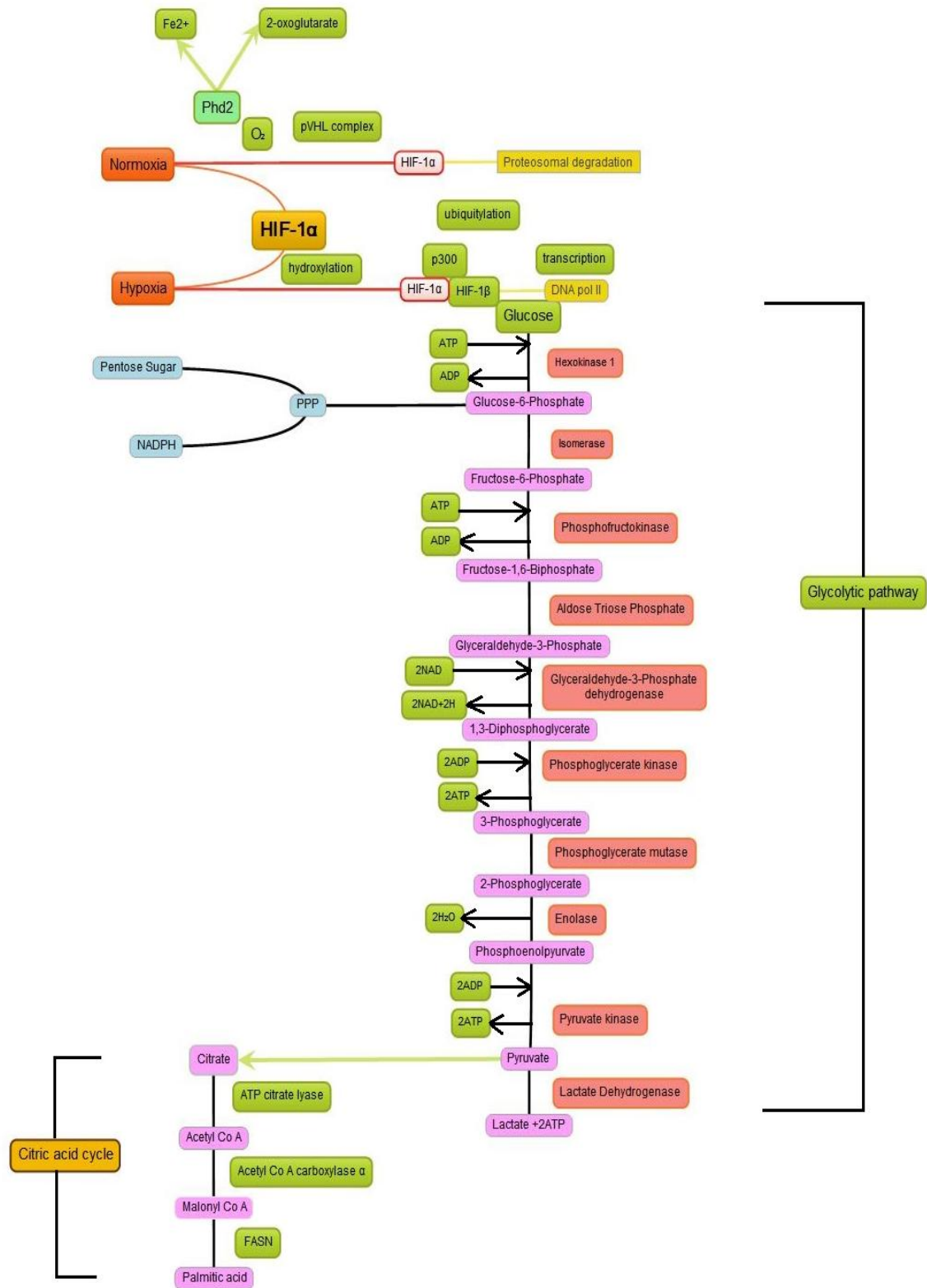
Initially, it was found that PHD-2 is the most critical hydroxylase in a variety of cultured cells and could be attributed to the fact that PHD-2 is more profoundly expressed than other PHDs [63]. The activity of PHDs can be restrained by post translational

mechanisms including proteasomal degradation and modulation of PHDs activity by collaborating proteins. It has been reported that all PHDs can downregulate HIF-1 α *in vitro* however the specific role of PHDs in cancer is still inconclusive [64].

1.7 Research Hypothesis

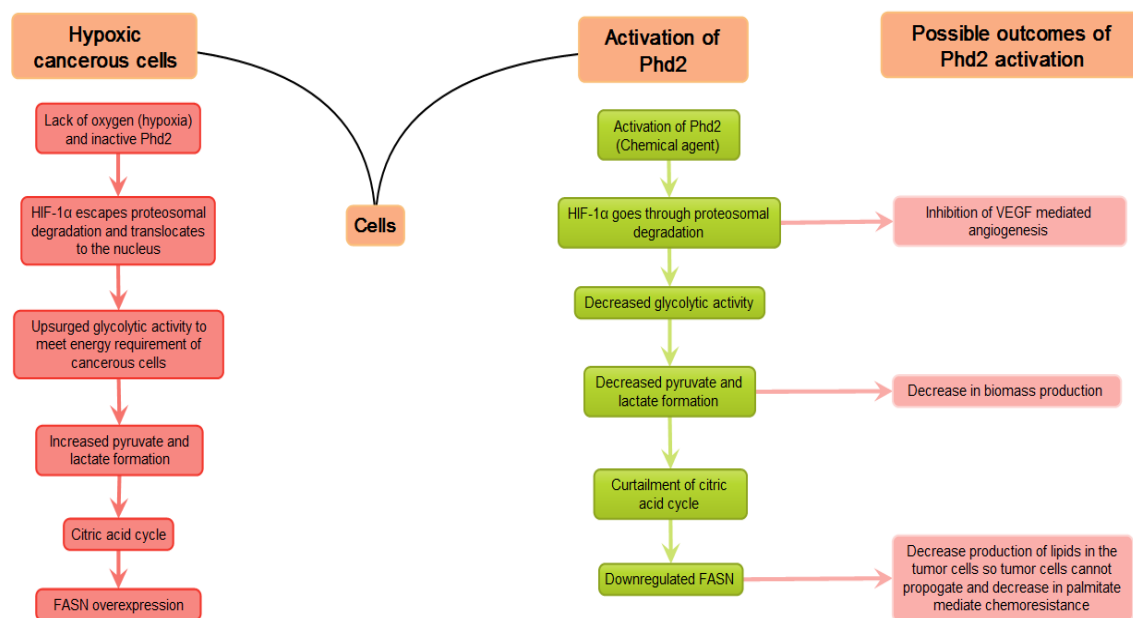
Notwithstanding, herewith it was hypothesized that the chemical activation of PHD-2 cause accelerated deterioration of HIF-1 α through proteasomal degradation which leads to the favourable outcomes against cancer. With the help of PHD-2 activators, the activity of HIF-1 α was curtailed and this cause decreased in glycolytic pathway and subsequent diminished in the FASN level which is recorded to be over expressed in tumor cells (Figure 3).

Figure 3: Regulatory pathway for FASN and its modulation by HIF-1 α and PHD-2



All in all, we hypothesized that activation of PHD-2 can affect cancerous cells in a multidirectional way. Firstly, by inhibiting the activation of HIF-1 α (a well established target in cancer chemoprevention); secondly, decreased production of lactate may help to cut down the biomass formation and lastly, by downregulating the FASN overexpression through curtailing the citric acid cycle (Figure 4).

Figure 4: Hypothesized outcomes of PHD-2 activation



1.8 Present scenario and future directions

As elaborated above, modifying the PHD-2 could be a viable target for cancer prognosis, which can be contemplated to have a momentous effect on the glycolytic pathway and thereby FASN expression in lipoidal cancers. It is to be noted that only three activators of PHD-2 namely KRH102053, KRH102140 and R59949 has been reported till date, with

KRH102053 and KRH102140 having a conspicuous effect on angiogenesis [35-37]. On the contrary, the R59949 (diacyl glycerol kinase II inhibitor) was also recorded with PHD-2 activating potential without much affecting the tumor progression [35]. It would be important to pen down that apart from activating the PHD-2, other physiological effects of KRH102053 and KRH102140 are unelucidated till date [36, 37]. In short, the underlying mechanism of these compounds is poorly understood, which we are in opinion could be transmutations in pathways of energy production and subsequent alteration in FASN over expression. We would also like to mention that the effect of KRH102053 and KRH102140 on glycolytic pathway and subsequent FASN overexpression could be a research question for future endeavours.

Down regulating the FASN overexpression in lipoidal cancer cells to customize tumor growth is a well studied and established phenomena [65]. Infact, a sufficient number of FASN inhibitors (e.g. cerulenin-3-derivative C75, β -lactone orlistat, green tea polyphenol epigallocatechin-3-gallate (EGCG) and other naturally occurring flavonoids as well as antibiotic triclosan) are proclaimed to have a profound effect on cell proliferation, angiogenesis, metastasis and apoptosis [66].

Most of the reported compounds are broad spectrum FASN inhibitors and mediate their action through ameliorating β -ketoacyl synthase. The compounds are well documented for their anti-cancer activity owing to their FASN inhibiting potential [67]. However, repercussion of FASN inhibition on glycolytic pathway, regulation of HIF-1 α and consequent effect on PHD-2 needs to be elucidated to full and stands still as a research question.

Additionally, most of the FASN inhibitors have several metabolic and pharmacological limitations which restrict their transformations from preclinical to clinical phase of drug discovery. Authors are in opinion that these impediments are the repercussion to the fact that FASN overexpression is the later consequence of hypoxic situation in cancerous cells and merely prohibiting the FASN, will not cater compelling detrimental effects on the tumor progression. In fact, we are not hesitant to put on records that activation of PHD-2 appears to be a more viable and constructive targets in terms of overseeing the hypoxic microenvironment and FASN overexpression in expeditiously dividing tumor cells.

With all above, authors are in strong accredit that activating PHD-2 could be a generous target to look after cancer progression and is hypothesized to be effectuated through down regulation of FASN over expression.

1.9 Literature Survey

- **Nunomiya et al (2017)** verified the direct contribution of HIF activation to running training without exposure to atmospheric hypoxia, they used PHD-2 conditional knockout mice (cKO), which exhibit HIF activation independent of oxygen concentration, and they examined their maximal exercise capacity before and after 4 weeks of treadmill exercise training. They conclude that the activation of the HIF pathway induced by PHD-2 deficiency enhances the effect of running training [68].
- **Kuchnio et al (2015)** explored the role of oxygen sensor PHD-2 in cancer as it is still a question for recent research. First, the role of PHD-2 in metastasis has not been studied in a spontaneous tumor model. In this study, they show that global PHD-2 haplodeficiency reduced metastasis without affecting tumor growth. Second, it is unknown whether PHD-2 regulates cancer by affecting cancer-associated fibroblasts (CAFs). They show that PHD-2 haplodeficiency reduced metastasis via two mechanisms: (1) by decreasing CAF activation, matrix production, and contraction by CAFs, an effect that surprisingly relied on PHD-2 deletion in cancer cells, but not in CAFs; and (2) by improving tumor vessel normalization. Third, the effect of concomitant PHD-2 inhibition in malignant and stromal cells (mimicking PHD-2 inhibitor treatment) is unknown. They show that global PHD-2 haplodeficiency, induced not only before but also after tumor onset, impaired metastasis [34].
- **Cheng et al (2014)** stated that cancer cells process a fundamental change in its bioenergetic metabolism from normal cells on an altered lipid metabolism, also known as the *de novo* fatty acid synthesis, for sustaining their high proliferation rates. Fatty acid

synthesis is now associated with clinically aggressive tumor behaviour and tumor cell growth and has become a novel target pathway for chemotherapy development [53].

- **Fan et al (2014)** stated that HIFs are oxygen-dependent transcriptional activators that play crucial roles in angiogenesis, erythropoiesis, energy metabolism and cell fate decisions. The group of enzymes that can catalyse the hydroxylation reaction of HIF-1 is PHDs. PHD inhibitors (PHIs) activate the HIF pathway by preventing degradation of HIF-1 α via inhibiting PHDs. Osteogenesis and angiogenesis are tightly coupled during bone repair and regeneration. Numerous studies suggest that HIFs and their target gene, VEGF, are critical regulators of angiogenic-osteogenic coupling [69].
- **Masson and Ratcliffe (2014)** stated that both tumor hypoxia and dysregulated metabolism are classical features of cancer. Recent analyses have revealed complex interconnections between oncogenic activation, hypoxia signalling systems and metabolic pathways that are dysregulated in cancer. These studies have demonstrated that rather than responding simply to error signals arising from energy depletion or tumor hypoxia, metabolic and hypoxia signalling pathways are also directly connected to oncogenic signalling mechanisms at many points [9].
- **Ackerman and Simon (2014)** stated that solid tumors typically develop hostile microenvironments characterized by irregular vascularization and poor oxygen (O₂) and nutrient supply. Whereas normal cells modulate anabolic and catabolic pathways in response to changes in nutrient availability, cancer cells exhibit unregulated growth even under nutrient scarcity. Recent studies have demonstrated that constitutive activation of growth-promoting pathways results in dependence on unsaturated fatty acids for survival

under O₂ deprivation. In cancer cells, this dependence represents a critical metabolic vulnerability that could be exploited therapeutically [70].

- **Yang M et al (2014)** stated that HIF and PHDs regulate the stability of HIF protein by post-translational hydroxylation of two conserved prolyl residues in its α subunit in an oxygen-dependent manner. Trans-4-prolyl hydroxylation of HIF-1 α under normal oxygen (O₂) availability enables its association with the pVHL tumor suppressor protein, leading to the degradation of HIF-1 α via the ubiquitin-proteasome pathway. Due to the obligatory requirement of molecular O₂ as a co-substrate, the activity of PHDs is inhibited under hypoxic conditions, resulting in stabilized HIF-1 α , which dimerizes with HIF-1 β and together with transcriptional co-activators CBP/p300, activates the transcription of its target genes. As a key molecular regulator of adaptive response to hypoxia, HIF plays important roles in multiple cellular processes and its overexpression has been detected in various cancers [71].
- **Tian and Ma (2014)** stated that FASN has been proven overexpressed in human breast cancer cells and consequently, has been recognized as a target for breast cancer treatment. Alpha-mangostin, a natural xanthone found in mangosteen pericarp, has a variety of biological activities, including anti-cancer effect. In their previous study, alpha-mangostin had been found both fast-binding and slow-binding inhibitions to FAS *in vitro*. This study was designed to investigate the activity of alpha-mangostin on intracellular FAS activity in FAS overexpressed human breast cancer cells and to testify whether the anti-cancer activity of alpha-mangostin may be related to its inhibitory effect on FAS. Alpha-mangostin could effectively suppress FAS expression and inhibit intracellular FAS activity and result in decrease of intracellular fatty acid accumulation. It could also

reduce cell viability, induce apoptosis in human breast cancer cells, increase in the levels of the PARP cleavage product and attenuate the balance between anti-apoptotic and pro-apoptotic proteins of the Bcl-2 family. Alpha-mangostin induced breast cancer cell apoptosis by inhibiting FAS, which provide a basis for the development of xanthone as an agent for breast cancer therapy [72].

- **Gilkes and Semenza (2013)** stated that breast cancer cells adapt to hypoxic conditions by increasing levels of HIFs, which induce the expression of multiple genes involved in angiogenesis, glucose utilization, resistance to oxidative stress, cell proliferation, resistance to apoptosis, invasion and metastasis. Breast cancer patients with increased HIF expression levels in primary tumor biopsies are at increased risk of metastasis. This is an important finding since 90% of breast cancer deaths are the result of metastasis, primarily to the bone, lungs, liver, brain and regional lymph nodes. Recent studies have implicated HIF target genes in every step of the metastatic process. Drugs, such as digoxin, show the potential therapeutic effects of blocking HIF activity by decreasing primary tumor growth, vascularization, invasion and metastasis in animal models of breast cancer [73].
- **Yoshii Y et al (2013)** stated that FASN expression is elevated in several cancers and this overexpression is associated with poor prognosis. Inhibitors of FASN, such as orlistat, reportedly show antitumor effects against cancers that overexpress FASN, making FASN a promising therapeutic target. However, large variations in FASN expression levels in individual tumors have been observed and methods to predict FASN targeted therapy outcome before treatment are required to avoid unnecessary treatment. In addition, how FASN inhibition affects tumor progression remains unclear. FASN-targeted therapy was

noticeably effective against tumors with high FASN expression, which was indicated by high acetate uptake. FASN inhibition not only suppressed cell proliferation but prevented pseudopodia formation and suppressed cell adhesion, migration, and invasion. FASN inhibition also suppressed genes involved in production of intracellular second messenger arachidonic acid and androgen hormones, both of which promote tumor progression. Collectively, the data demonstrated that uptake of radiolabeled acetate is a useful predictor of FASN targeted therapy outcome. FASN targeted therapy could be an effective treatment to suppress multiple steps related to tumor progression in prostate cancers selected by [1-¹¹C] acetate PET [74].

- **Zhao Y et al (2013)** stated that the metabolic properties of cancer cells diverge significantly from those of normal cells. Energy production in cancer cells is abnormally dependent on aerobic glycolysis. In addition to the dependency on glycolysis, cancer cells have other atypical metabolic characteristics such as increased fatty acid synthesis and increased rates of glutamine metabolism. Emerging evidence shows that many features characteristic to cancer cells, such as dysregulated Warburg-like glucose metabolism, fatty acid synthesis and glutaminolysis are linked to therapeutic resistance in cancer treatment. Therefore, targeting cellular metabolism may improve the response to cancer therapeutics and the combination of chemotherapeutic drugs with cellular metabolism inhibitors may represent a promising strategy to overcome drug resistance in cancer therapy. The author discussed the relationship between dysregulated cellular metabolism and cancer drug resistance and how targeting of metabolic enzymes, such as glucose transporters, hexokinase, pyruvate kinase M2, lactate dehydrogenase A, pyruvate

dehydrogenase kinase, fatty acid synthase and glutaminase can enhance the efficacy of common therapeutic agents or overcome resistance to chemotherapy or radiotherapy [57].

- **Smirnova NA (2012)** told about the catalytic mechanism, substrate specificity, and structural peculiarities of 2-OG dependent nonheme iron dioxygenases catalyzing prolyl hydroxylation of HIF. Distinct localization and regulation of three isoforms of HIF prolyl hydroxylases suggest their different roles in cells. The recent identification of novel substrates other than HIF, namely β 2-adrenergic receptor and the large subunit of RNA polymerase II, places these enzymes in the focus of drug development efforts aimed at development of isoform-specific inhibitors. They discussed the challenges and prospects of designing isoform-specific inhibitors [75].
- **Nepal M et al (2011)** stated that HIFs play a pivotal role in the response of cells to hypoxia. HIFs are dimers of an oxygen-sensitive α -subunit (HIF-1 α or HIF-2 α) and a constitutively expressed β -subunit. In normoxia, HIF-1 α is destabilized by post-translational hydroxylation of Pro-564 and Pro-402 by a family of oxygen-sensitive dioxygenases. PHDs lead to pVHL-dependent ubiquitination and rapid degradation of HIF-1 α . They previously reported that KRH102053, an activator of PHD-2, rapidly decreased HIF-1 α and eventually inhibited angiogenesis. The results suggest that KRH102140 has potential therapeutic effects in alleviating various diseases associated with HIFs [36].
- **Jokilehto and Jaakkola (2010)** stated that tumour hypoxia is a well-known microenvironmental factor that causes cancer progression and resistance to cancer treatment. This involves multiple mechanisms of which the best understood ones are mediated through transcriptional gene activation by the HIFs. HIFs in turn are regulated

in response to oxygen availability by a family of iron and 2-OG dependent dioxygenases, the HIF-PHDs. PHDs inactivate HIFs in normoxia by activating degradation of the HIF-1 α subunit but release HIF activation in poorly oxygenated conditions. They review the function of PHDs on the HIF system, the expression of PHDs in human tumours as well as their putative function in cancer [64].

- **Chan and Giaccia (2010)** stated that the role of PHD proteins have remained elusive. Of the four identified PHD enzymes, PHD-2 is considered to be the key oxygen sensor, as knockdown of PHD-2 results in elevated HIF protein. Several recent studies have highlighted the importance of PHD-2 in tumourigenesis. However, there is conflicting evidence as to the exact role of PHD-2 in tumour angiogenesis. This review summarises the current understanding of PHD-2 and tumour angiogenesis, focusing on the influences of PHD-2 on vascular normalisation and neovascularisation [76].
- **Flavin R et al (2010)** stated that FASN is a key enzyme involved in neoplastic lipogenesis. Overexpression of FASN is common in many cancers and accumulating evidence suggests that it is a metabolic oncogene with an important role in tumor growth and survival, making it an attractive target for cancer therapy. Several potent inhibitors have recently been reported that may help to unravel and exploit the full potential of FASN as a target for cancer therapy in the near future. Furthermore, novel sources of FASN inhibitors, such as green tea and dietary soy, make both dietary manipulation and chemoprevention potential alternative modes of therapy in the future [44].
- **Choi et al (2008)** stated that HIF is a transcription factor induced by hypoxia and degraded by ubiquitin-dependent proteasomes in normoxic conditions. Under hypoxic conditions, hydroxylation of HIF-1 α subunit by PHD is suppressed, thus leading to

increased levels of HIF. Although PHD-2 plays a key role in regulating the levels of HIF, chemical activators of PHD-2 are relatively unknown. The aim of this study was to identify small molecule activators of PHD-2 that could be used, eventually, to suppress the level of HIF-1 α . They found a potent activator of PHD-2, KRH102053 (2-amino-4-methylsulphonyl-butylidene-4-methoxy-6-(4-methoxy-benzylamino)-2, 2-dimethylchroman-3-yl ester). The results suggest that KRH102053 and its structural analogues have the potential for use as therapeutic agents against various diseases associated with HIF [37].

- **Lisy and Peet (2008)** stated that the HIFs are critical for cellular adaptation to limiting oxygen and regulate a wide array of genes when cued by cellular oxygen-sensing mechanisms. HIF is able to direct transcription from either of two transactivation domains, each of which is regulated by distinct mechanisms. The oxygen-dependent asparaginyl hydroxylase factor-inhibiting HIF-1 α (FIH-1) is a key regulator of the HIF C-terminal transactivation domain and provides a direct link between oxygen sensation and HIF mediated transcription [77].
- **Young and Anderson (2008)** stated that tumor cells exhibit an altered metabolism, characterized by increased glucose uptake and elevated glycolysis, which was first recognized by Otto Warburg 70 years ago. In recent years it has become clear that loss of p53 and activation of Akt can induce all or part of the metabolic changes reflected in the Warburg effect. Likewise, changes in expression of lactate dehydrogenase and other glycolytic control enzymes can contribute to increased or altered glycolysis. It is also clear that changes in lipid biosynthesis occur in tumor cells to support increased membrane biosynthesis and perhaps the altered energy needs of the cells. Changes in

FASN, Spot 14, Akt, and DecR1 (2, 4-dienoyl-coenzyme A reductase) may underlie altered lipid metabolism in tumor cells and contribute to the ability of tumor cells to proliferate or metastasize. Although these advances provide new therapeutic targets that merit exploration, there remain critical questions to be explored at the mechanistic level; this work may yield insights into tumor cell biology and identify additional therapeutic targets [78].

- **Furuta E et al (2008)** stated that the FASN gene is significantly up-regulated in various types of cancers and blocking the FAS expression results in apoptosis of tumor cells. Therefore, FAS is considered to be an attractive target for anticancer therapy. However, the molecular mechanism by which the FAS gene is up-regulated in tumor cells is poorly understood. They found that FAS was significantly up-regulated by hypoxia, which was also accompanied by reactive oxygen species (ROS) generation in human breast cancer cell lines. They also found that the hypoxia significantly up-regulated SREBP-1, the major transcriptional regulator of the FAS gene, via phosphorylation of Akt followed by activation of HIF-1. In their xenograft mouse model, FAS was strongly expressed in the hypoxic regions of the tumor. In addition, the results of immunohistochemical analysis for human breast tumor specimens indicate that the expressions of both FAS and SREBP-1 were colocalized with hypoxic regions in the tumors. Furthermore, they found that hypoxia-induced chemoresistance to cyclophosphamide was partially blocked by a combination of FAS inhibitor and cyclophosphamide. Taken together, the results indicate that FAS gene is up-regulated by hypoxia via activation of the Akt and HIF-1 followed by the induction of the SREBP-1 gene, and that hypoxia-induced chemoresistance is partly due to the up-regulation of FAS [48].

- **Horn M et al (2007)** stated that a major feature of solid tumors is hypoxia, decreased availability of oxygen, which increases patient treatment resistance and favours tumor progression. Massive tumor-cell proliferation distances cells from the vasculature, leading to a deficiency in the local environment of blood carrying oxygen and nutrients. Such hypoxic conditions induce a molecular response, in both normal and neoplastic cells, that drives the activation of a key transcription factor; the HIF. Although now recognized as a major contributor to cancer progression and to treatment failure, the precise role of hypoxia signalling in cancer and in prognosis still needs to be further defined. It is hoped that a better understanding of the mechanisms implicated will lead to alternative and more efficient therapeutic approaches [79].
- **Menendez and Lupu (2007)** stated that there is a renewed interest in the ultimate role of FASN, a key lipogenic enzyme catalysing the terminal steps in the de novo biogenesis of fatty acids in cancer pathogenesis. A recent identification of cross-talk between FASN and well-established cancer-controlling networks begins to delineate the oncogenic nature of FASN-driven lipogenesis [80].
- **Ke and Costa (2006)** stated that adaptation to low oxygen tension (hypoxia) in cells and tissues leads to the transcriptional induction of a series of genes that participate in angiogenesis, iron metabolism, glucose metabolism, and cell proliferation/survival. Overexpression of HIF-1 has been found in various cancers, and targeting HIF-1 could represent a novel approach to cancer therapy [81].
- **Kuhajda FP (2006)** stated that FASN is the sole mammalian enzyme which is capable of de novo fatty acid synthesis and it is highly expressed in most human carcinomas. FASN is associated with poor prognosis in breast and prostate cancer, is elaborated into the

blood of cancer patients, and its inhibition is selectively cytotoxic to human cancer cells. Thus, FASN and fatty acid metabolism in cancer has become a focus for the potential diagnosis and treatment of cancer [82].

- **Zhou J et al (2006)** stated that aerobic life consumes oxygen for efficient production of high energy compounds. The discovery of HIF-1 allowed the identification of molecular mechanisms by which changes in oxygenation are transduced to adequate intracellular adaptive responses. Likely, secondary stressors such as pH changes, i.e. acidosis, and the context of genetic alterations will shape the role of HIF-1 to affect susceptibility of cells to undergo hypoxia-induced cell death or to allow adaptation and progression towards malignancy [83].
- **Temes E et al (2005)** stated that HIF are heterodimeric (α/β) transcription factors that play a fundamental role in cellular adaptation to low oxygen tension. They previously shown that the hypoxia-induced accumulation of HIF- α protein is strongly impaired by the inhibitor of diacylglycerol kinase, R59949. They investigated the mechanisms through which this inhibitor exerts its effect. They found that R59949 inhibits the accumulation of HIF-1/2 α protein without affecting the expression of their mRNAs. They also determined that R59949 could only block the accumulation of HIF- α in the presence of pVHL protein [36].
- **Menendez J A et al (2005)** stated that Her-2/neu (erbB-2) oncogene overexpression is associated with increased tumor progression and metastasis. Interestingly, they recently established that both pharmacological inhibition of FASN activity and silencing of FASN gene expression specifically suppress Her-2/neu oncoprotein expression and tyrosine-kinase activity in breast and ovarian Her-2/neu overexpressors. Unravelling the

functional organization of this novel bi-directional molecular connection between Her-2/neu and FASN-dependent neoplastic lipogenesis is a major challenge that the field is only beginning to take on. It is tempting to suggest that an intact FAS-catalyzed endogenous fatty acid metabolism is a necessary metabolic adaptation to support the enhanced ability of Her-2/neuoverexpressing cancer cells to survive cellular hypoxia in a HIF- α -dependent manner [84].

1.10 Research Envisaged

FASN is an enzyme responsible for fatty acid synthesis and is reported to be overexpressed in cancers particularly in mammary gland cancers. The FASN overexpression in cancers has been attributed to hypoxic environment in cancer and increased lipid requirement of cancer. The inhibitors of FASN have been previously reported to exhibit good anti-cancerous effects.

The hypoxic environment in cancerous cells is due to inhibition of PHD-2 leading to induction of HIF-1 α , which in further regulates the glycolytic pathway and hence modulates FASN overexpression.

The present study was proposed to screen the PHD-2 inducers using computer modelling and to evaluate the effect of PHD-2 inducers on FASN expression in tumor cells. The study further extends its horizon to enumerate the effect of PHD-2 inducers in tumor growth, angiogenesis, metastasis and apoptosis.

The work was proposed to be carried out mammary gland cancer considering the fact FASN overexpression is more pronounced in lipoidal tissues.

The proposed work was based upon the hypothesis that PHD-2 induction will inhibit HIF-1 α production, leading to decreased FASN expression and thereby decreased cancer growth.

1.11 Aim & objectives of the study

The proposed study was aimed to screen/ identify possible inducers of PHD-2 and to evaluate them against mammary gland tumors with following specific objectives:

- ✓ To screen the possible legends for PHD-2 inducers using computational approach.
- ✓ To evaluate the HIF-1 α inhibitory, glycolytic inhibitory activity of PHD-2 inducers *in vitro*.
- ✓ To investigate the effects of PHD-2 inducers on FASN expression and fatty acid composition of cancer cells in tumour cells.
- ✓ To enumerate the effect of PHD-2 inducers on angiogenic and metastatic status of a fastly growing tumours.

1.12 Plan of work

1. Literature survey & procurement of materials

2. *In silico* study

- ✓ Virtual screening of compounds
- ✓ Anti-cancer potential screening using CDRUG web server
- ✓ Docking using Autodock 4.2
- ✓ Metabolic profiling
- ✓ *In vitro* PHD-2 activation assay

3. *In vitro* study

- ✓ MTT assay

- ✓ Acridine orange/ethidium bromide (AO/EtBr) staining
- ✓ JC-1 staining
- ✓ Cell cycle analysis

4. *In vivo* study

- ✓ Hemodynamic study
- ✓ Morphological analysis
- ✓ Anti-oxidant parameters
- ✓ Caspase 3 and caspase 8 estimation
- ✓ Western blotting
- ✓ qRT-PCR

5. Statistical analysis

6. Compilation of data

CHAPTER 2

SCREENING OF

COMPOUNDS

2.1 Scrutiny of compounds using Zinc and Asinex database

Based on the hypothesis, approximately 28000 compounds were screened using the criteria of 50% structure similarity with the previously reported PHD-2 activators: R59949 [35] and KRH102140 [36]. The compounds were further screened from the Zinc database and Asinex database using Maestro (version 9.3, Schrödinger, LLC New York, NY, 2012) [85]. Only 1355 hits were retrieved and further docked with PHD-2 enzyme (PDB id-2G19). After that, the compounds were screened through various filters of drug likeliness including ADME, Lipinski, and reactive group filter from Maestro (version 9.3, Schrödinger, LLC New York, NY, 2012) [85].

2.1.1 Anticancer potential screening of compounds through CDRUG server

One thousand three hundred fifty five hits were retrieved through structural similarity search, which were further screened for their anticancer potential using CDRUG web server. CDRUG is an online web server, which is used to evaluate the *in silico* anticancer potential of a compound by using molecular description method (relative frequency-weight fingerprint). The results are represented by a set of variables, including query compound(s), matched compound(s), average GI50 value of the matched compound(s), the maximum H-score and P-value. It categorizes the result as green (highly possible), black (possible), and gray (less likely) depending on the P-value [86]. The CDRUG screening retrieved BBAP-1 (2-[4-(difluoromethoxy)phenyl]-1, 2, 3, 4-tetrahydroquinazolin-4-one) and BBAP-2 (4-[7-(acetyloxy)-2-ethyl-2H-chromen-3-yl] phenyl acetate) as a highly possible anti-cancer compounds.

2.1.2 Protein ligand interaction and toxicity prediction

The BBAP-1 and BBAP-2 were further docked with PHD-2 enzyme (PDB id-2G19) using Autodock 4.2 [87] and the binding energy was found to be -3.97 and -3.33

Kcal/mol. The toxicity profile was predicted using *in silico* toxicity estimation software tool (TEST) [88].

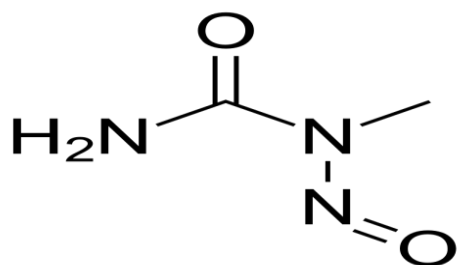
2.1.3 Predicted metabolites of BBAP-1 and BBAP-2

The metabolic profile of BBAP-1 and BBAP-2 were evaluated using Metaprint2D, licensed under the Apache license, 2.0 [89]. The BBAP-1 and BBAP-2 were further screened for the type of CYP450 isoform involved in its metabolism using WhichCyp web server [90].

2.2 Toxicant

MNU is a highly reliable carcinogen, mutagen, and teratogen. MNU is an alkylating agent and exhibits its toxicity by transferring its methyl group to nucleobases in nucleic acids, which can lead to AT: GC transition mutations. MNU is the traditional precursor in the synthesis of diazomethane. However, because it is unstable at temperatures beyond 20 °C and somewhat shock-sensitive, it has become obsolete for this purpose and replaced by other N-nitroso compounds: (N-methyl) nitrosamides and nitrosamines. Acute exposure to MNU in humans can result in skin and eye irritation, headache, nausea, and vomiting. MNU is reasonably anticipated to be a human carcinogen based on sufficient evidence of carcinogenicity in experimental animals. Various cancers induced in animal models include: squamous cell carcinomas of the forestomach, sarcomas and gliomas of the brain, adenocarcinomas of the pancreas, mammary carcinomas, leukemia, and lymphomas. However, the actual potential for human exposure is quite limited, as the chemical is not produced or used in large quantities. MNU is teratogenic and embryotoxic, resulting in craniofacial (cleft palate) and skeletal defects, fetal growth retardation and increased fetal resorption. Exposure to MNU during pre-implantation, post-implantation,

organogenesis or by paternal exposure can result in these effects. MNU doesn't need the involvement of any other intermediate [91].



Molecular formula: C₂H₅N₃O₂

Molecular weight: 103.081 g/mol

Physical description: Pale yellow crystals or light yellow moist powder

The toxicant was prepared in glacial acetic acid and water with pH 4.5-5. The MNU was given in a dose of 8mg/kg, i.v. twice in the whole study.

CHAPTER 3
MATERIALS AND
METHODS

3.1 Materials

3.1.1 Drugs and chemicals

2-[4-(Difluoromethoxy) Phenyl]-1, 2, 3, 4-Tetrahydroquinazoline 4-one (BBAP-1) was purchased from AKos Consulting & Solutions Deutschland GmbH, Germany. 4-[7-(acetyloxy)-2-ethyl-2H-chromen-3-yl] phenyl acetate (BBAP-2) was received as a generous gift from National Cancer Institute, National Institutes of Health, USA (export reference: SL#201500077, Job number-0348). RPMI 1640 medium (Gibco-11875093); l-glutamine (Gibco-25030081); fetal bovine serum (FBS) (Gibco-10270); trypsin (Gibco-R001100); eagle's balanced salt solution (EBSS) (Gibco-2018-11); hank's balanced salt solution (HBSS) (Himedia-TL1190); EtBr (Himedia-MB071-1G); AO (Himedia-MB116-10G); propidium iodide (PI) (SC-3541); JC-1 assay kit (Thermo Scientific M34152); tamoxifen citrate (Biochem Pharmaceuticals); penicillin-streptomycin (Thermo Scientific, 15410-163); gentamycin (Thermo Scientific, 15710-049); 3-(4,5-Dimethyl-2-thiazolyl)-2,5-diphenyl-2H-tetrazolium bromide (MTT) (TC191-1G); RNase (SRL, 9001-99-4); dimethyl sulfoxide (DMSO) (Merk, 1.16743.0521); ponceau S (Himedia-ML045); sodium cacodylate (Sigma-Aldrich, C0250); collagenase type IV (TC214); hyaluronidase (TC331); hematoxylin (Himedia-S058); eosin (Himedia-S007); RIPA lysis buffer (Amresco, N653); protein assay kit (Amresco, M173); bovine serum albumin (BSA) (Genetix, PG-2330); transfer buffer (Genetix, GX-9411AR); MNU (Sigma-Aldrich, N1517). Caspase 3 (SC-4263) and caspase 8 (SC-4267) assay kit was procured from Santacruz Biotechnology Inc., California, Delaware. All other chemicals used in the study are of molecular biology and purchased from Genetix Biotech Asia Pvt. Ltd. India; else otherwise stated in the text.

3.1.2 In silico software used

- Maestro (version 9.3, Schrödinger, LLC New York, NY, 2012)
- CDRUG server
- Autodock 4.2
- TEST
- Metaprint2D
- WhichCyp web service tool

3.1.3 Equipment used**Table 1: Lists of equipments used**

Serial no.	Equipment	Manufacturer and Model
1.	Cooling centrifuge	Eppendorf India Limited, Chennai 5418R
2.	Vortex shaker	Remi Mumbai CM101
3.	Refrigerator	Godrej, Lucknow
4.	Homogenizer	Remi, Mumbai RQT-127A
5.	Microvolume Spectrophotometer	Agilent Technologies, Mumbai Carry 500
6.	Weighing balance	Sartorius, Mumbai BSA224S-CW
7.	pH meter	Labman Scientific Instruments, Lucknow LMPH-10
8.	Micropipette	Genetix Biotech Asia Pvt. Ltd. New Delhi
9.	Deep freezer	Celfrost, Lucknow
10.	Microplate Reader	Bio-Rad Laboratories Inc. Model 680XR
11.	Inverted fluorescence microscope	Niken Leica M165FC
12.	Fluorescence activated cell sorter (FACS)	BD Influx cell sorter

13.	Bio-amplifier (ML-136) and channel power lab (ML-826)	AD Instruments, Australia
14.	Digital biological microscope	N 120, BR-Biochem Life Sciences, New Delhi
15.	Scanning electron microscope (SEM)	JEOL JSM-6490LV
16.	SDS-PAGE	GX-SCZ2, Genetix Biotech Asia Pvt. Ltd. New Delhi
17.	Semidry transfer unit	GX-ZY3, Genetix Biotech Asia Pvt. Ltd. New Delhi
18.	Light cycler-480 machine	Roche Diagnostics, Germany

3.2 Methodology

3.2.1 *In silico study*

3.2.1 Screening of compounds through *in silico* tools

The compounds were screened by 50% structure similarity with the previously reported PHD-2 activator R59949 [35] and KRH102140 [36] from the zinc and asinex database using Maestro (version 9.3, Schrödinger, LLC New York, NY, 2012) [92].

3.2.2 Anticancer potential screening of compounds through CDRUG server

One thousand three hundred fifty five hits were retrieved through structural similarity search, were further screened for their anticancer potential with CDRUG web server [86]. The CDRUG screening retrieved BBAP-1 (2-[4-(difluoromethoxy) phenyl]-1, 2, 3, 4-tetrahydroquinazolin-4-one) and BBAP-2 (4-[7-(acetyloxy)-2-ethyl-2H-chromen-3-yl]) phenyl acetate as a highly possible anti-cancer compound.

3.2.3 Protein ligand interaction and toxicity prediction

The BBAP-1 and BBAP-2 were docked with PHD-2 enzyme (PDB id-2G19) using Autodock 4.2 [87]. The toxicity profile was estimated through TEST [88].

3.2.4 Metabolic profiling of BBAP-1 and BBAP-2

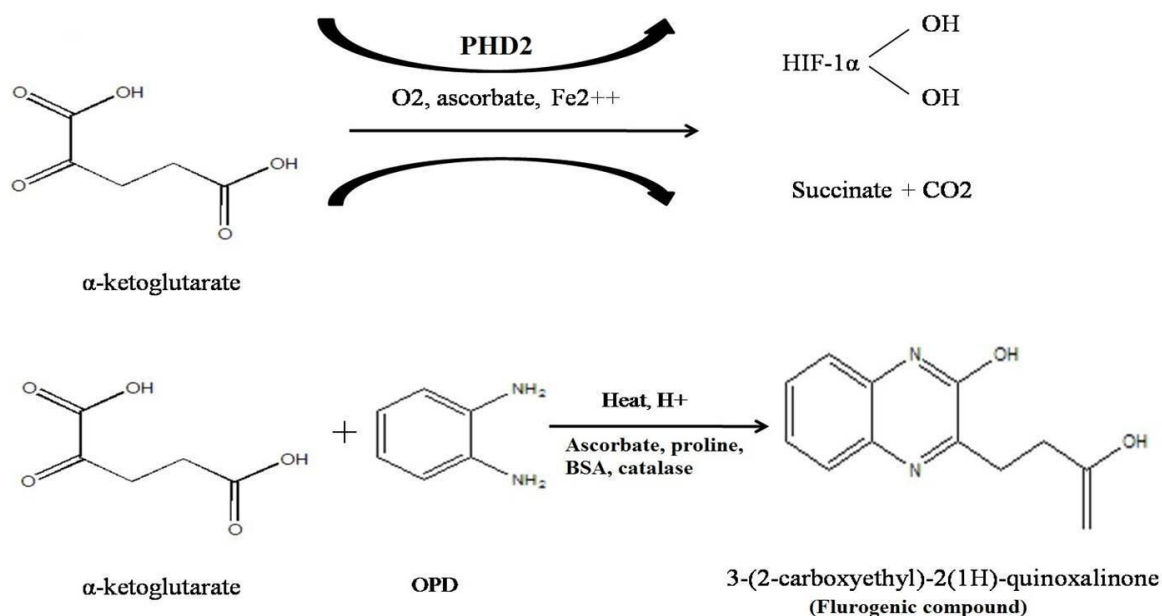
The metabolic profile of BBAP-1 and BBAP-2 was evaluated by using Metaprint2D [89]. The BBAP-1 and BBAP-2 were further screened for the type of isoform CYP450 involved in its metabolism using WhichCyp web service tool [90].

3.2.5 2-OG dependent PHD-2 activation assay

The effect of BBAP-1 and BBAP-2 on PHD-2 activity was scrutinized through fluorescence-based assay. The serum sample from a separate group of control animals was collected and homogenized in five volumes of 0.25 M sucrose containing HEPES buffer (50mM, pH 7.0). The homogenizing medium also contained PMSF (50µg/ml), dithiothreitol (DTT) (10^{-4} M), EDTA (10^{-5} M) and Triton X-100 (0.1%). The

homogenates were centrifuged at 14,000 rpm for 10 min and the supernatants were used for enzyme activation. Activation of PHD-2 was done as follows: 100 μ l of the supernatant was incubated with proline (1mM), sodium ascorbate (1mM), BSA (0.2%), catalase (0.04%) and 2-OG (0.1mM) in a total volume of 1ml. After incubation for 3 h at 30°C, 100 μ l of this mixture was assayed for PHD-2 activity [92]. The reaction was stopped after 5 min by addition of 100 μ l, 0.5 M HCl. Subsequently, derivatization was achieved by the addition of 50 μ l, 10mg/ml of o-phenylenediamine (OPD) in 0.5 M HCl and heated for 10 min at 95°C. After the centrifugation for 5 min, the supernatant (100 μ l) was made basic by the addition of 60 μ l of 1.25M NaOH and fluorescence was measured with excitation filter 340 nm and emission filter at 420 nm [93]. The assay was divided into four groups: control (serum), inhibitor [serum + cobalt (inhibitor)], activator 1 [serum + BBAP-1] and activator 2 [serum + BBAP-2]. The related PHD-2 activity of the cobalt, BBAP-1 and BBAP-2 was calculated considering 100% activity in the control samples.

Figure 5: Principle of *in vitro* PHD-2 assay



3.3 *In vitro* studies

3.3.1 *Cell line and culture condition*

ER+ MCF-7 cells were cultured and routinely maintained in RPMI 1640 medium supplemented with 10% heat-inactivated FBS, penicillin (100 units/ml), streptomycin (100µg/ml), gentamycin (0.25µg/ml) and were incubated at 37°C in a humidified atmosphere containing 5% CO₂ inside a CO₂ incubator. Single cell suspensions were obtained by trypsinization (0.05%trypsin/EDTA) and cells were counted using a hemocytometer [94].

3.3.2 *Cytotoxicity study using MTT*

ER+MCF-7 cells (1×10^5) were seeded in 96- well sterile plates and treated with different concentrations of BBAP-1 and BBAP-2 (1µM, 5µM, 10µM, 15µM, 20µM, 25µM) for 24h, against control and standard treated cells (tamoxifen) respectively. Subsequently, after treatment for 24 h, the media from upper layer was removed and incubated with 20µl MTT (5mg/ml) and 100µl of fresh media for 2h, then 1% DMSO was added to solubilize the formazan crystals. After 30 min incubation, the absorbance of the colour solution was quantified by measuring at a wavelength of 570 nm using micro plate reader (Reader type: Model 680 XR Bio-Rad laboratories inc). The IC₅₀ and ½ IC₅₀ values of BBAP-1 and BBAP-2 against ER+MCF-7 cells were determined after 24 h [95].

3.3.3 *Morphological evaluation for apoptosis using AO/EtBr dual staining*

AO/EtBr staining was carried out to identify morphological evidence of apoptosis. ER+MCF-7 cells were treated with the IC₅₀ value of BBAP-1 and BBAP-2 for 24 h. The cells were washed with phosphate buffer saline (PBS) (pH 7.4) and 10µl of AO/EtBr solution (100µg/ml of AO and 100µg/ml of EtBr) and made up to 100µl

using PBS and incubated for 5 min. The cells were again washed with PBS and examined under an inverted fluorescence microscope (Nikon Leica M165 FC) [96].

3.3.4 Effect of BBAP-1 and BBAP-2 on mitochondrial membrane potential

ER+MCF-7 cells were seeded at a density of 500,000 cells in a 25 cm² culture flask and incubated overnight. The cells were then treated with IC₅₀ dose of BBAP-1 and BBAP-2. After 24 and 48 h, 200µl of JC-1 staining solution (1:10 dilution in culture medium) was added to each 1 ml of culture medium and incubated for 15 min at 37°C in a CO₂ incubator. Subsequently, the cells were trypsinized and collected by centrifugation at 10,000 rpm for 5 min. The cells were washed twice with 1ml of assay buffer. Finally, 500µl of assay buffer was added to the cell pellet in each tube and re-suspended well. After incubation for 20 min, cells were washed three times with PBS and imaged using an inverted fluorescence microscope (Nikon Leica M165 FC) [97].

3.3.5 Cell cycle analysis using PI staining

1x10⁶ cells were treated with BBAP-1 (IC₅₀ dose and ½ IC₅₀ dose) and BBAP-2 (individual IC₅₀ dose) for 18 h. Cells were washed with PBS, fixed with methanol and kept at -20 °C for 3 min. Subsequently, cells were suspended in cold PBS and kept at 4 °C for 90 min. Cells were pellet down, dissolved in PBS, treated with RNase for 30 min at 37 °C. Subsequently cells were stained with PI and kept in the dark for 15 min. Cell cycle phase distribution of nuclear DNA was determined on FACS (BD Influx cell sorter), fluorescence detector equipped with 488 nm argon laser light source and 623 nm band pass filter (linear scale) using BD FAX Software 1.2.0.87 [98].

3.4 *In vivo* evaluation

3.4.1 *Experimental animals and treatment schedule*

Thirty-two female albino wistar rats (100-120g) were divided into four groups of eight animals each. The animals were subjected to the treatment as: Group I (normal control, 0.9% normal saline ml/kg, p.o.), Group II (toxic control, MNU 8 mg/kg, i.v.), Group III (BBAP-1, 56.62 µg/kg, s.c. + MNU 8 mg/kg, i.v.) and Group IV (BBAP-1, 113.25 µg/kg, s.c. + MNU 8 mg/kg, i.v.). The animal dose of BBAP-1 was calculated with the help of IC₅₀ dose of BBAP-1 and tamoxifen. MNU was administered on day 1st and 31st followed by daily administration of BBAP-1 upto 38th day of the study. The hemodynamic profiling of animals was perceived through electrocardiogram (ECG) and heart rate variability (HRV) recording on the 39th day. The animals were anesthetized using light chloroform to collect serum and subsequently sacrificed through cervical dislocation to obtain 4th mammary gland tissue. The animals were procured from central animal house facility and fed with standard laboratory chow diet and water *ad libitum*. All the experimental procedures were approved by the Institutional Animal Ethics Committee (UIP/IAEC/2014/FEB/16) and were performed as per the guidelines laid by Department of Animal Welfare, Government of India.

3.4.2 *Hemodynamic changes*

The animals were anesthetized on 39th day of the study by using the combination of ketamine hydrochloride (50 mg/kg, i.m.) and diazepam (2.5 mg/kg, i.m.) and mounted on a wax tray. The platinum hook electrodes were placed on the skin of the dorsal and ventral thorax to record the ECG signal. The electrodes were connected to Bio-amplifier (ML-136) and channel power lab (ML-826) to convert analogue to digital

signals (AD Instruments, Australia). The ECG signals were saved on the hard disk and analyzed offline using Lab Chart Pro-8 (AD Instruments, Australia).

HRV analysis was conducted on multiple segments of continuous ECG signals. Firstly, all the raw signals were inspected manually to ensure that all the R-waves were detected correctly. Subsequently, heart rate (HR) was calculated by plotting the number of R waves per unit time. Following the same, time and frequency domain parameters of HRV were also calculated using the Lab Chart Pro-8 (AD Instruments, Australia) [99].

3.4.3 Morphological evaluation of tissues using carmine staining, histopathology, and SEM

3.4.3.1 Carmine staining of whole mounts mammary gland

The mammary glands obtained from female albino wistar rats were stretched onto a slide and placed in a fixative solution (60:30:10 ratio of ethanol: chloroform: acetic acid), stained with a carmine solution for 2 days, washed with 90%, 70%, 35% and 15% ethyl alcohol for 1h respectively and lastly rinsed with distilled water for 3 times at 5 min interval. The tissue sample was dehydrated in ascending grades of alcohol and dipped in xylene at least for two days. For the preparation of carmine alum stain; 1gm carmine and 2.5gm aluminum potassium sulfate in 450ml distilled water was boiled for 20 min. The final volume was adjusted to 500ml with distilled water. Whole mounts were examined under the 4X microscope and evaluated for the number of alveolar buds (ABs). Mammary gland differentiation (DF) was determined by scoring the number of ABs type 1 and type 2. The score values (0–5) from AB1 and AB2 were added for a final DF score (0–10). The average rating values (0–5) from AB1 and AB2 were added to the lobule score values (0–5) for a final differentiation score (0–10) [100, 101].

3.4.3.2 Histopathology of mammary gland tissue

A small portion of the mammary gland was fixed overnight in 10% neutral buffered formalin and processed into paraffin blocks. The tissues were cut into 5µm sections by using microtome and stained with hematoxylin and eosin (H&E). The sections were visualized and photographed at 40X using a digital biological microscope (N120, BR-Biochem Life Sciences, New Delhi, India [102]).

3.4.3.3 Surface texture analysis through SEM

The HCl-collagenase and enzymatic digestion methods were used for the purpose of SEM. Small sections of mammary glands were treated with HBSS containing 100µg/ml collagenase (type IV) and 2.5 TRU (turbidity reduction unit)/ml of hyaluronidase for 30min at 37°C. After digestion, the tissues were rinsed in the balanced solution and then fixed in 4% glutaraldehyde in 0.1 M cacodylate/HCl buffer (pH 7.2) at room temperature for 3h and then placed in 8 N HCl for 30 min at 60°C. After HCl digestion, the tissues were rinsed three times with distilled water to remove the acid. The samples were dried with 70%, 80%, 90%, and 100% acetone. All the specimens were dehydrated, dried by the critical point method and examined under SEM (JEOL JSM-6490LV) [103, 104].

3.4.4 Antioxidants markers

The mammary gland tissues (10 % w/v) were homogenized in 0.15 M KCl and centrifuged at 10,000 rpm. The supernatants were evaluated for oxidative stress markers, including thiobarbituric acid reactive substances (TBARs), superoxide dismutase (SOD), catalase, glutathione (GSH) and protein carbonyl (PC) using the methods established in our laboratory [105, 106].

3.4.5 Evaluation of caspase 3 and caspase 8

Caspase 3 and caspase 8 were evaluated using the commercial kits. In casapase 3, DEVD-AFC synthetic substrate was used and in caspase 8, IETD-AFC synthetic substrate was used. The assay was carried out in a 96-well plate. Equal volumes of the serum sample from both control and experimental animals were diluted with reaction buffer and DTT was added to a final concentration of 10mM. To the reactant mixture, 5 μ l of IETD-AFC/DEVD-AFC substrate was added and incubated for 1 h at 37°C. Free AFC levels formed were measured in a plate reader with a 400 nm excitation and a 505 nm emission. The results were expressed as fluorescence units/mg of protein [107].

3.4.6 Western blotting

Protein samples were prepared from the mammary gland tissue through acetone precipitation and quantified using the Bradford reagent [108]. SDS-PAGE analysis was performed following the principles of Laemmli with slight modifications [109]. Briefly, protein samples were mixed with sample buffer (125mM Tris-HCl, pH6.8; 20% glycerol; 4% SDS; 0.05% bromophenol blue; 10% 2-mecaptoethanol). A 30 μ g of protein sample was allowed to resolve through 12% polyacrylamide gel using SDS-PAGE (GX-SCZ2, Genetix Biotech Asia Pvt. Ltd, New Delhi). The proteins as resolved by SDS-PAGE were transferred to a PVDF membrane (IPVH 00010 Millipore, Bedford, MA USA) using semidry transfer (GX-ZY3, Genetix Biotech Asia Pvt. Ltd, New Delhi). Subsequently, membrane was blocked with 3% BSA and 3% not fat milk in TBST for 3h and incubated overnight with primary antibody against Bcl-xl (MA-5-15142), Bcl-2 (SC-7382), BAX (SC-23959),VDAC (SC-390996), cytochrome c (SC-13561), Apaf-1 (SC-65891), procaspase 9 (SC-73548), NF κ Bp65 (MA5-1616), UCHL-1 (MA1-83428), PHD-2 (SC-67030), HIF-1 α (SC-

13515), FASN (SC-55580) and SREBP-1c (SC-13551). β -actin (MA5-15739-HRP) was used as a standard reference. The membrane was washed with TBST thrice and incubated with the corresponding anti-rabbit (SC-2030), anti-goat (SC-2020) and anti-mouse (31430, Pierce Thermo Scientific, USA) HRP conjugated secondary antibody (1:5000 dilutions) at room temperature for 3h. The signals were detected using an enhanced chemiluminescence substrate (Western Bright ECL HRP substrate, Advansta, Melanopark, California, US). The quantification of protein was done through densitometric digital analysis of protein bands using Image J software [110].

3.4.7 qRT-PCR

Primers for real time were designed online using primer quest tool from the IDT DNA Technologies website (www.idtdna.com). The amplicon size was kept between 100 to 200 base pairs; GC% was held above 50% and melting temperature was maintained between 58°C to 62°C. The specific sequences of the forward and reverse primers are specified in table 2.

Total RNA was extracted from mammary gland tissue using trizol reagent (Invitrogen, Life Technologies) according to the manufacturer's instructions. Briefly, tissues were washed off treatment plates using 0.1% DEPC water. The tissues were crushed in 250 μ l trizol reagent using micro pestles. Another 750 μ l of trizol reagent was added to make the final volume to 1ml, followed by addition of 200 μ l of chloroform and mixing for 2 to 5 min on a vortex mixer. The suspension was then centrifuged at 14,000rpm, 4°C for 15 min and upper aqueous phase was gently pipette out in the fresh vials. RNA was precipitated by addition of 500 μ l chilled isopropanol. The vials were kept at room temperature for 10 min and were centrifuged at 14,000 rpm, 4°C for 10 min and RNA pellet so obtained was washed twice with 75% ethanol (chilled) at 7,500 rpm, 4°C for 5 min. The RNA pellet was finally dissolved in 15 μ l of

0.1% DEPC water. To quantify RNA, absorbance was read using Nanodrop (Qua Well Q5000). cDNA synthesis was done from 1µg of total mammary gland RNA in a 96 well thermal cycler (BioRad, C1000) with steps including, incubation at 25°C for 10 min, 37°C for 120 min, 85°C for 5 min and 4°C forever RNA using high capacity cDNA Synthesis Kit (Applied Biosystems). cDNA sample was quantified using Nanodrop and was stored at -80°C until use. 125ng of cDNA was used as a template for each reaction of qRT-PCR with β-actin as housekeeping control using light cycler 480 machine (Roche Diagnostics, Germany). For each primer pair, a melting curve analysis was performed according to the instrument. The program in brief was an initial incubation of 50°C for 2 min hold (UDG incubation) and 95°C for 10 min followed by 40 cycles at 95°C for 15 s (denaturation), 58°C for 30 s (annealing) and final extension at 72°C for 20 s. Differential expression was calculated by the 2- $\Delta\Delta$ CT method. β-actin was used as internal control and used to normalize ratios between samples [111, 112].

3.5 Statistical analysis

All data were presented as mean \pm SD and analyzed by one-way ANOVA followed by Bonferroni test and for the possible significance identification between the various groups. ($p < 0.05^*$), ($p < 0.01^{**}$), ($p < 0.001^{***}$) were considered as statistically significant. Statistical analysis was performed using Graph Pad Prism software (5.02).

Table 2: Sequence of forward and reverse primers used for qRT-PCR

Primer	Sequence
Bcl2 F	GTGGATGACTGAGTACCTGAAC
Bcl2 R	GAGACAGCCAGGAGAAATCAA
Bcl-x1 F	CCCTCGTATCTGGAAGCCAC
Bcl-x1-R	CAGCGGAGACCTCGTTTTCT
BAX F	TGCTACAGGGTTTCATCCAG
BAX R	GACACTCGCTCAGCTTCTT
VDAC F	GGAGTTTGGTGGCTCCATTTA
VDAC R	GACCTGATACTTGGCTGCTATTC
Cytochrome-c F	TCCATTTCCTTCCTTGGGC
Cytochrome-c R	ATCGGGGCTGTCCAACAAAA
Apaf-1F	GAACATAGACTCCCGGGTAAAG
Apaf-1R	CTTGTCTCCAGACCCTTATTG
Procaspase9F	GGCTCTCTGGCTTCATTCTT
Procaspase9R	GGGTCCAGCTTCACTACTTTC
PHD-2 F	ACGCAGTTCATACCCAGTTAG
PHD-2 R	CCTGTCCACTCTCAGCTTTAC
HIF1- α F	GATGGGTATGAGCCAGAAGAA
HIF1- α R	CTGTGGTGACTTGTCTTTAGT
FASN F	GGCGAGTCTATGCCACTATTC
FASN R	GCTGATACAGAGAACGGATGAG
SREBP-1cF	TCCGAGTTCAGGTAGGGTT
SREBP-1cR	CTTGGCGCACACCAAATACC
UCLH-1 F	CGCTCTGCCCTGAGTTATT
UCLH-1 R	CCGTCTGGGTCAATCCTCTG
NF κ Bp65 F	GGGCTACGAAGTCAAACCCA
NF κ Bp65 R	TTCTCCTCAATCCGGTGACG
β -actin F	TGCAGGATCGTGAGGAACAC
β -actin R	AGCGTGATTGTAACGCCTGA

CHAPTER 4
RESULTS AND
DISCUSSION

4. Results

4.1 Virtual screening

Twenty eight thousand compounds were retrieved from Zinc and Asinex database by 50% structure similarity with the previously reported PHD-2 activators R59949 and KRH102140. One thousand three hundred fifty five hits were retrieved after the docking with PHD-2 enzyme (PDB id-2G19) and screened through filters like ADME, Lipinski and reactive group filter using the Maestro version 9.3 (Maestro, version 9.3, Schrödinger, LLC, New York, NY, 2012) (Figure 6A and B). The compounds were estimated for their possibility of being anticancer by CDRUG web server and two compounds BBAP-1 (2-[4-(difluoromethoxy) phenyl]-1, 2, 3, 4-tetrahydroquinazolin-4-one) and BBAP-2 (4-[7-(acetyloxy)-2-ethyl-2H-chromen-3-yl] phenyl acetate) were found as an anti-cancerous agent. The BBAP-1 and BBAP-2 were further docked with PHD-2 (PDB id-2G19) enzyme using software Autodock 4.2 and the binding energy was found be -3.97 and -3.33Kcal/mol. The predicted oral rat LD50 value of BBAP-1 was observed to be 2802.36 mg/kg and for BBAP-2 was 935.58mg/kg using TEST. BBAP-1 and BBAP-2 were also noted to be non-mutagenic (Figure 6A and B). The virtual screening, toxicity profiling with subsequent *in silico* docking studies, revealed BBAP-1 and BBAP-2 as a potential lead molecule for further evaluations.

In silico metabolic profiling of BBAP-1 revealed 6th, 10th, 19th and 20th carbon positions as a major site for metabolism through hydroxylation whereas the metabolic positions of BBAP-2 were 11th, 12th, 21st and 22nd carbon positions as major site for metabolism through 12 and 22-dealkylation and 11 and 21-ester hydrolysis. For BBAP-1; CYP2C9, CYP2C19, and CYP1A2 were observed to be the major cytochrome P450 enzymes in hydroxylation whereas for BBAP-2; CYP3A4 and

CYP2D6 were the major cytochrome P450 enzymes involved in their metabolism (Figure 7A and B).

Flow diagram for screening of compounds

Approximately 28000 compounds were screened from Zinc database and Asinex database from Maestro version 9.3 (Schrödinger) on the basis of 50% structural similarity with R59949 and KRH102140



Compounds were docked with PHD-2 enzyme (PDB id-2G19) using Autodock 4.2 and various filters were applied like ADME, Lipinski and reactive group filter.



1355 hits were found and further screened with CDRUG web server for anti-cancer potential. Two compounds, BBAP-1 and BBAP-2 were selected for on the basis of CDRUG result and estimated through TEST.



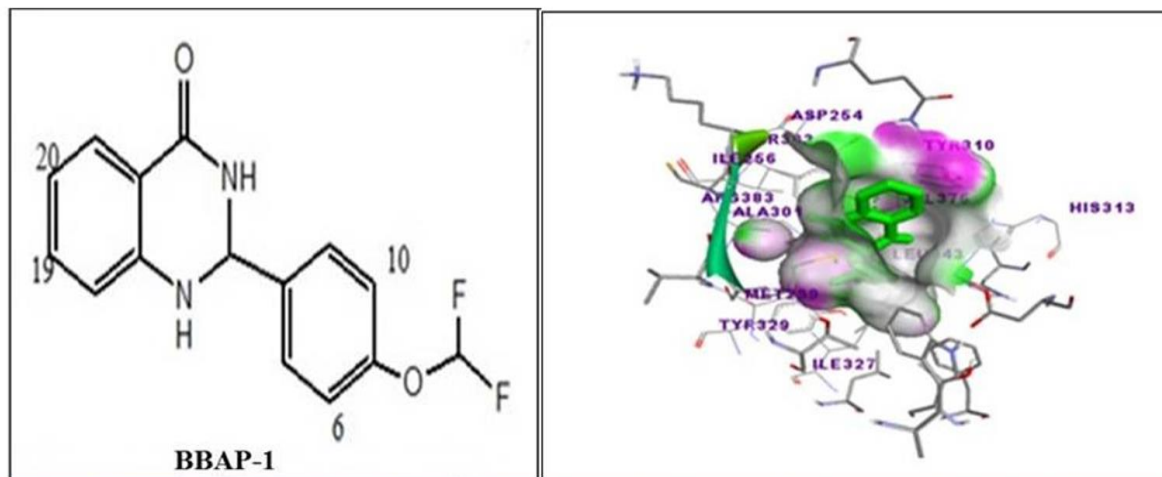
Both the compounds were evaluated against ER+MCF-7 cells using experiments like MTT assay, AO/EtBr staining, JC-1 staining along with cell cycle analysis.



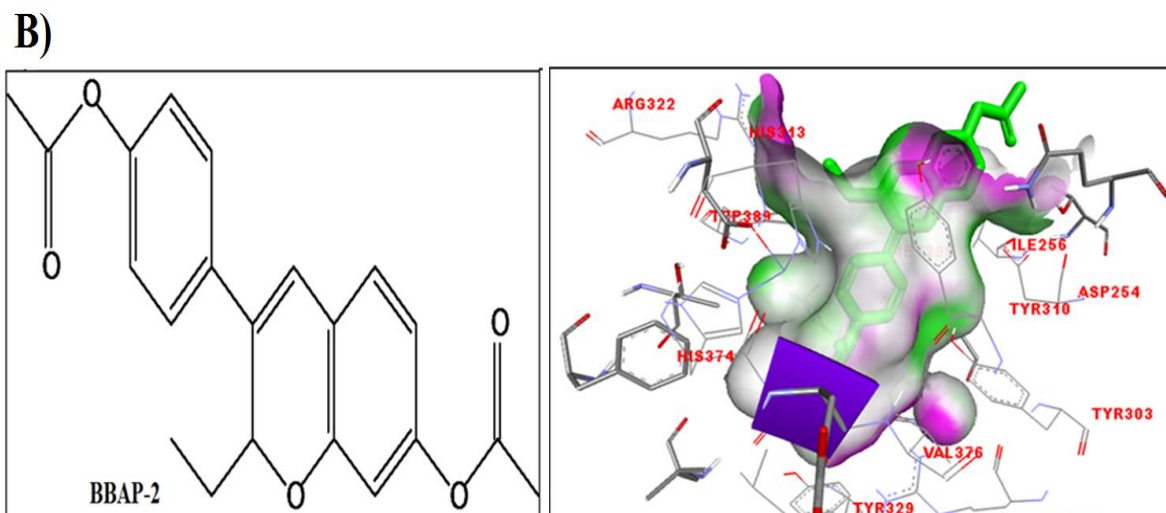
Only BBAP-1 was further evaluated against MNU induced mammary gland model.

Figure 6 (A and B): *In silico* binding efficacy and toxicity profiling of BBAP-1 and BBAP-2

A)



Binding energy				Hydrogen bond				Amino acid			
-3.97				UNK 0:H1 and ARG 322:HH12 1				LEU 343, VAL 376, TYR 303, HIS 374, TYR 310, MET 299, TRP 389, ASP 315, ARG 322			
Oral rat LD ₅₀				Developmental toxicity				Mutagenicity value			
Oral rat LD50-log10 (mol/kg)		Oral rat LD 50 mg/kg		Developmental toxicity value		Developmental toxicity result		Mutagenicity value		Mutagenicity result	
Expected value	Predicted value	Expected value	Predicted value	Expected value	Predicted value	Expected value	Predicted value	Expected value	Predicted value	Expected value	Predicted value
N/A	2.02	N/A	2802.36	N/A	1.00	N/A	toxicant	N/A	0.46	N/A	negative

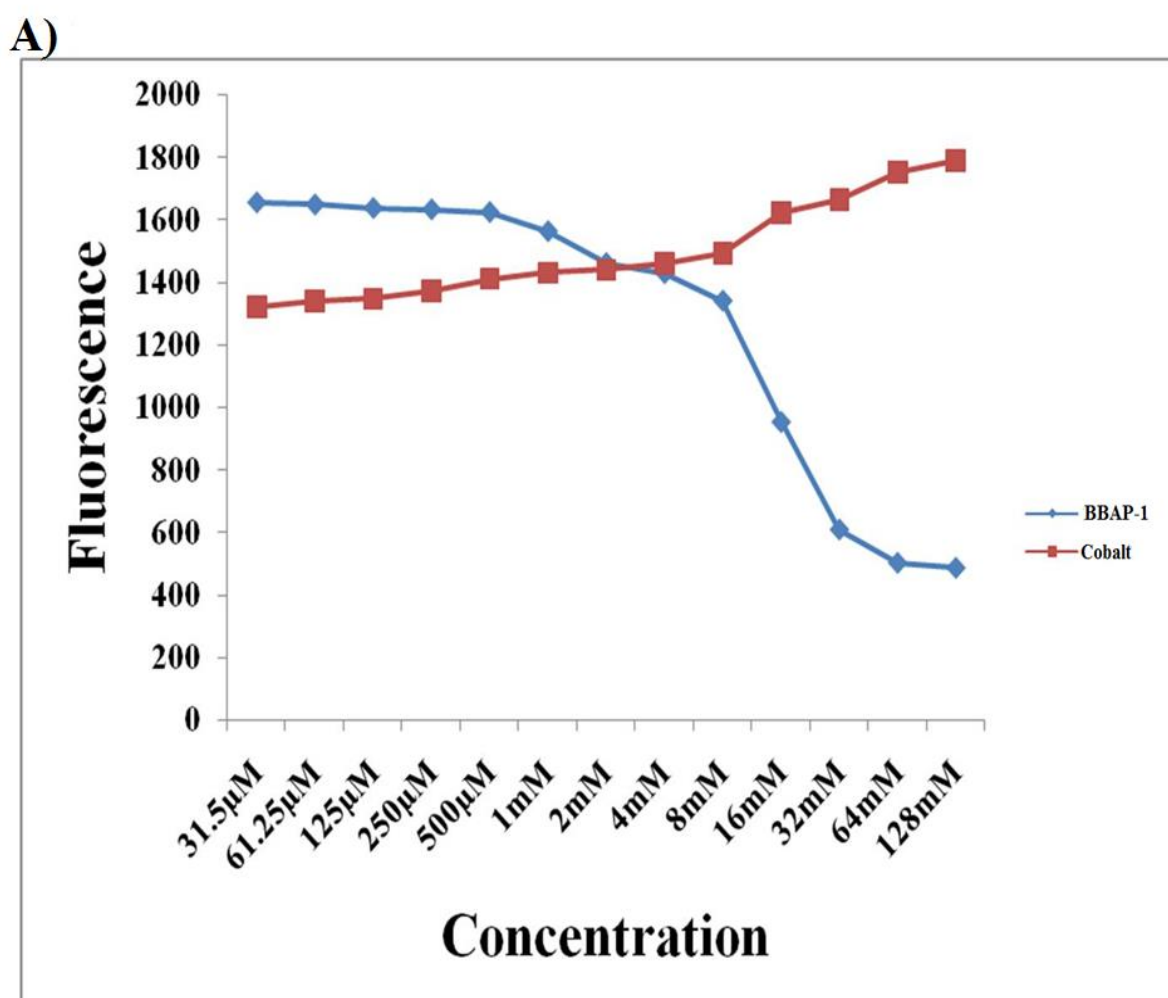


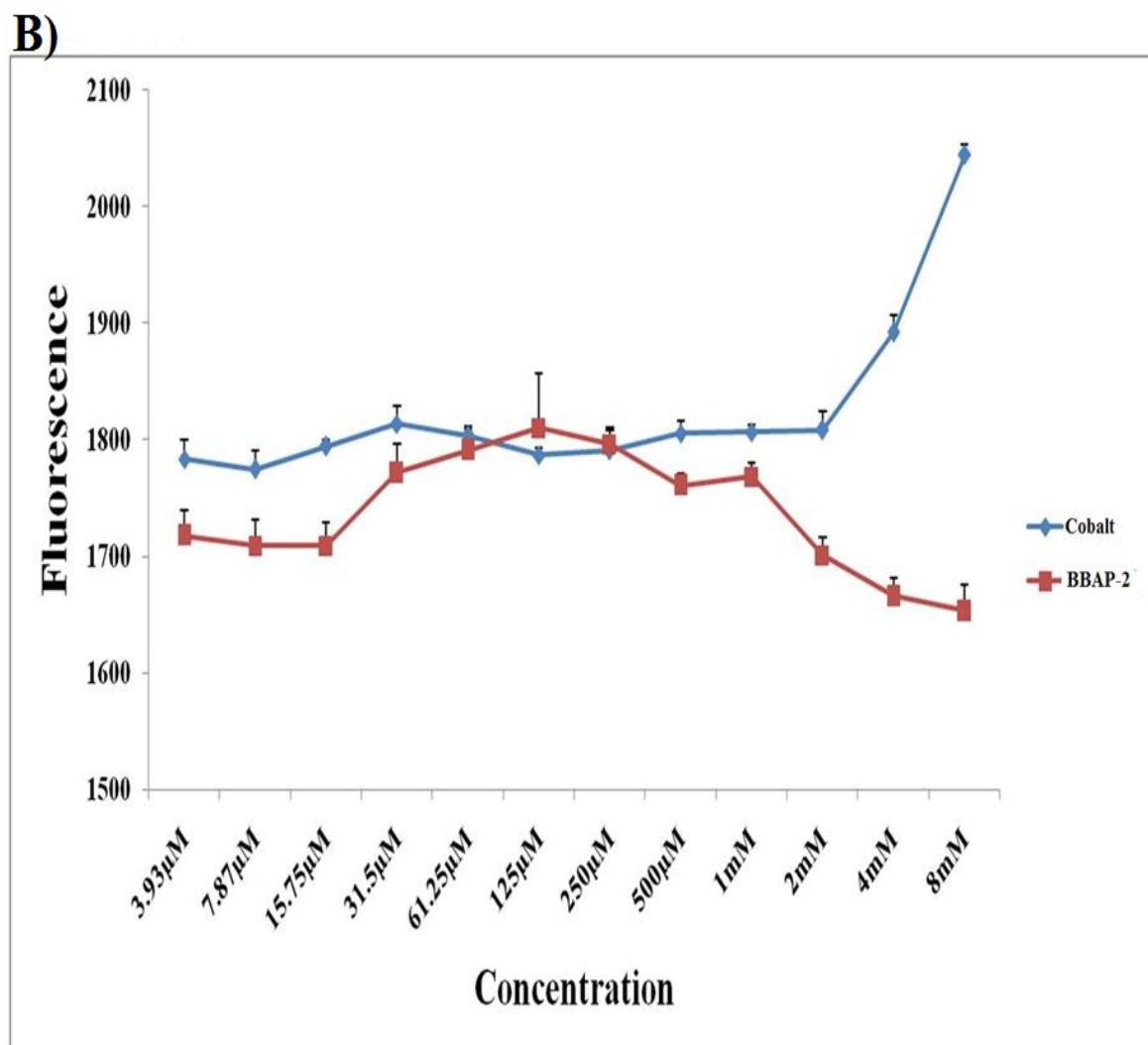
Binding Energy		Hydrogen Bond		Amino Acid							
-3.33		No hydrogen bond		ARG 322,HIS 313,TRP 389,HIS 374, TYR 329, VAL 376, TYR 303, TYR 310, ASP 254, ILE 256, MET 299							
Oral LD50				Developmental Toxicity				Mutagenicity value			
Oral rat LD50-log10 (mol/kg)		Oral rat LD 50 mg/kg		Developmental Toxicity value		Developmental Toxicity result		Mutagenicity value		Mutagenicity result	
Expected value	Predicted value	Expected value	Predicted value	Expected value	Predicted value	Expected value	Predicted value	Expected value	Predicted value	Expected value	Predicted value
N/A	2.58	N/A	935.58	N/A	0.95	N/A	toxicant	N/A	0.04	N/A	Negative

4.2 2-OG dependent PHD-2 activation assay

In vitro PHD-2 assay revealed that in the case of inhibitor (cobalt), the amount of 2-OG was increased which represents the decreased PHD-2 activity. On the other side, in the event of activator (BBAP-1 and BBAP-2), the quantity of 2-OG was reduced suggesting increased PHD-2 activity (Figure 8A and B).

Figure 8 (A and B): Effect of BBAP-1, BBAP-2 and cobalt upon *in vitro* PHD-2 activity



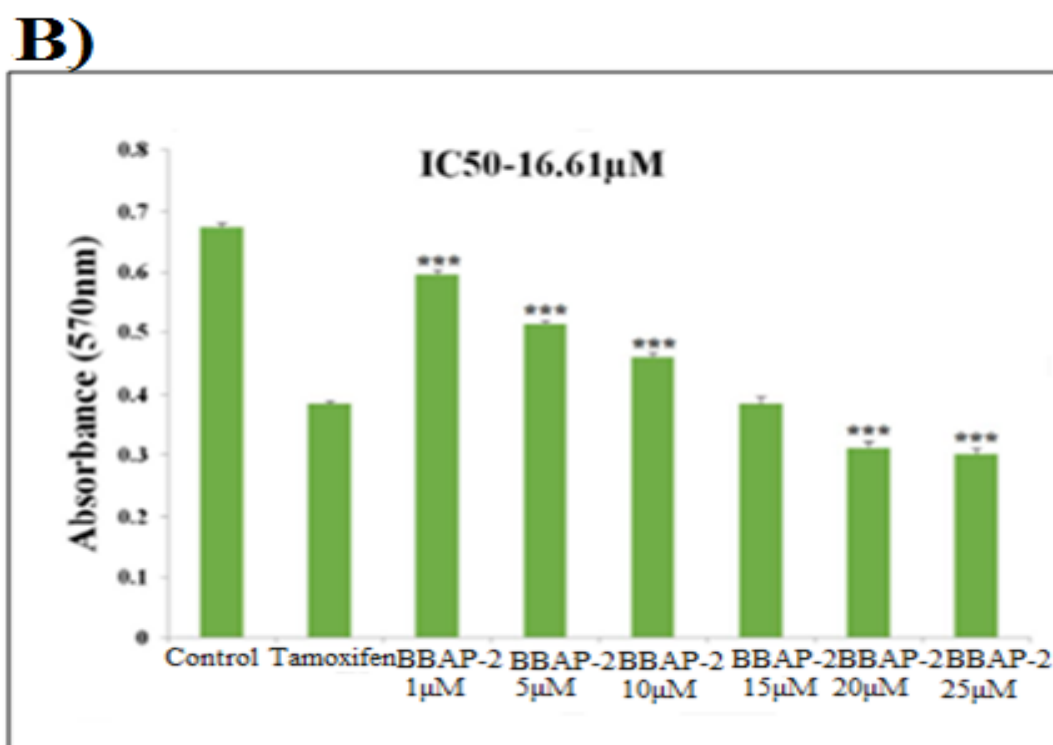
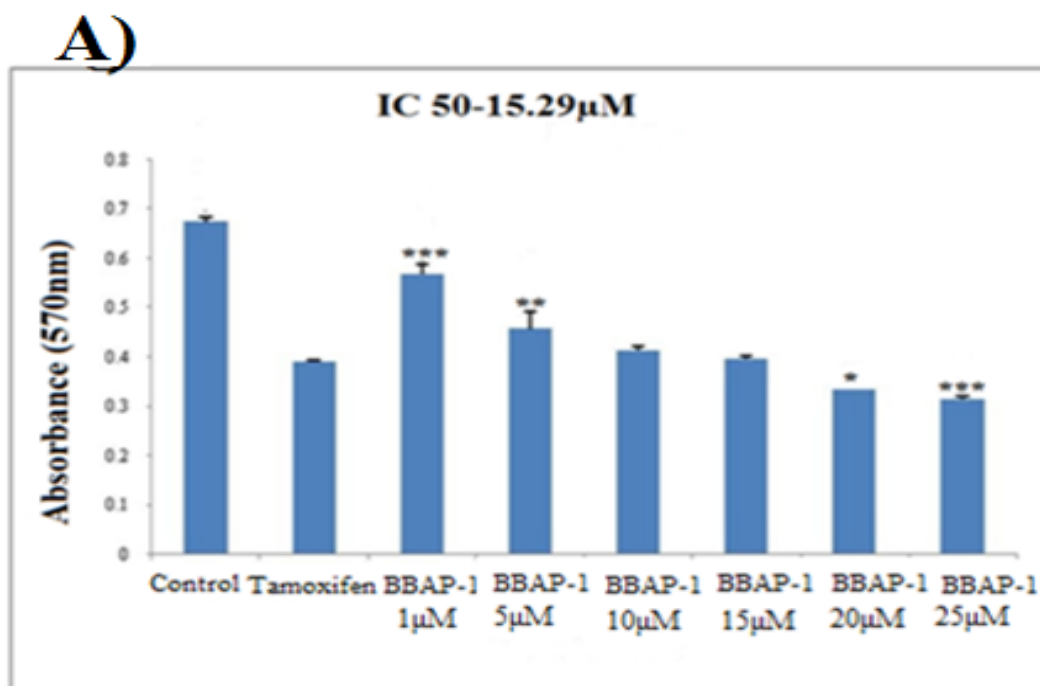


4.3 *In vitro* study

4.3.1 Cytotoxicity study using MTT

BBAP-1 and BBAP-2 at concentrations of 1µM, 5µM, 10µM, 15µM, 20µM and 25µM significantly inhibited the growth of ER+ MCF-7 cells compared with that of the control cells. The IC₅₀ value of BBAP-1 and BBAP-2 were recorded to be 15.29µM and 16.61µM respectively against ER+MCF-7 cells (Figure 9A and B).

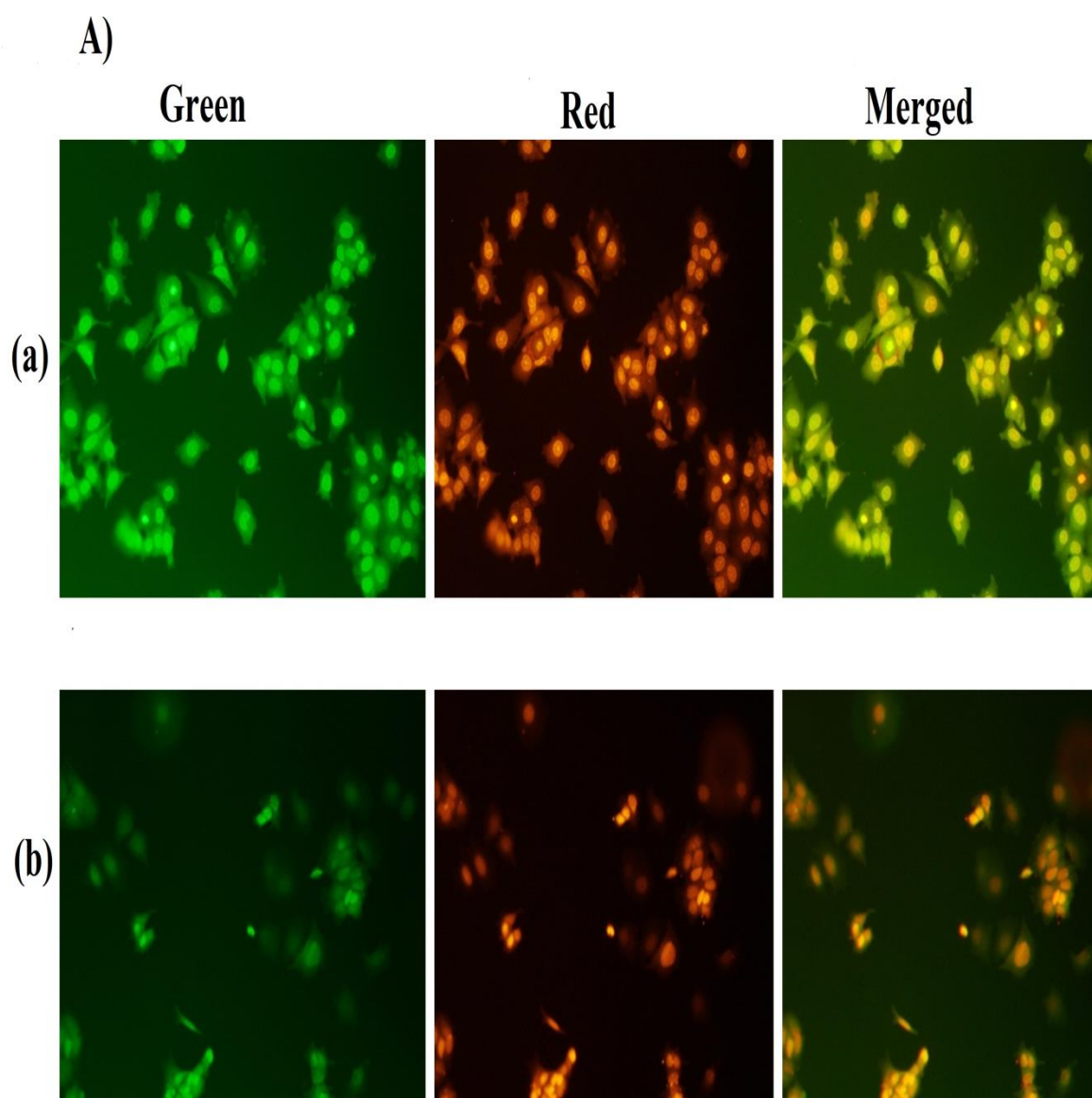
Figure 9 (A and B): Effect of BBAP-1 and BBAP-2 upon MTT assay

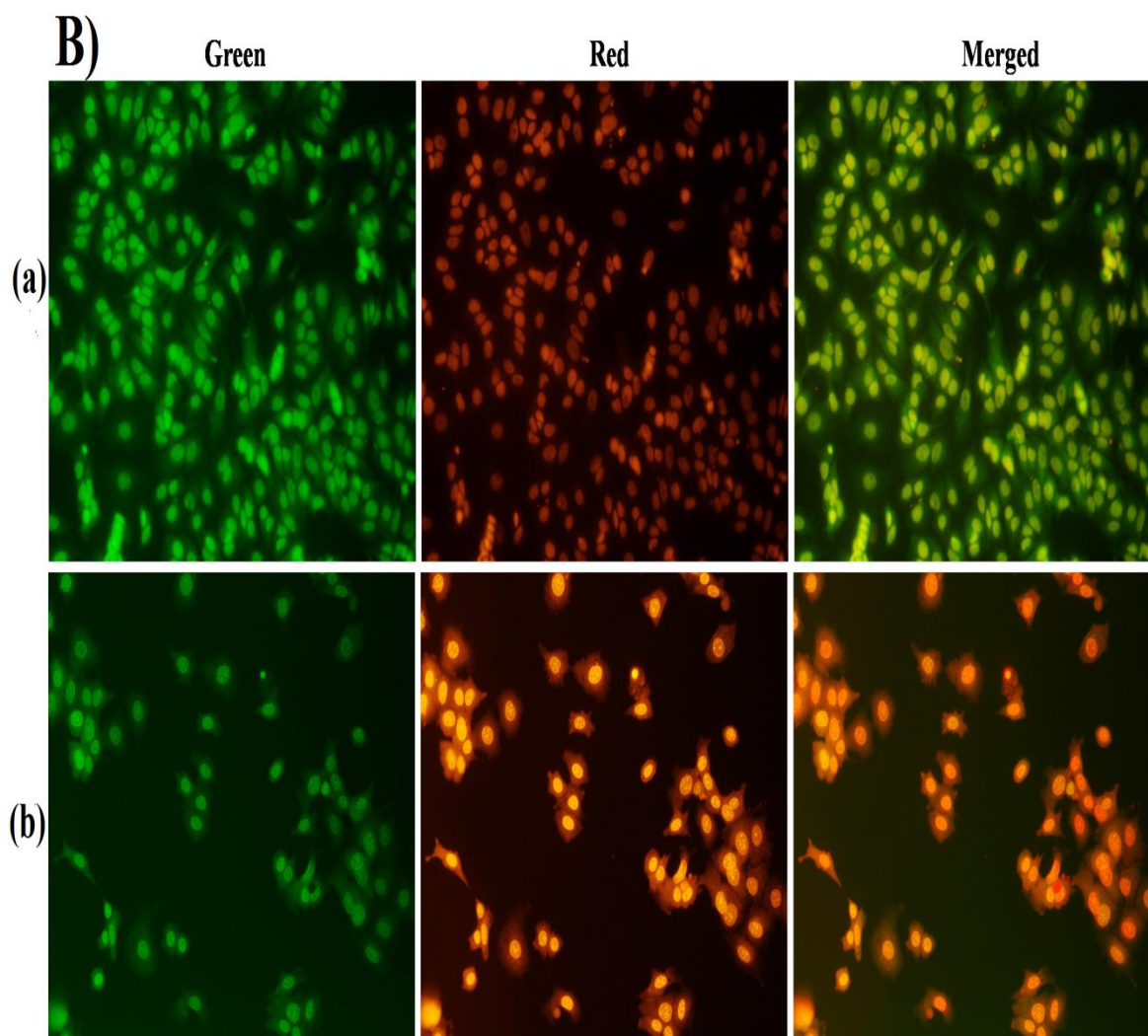


4.3.2 Morphological evaluation for apoptosis using AO/EtBr staining

An array of nuclear changes including chromatin condensation, apoptotic body formation, membrane blebbing and dotted nuclei were observed after BBAP-1 and BBAP-2 treatment through AO/EtBr staining that are indicative of apoptosis (Figure 10A and B).

Figure 10 (A and B): Effect of BBAP-1 and BBAP-2 upon morphological symptoms of apoptosis

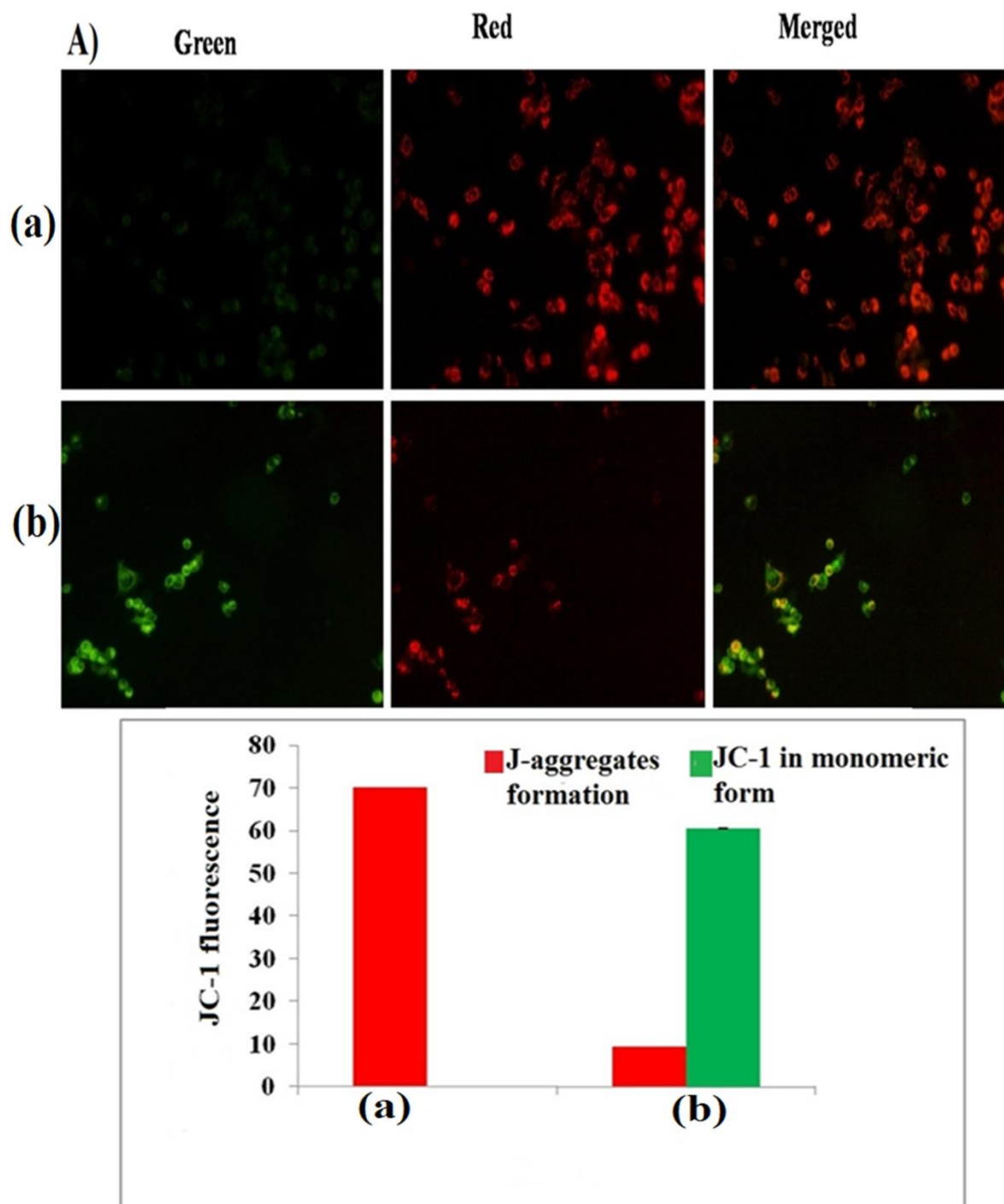


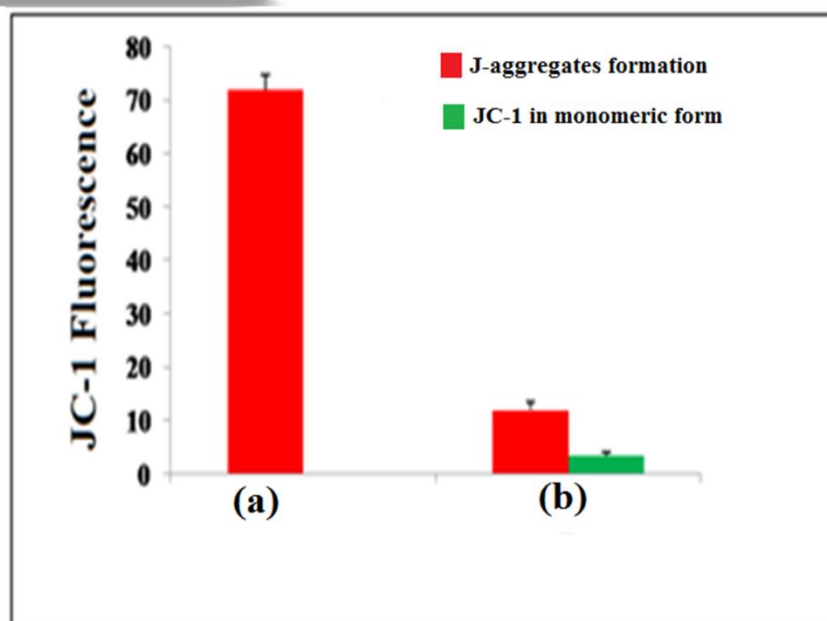
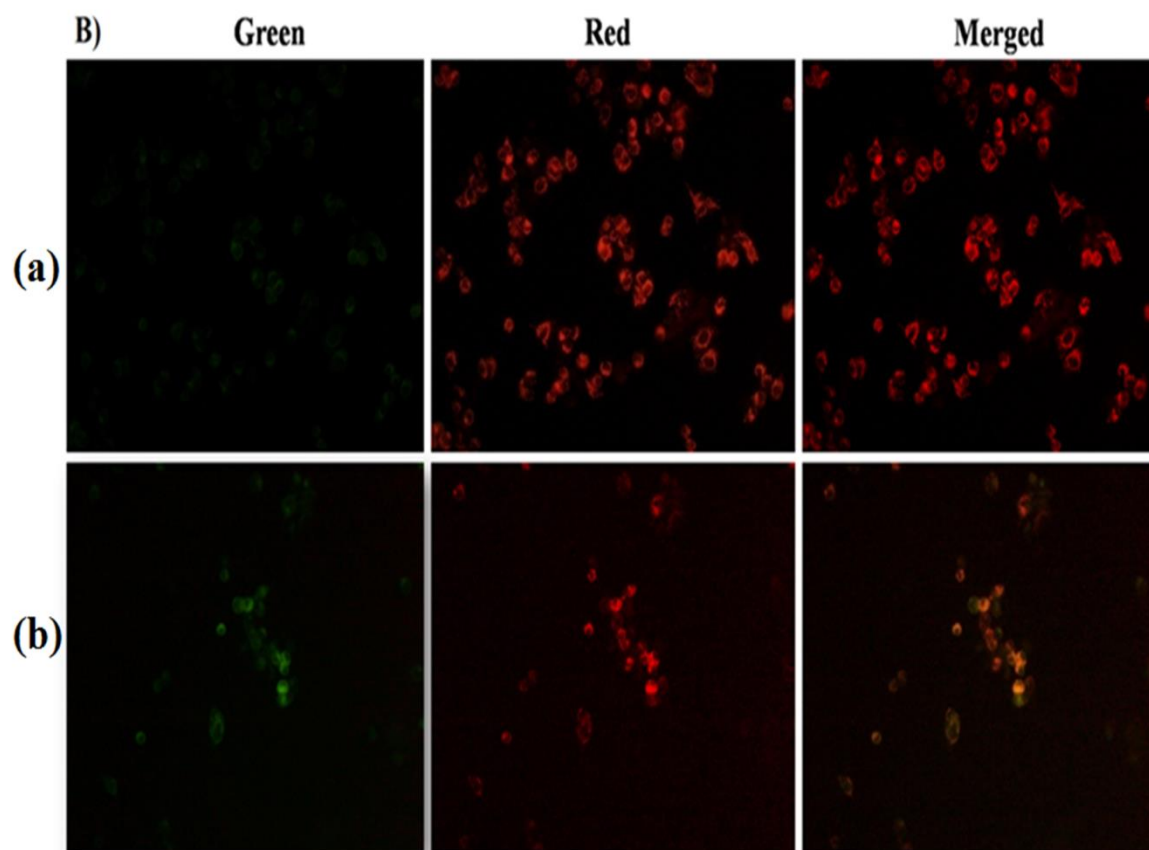


4.3.3 Effect of BBAP-1 and BBAP-2 on mitochondrial membrane potential

JC-1 is a cationic dye that exhibits potential-dependent accumulation in mitochondria, indicated by a fluorescence emission shift from green (~525 nm) to orange (~590 nm). Consequently, mitochondrial depolarization is indicated by an increase in the orange/green fluorescence intensity ratio. Mitochondrial depolarization was recorded after BBAP-1 and BBAP-2 treatment by an increase in orange/green fluorescence intensity ratio (Figure 11A and B).

Figure 11 (A and B): Effect of BBAP-1 and BBAP-2 upon mitochondria membrane potential

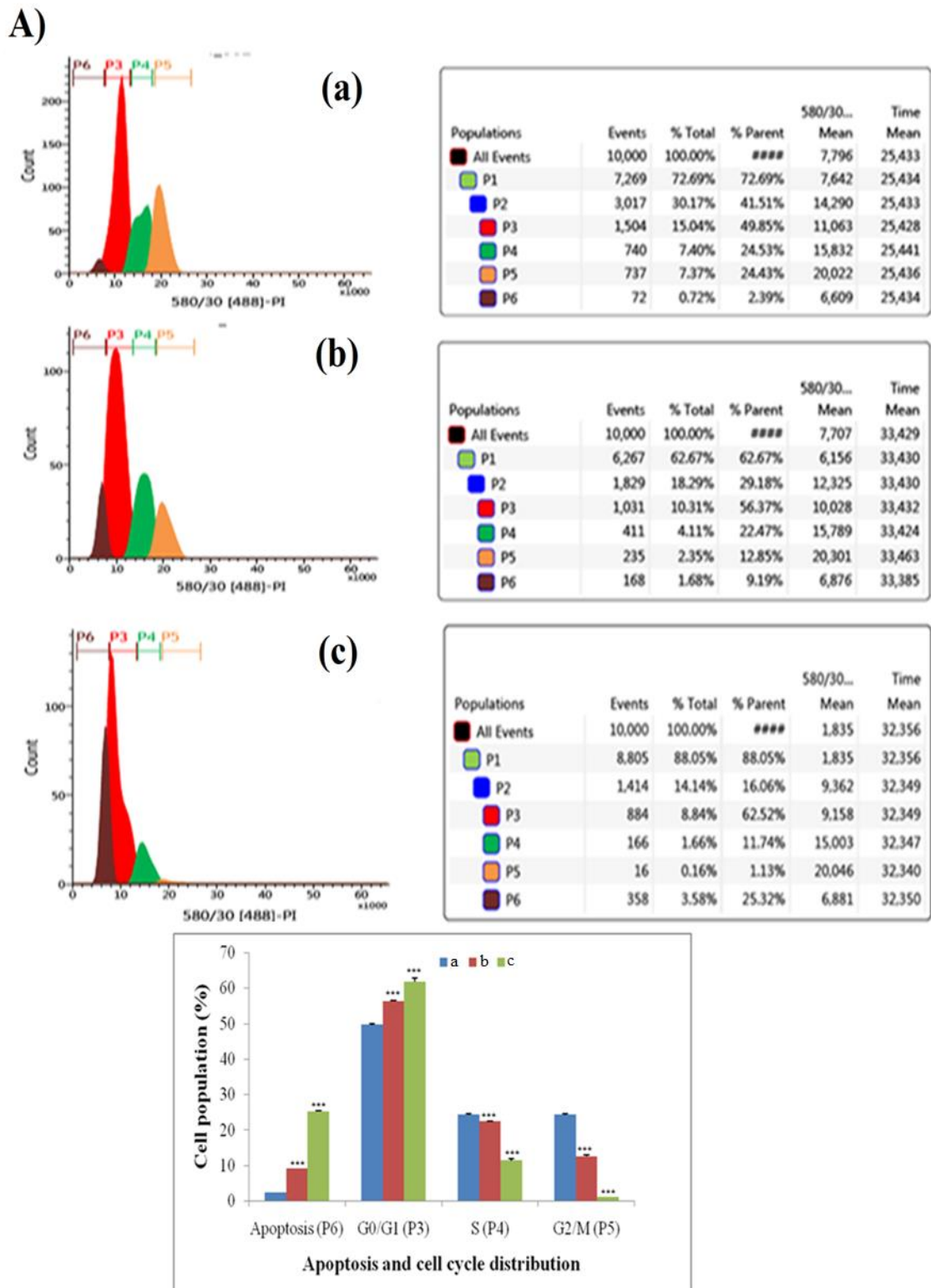


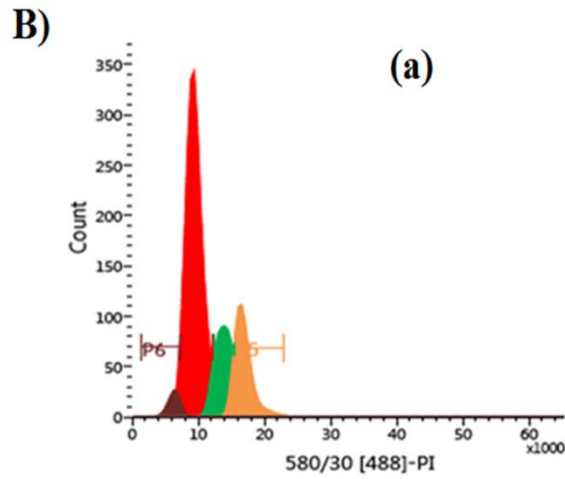


4.3.4 Cell cycle analysis using PI staining

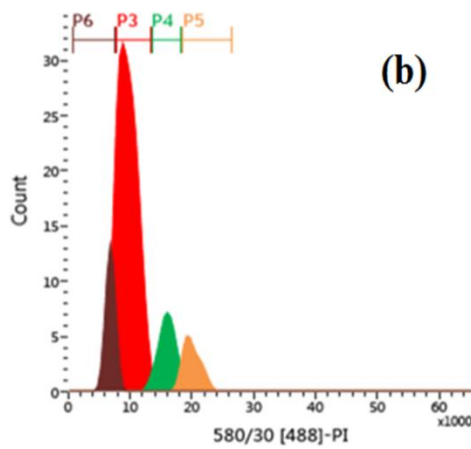
PI is a fluorogenic compound that binds stoichiometrically to nucleic acids so that fluorescence emission is proportional to the DNA content of the cell. DNA content was increased by 1.13 and 1.31 fold in the G₀/G₁ phase after treatment with ½ IC 50 and IC 50 dose of BBAP-1. Apoptotic cell burden was also multiplied to 3.84 and 10.59 fold by ½ IC 50 and IC 50 dose of BBAP-1 (Figure 12A). Treatment with BBAP-2 was distinct for the increase in DNA content by 1.094 fold in G₀/G₁ in comparison to control (66.67 % against 60.90%). Apoptotic cell burdens were multiplied to 3.75 fold after BBAP-2 treatment in comparison to control (12.90% against 3.44%). Cell cycle was arrested in G₂/M phase as the number of cells was decreased in G₂/M phase in comparison to control with the larger population of cells in G₀/G₁ phase (8.27% against 19.25%) (Figure 12B).

Figure 12 (A and B): Effect of BBAP-1 and BBAP-2 upon cell cycle arrest and apoptotic cell burden

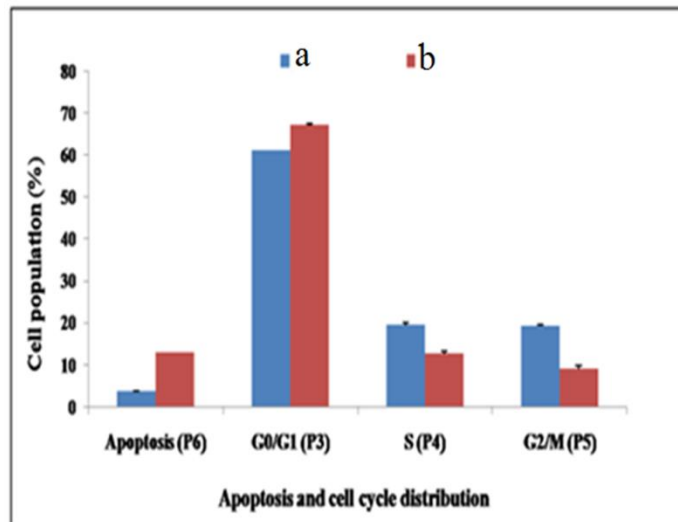




Populations	Events	% Total	% Parent	580/30... Mean	Time Mean
All Events	10,000	100.00%	###	7,115	2,185
P1	9,507	95.07%	95.07%	7,327	2,185
P2	3,430	34.30%	36.08%	11,547	2,185
P3	2,089	20.89%	60.90%	9,485	2,185
P4	651	6.51%	18.98%	13,904	2,183
P5	667	6.67%	19.45%	16,920	2,187
P6	118	1.18%	3.44%	6,439	2,185



Populations	Events	% Total	% Parent	580/30... Mean	Time Mean
All Events	10,000	100.00%	###	4,985	34,589
P1	5,369	53.69%	53.69%	1,754	34,588
P2	411	4.11%	7.66%	10,973	34,596
P3	274	2.74%	66.67%	9,687	34,593
P4	50	0.50%	12.17%	16,087	34,589
P5	34	0.34%	8.27%	20,144	34,625
P6	53	0.53%	12.90%	6,915	34,604



4.4 In vivo study

4.4.1 ECG and HRV

ECG analysis of the ECG signals revealed an increase in HR after MNU treatment (361.1 ± 8.42 beats/min). Treatment with BBAP-1 helped to restore the HR significantly to normal ($322.43 \pm 6.79^{***}$ beats/min). No significant variability could be perceived in the P wave duration after either of the treatments (Table 3). The HRV analysis of the ECG complex revealed the sharp decrease in the low frequency (LF) (9.60 ± 0.01 ms²), high frequency (HF) (40.96 ± 0.05 ms²) and LF/HF (0.23 ± 0.04) after the MNU treatment. Treatment with BBAP-1 perceived dose-dependent restoration of the HRV parameters (Table 4).

Table 3: Effect of BBAP-1 on electrocardiographic changes in mammary gland carcinoma

ECG Parameters	Control (0.9% normal saline, p.o)	Toxic control (MNU 8 mg/kg, i.v.)	MNU +BBAP-1 (8 mg/kg i.v. + 56.62µg/kg , s.c.)	MNU + BBAP-1 (8 mg/kg i.v. +113.25µg/kg s.c.)
RR Interval (s)	0.17±0.01	0.16±0.01	0.15±0.009	0.18±0.01
Heart Rate (BPM)	391.05±5.17***	361.1±8.42	370.8±8.09	322.43±6.79***
PR Interval (s)	0.04±0.002	0.04±0.002	0.04±0.003	0.05±0.004***
P Duration (s)	0.01±0.004	0.01±0.001	0.01±0.001	0.01±0.002
QRS Interval (s)	0.01±0.004	0.01±0.004	0.01±0.003	0.02±0.006
QT Interval (s)	0.04±0.01	0.05±0.08	0.06±0.09	0.04±0.01
QTc (s)	0.1±0.02	0.1±0.01	0.1±0.02	0.1±0.02
JT Interval (s)	0.02±0.01	0.03±0.01	0.09±0.01	0.02±0.01
T peak Tend Interval (s)	0.01±0.007	0.02±0.009	0.02±0.007	0.01±0.005
P Amplitude (mV)	0.05±0.01	0.09±0.03	0.1±0.2	0.06±0.007
Q Amplitude (mV)	0.03±0.03	-0.007±0.01	0.01±0.03	0.001±0.07
R Amplitude (mV)	1.4±0.48	1.4±0.02	1.2±0.2	1.2±0.4
S Amplitude (mV)	-0.2±0.1	-0.3±0.006	-0.04±0.005*	-0.1±0.2
ST Segment (mV)	-0.08±0.1	-0.01±0.06	0.01±0.05	0.05±0.08
T Amplitude (mV)	0.3±0.06	0.2±0.1	0.1±0.1	0.03±0.1

(Values are presented as mean ± SD). Each group contains eight animals. Comparisons are made on the basis of one-way ANOVA followed by Bonferroni multiple test. All groups are compared to the toxic control group (*p<0.05, **p<0.01, ***p<0.001).

Table 4: Effect of BBAP-1 on HRV changes in MNU induced mammary gland carcinogenesis

	Control (0.9% normal saline, p.o)	Toxic control (MNU 8 mg/kg, i.v.)	MNU +BBAP-1 (8 mg/kg i.v. + 56.62µg/kg , s.c.)	MNU + BBAP-1 (8 mg/kg i.v. +113.25µg/kg s.c.)
Time Domain				
Average RR (ms)	176.2±0.01***	164.9±0.03	155.3±0.08***	167.01±0.07***
Median RR (ms)	173.3±0.06	165.3±0.05	155.5±0.09***	185.16±0.09***
SDRR (ms)	7.25±0.01	5.44±0.7	3.47±0.01***	8.38±0.01***
CVRR	0.02±0.01	0.03±0.01	0.02±0.02	0.04±0.02
Frequency Domain				
LF (ms²)	11.32±0.06***	9.6±0.01	8.19±0.04***	12.62±0.06***
HF (ms²)	49.7±0.09***	40.96±0.05	45.96±0.09***	50.84±0.07***
LF/HF	0.34±0.02	0.23±0.04	0.23±0.08	0.26±0.1
VLF (ms²)	38.8±0.07***	30.47±0.08	26.36±0.04***	39.35±0.09***

(Values are presented as mean ± SD). Each group contains eight animals. Comparisons are made on the basis of one-way ANOVA followed by Bonferroni multiple test. All groups are compared to the toxic control group (*p<0.05, **p<0.01, ***p<0.001).

4.4.2 Morphological evaluation

4.4.2.1 Carmine staining of whole mounts mammary gland

In the toxic control group, there was a marked increase in the AB count and lobules and BBAP-1 afforded a marked protection against the same. As a marker for growth and proliferation of the mammary gland tissue, BBAP-1 also regulated the DF score favorably (Table 5) (Figure 13A-D).

4.4.2.2 H&E staining of mammary gland tissue

Histopathological examination of the mammary gland tissue revealed the presence of duct, adipocytes, loose connective tissue (LCT), dense connective tissue (DCT), lymphocytes, cuboidal epithelial cells (CEC) and myoepithelial cells (MC) in case of control. In the toxic group, there was a loss of LCT, DCT, and adipocytes. Scattered CEC were recorded in toxic groups. However, after treatment with BBAP-1, dose-dependent restoration of mammary gland architecture was observed (Figure 13E-H).

4.4.2.3 SEM analysis of mammary gland tissue

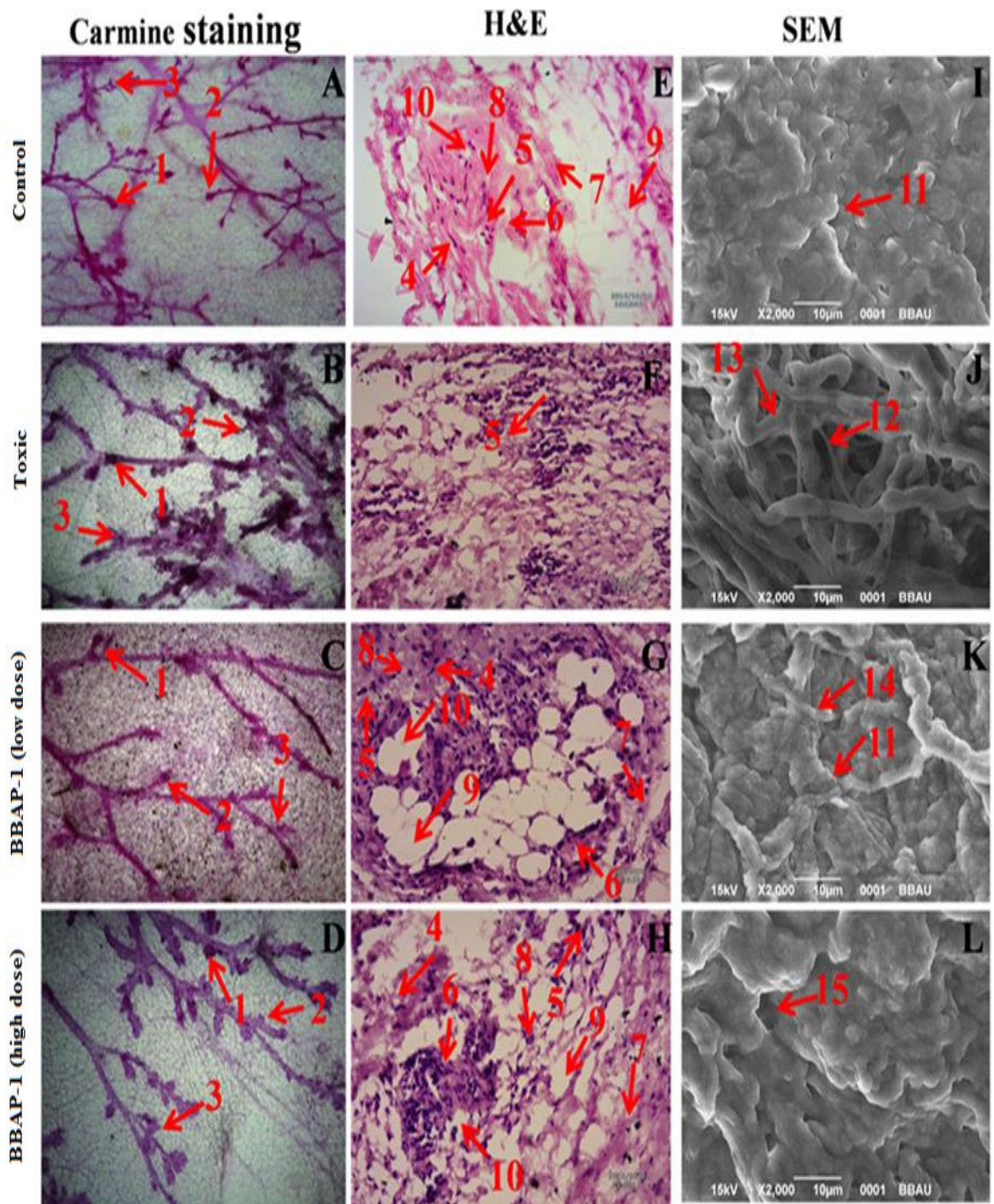
Mammary gland tissues from all the groups were further subjected to SEM to elucidate the surface features like intra-arterial cushions due to presence of collagenous fibers, duct and large blood vessels in control tissues. The tissue from the MNU treated group revealed formation of small capillary networks representing tumor microvessels, nodules formation with loss of intra-arterial cushions. BBAP-1 treatment successfully curtailed the number of the microvessels and had a profound impression on branching sites which is an indication for restoration of intra-arterial cushion (Figure 13I-L).

Table 5: Effect of MNU and BBAP-1 on differentiation of mammary gland

Groups	AB1	AB2	AB1+AB2	Lobules	DF Score (AB1+AB2+Lobules)
Control (0.9% normal saline, p.o)	240.89±3.45***	301±9.76***	541.89±13.21***	543±12.76***	1084.89±25.97***
Toxic control (MNU 8 mg/kg, i.v.)	2489±12.08	1567.77±2.98	4056.77±15.06	4127±10.72	8183.77±25.78
MNU +BBAP-1 (8 mg/kg i.v. + 56.62µg/kg , s.c.)	709±8.87***	800.34±4.76***	1509.34±13.63***	1992±9.21***	3501.34±22.84***
MNU + BBAP-1 (8 mg/kg i.v. +113.25µg/kg s.c.)	349±3.78***	288.33±21.89***	637.33±25.67***	432±9.87***	1069±35.54***

(Values are presented as mean ± SD). Each group contains eight animals. Comparisons are made on the basis of one-way ANOVA followed by Bonferroni multiple test. All groups are compared to the toxic control group (*p<0.05, **p<0.01, ***p<0.001).

Figure 13: Effect of BBAP-1 upon cellular, morphological and surface architecture of mammary gland tissue



4.5 Antioxidant markers

Treatment with BBAP-1 validated the restoration of antioxidant defense system in comparison to toxic control. The protein and lipid peroxidation was very well evident after MNU treatment. The BBAP-1 successfully curtailed down the level of PC ($31.30 \pm 4.10^{***}$ nM/ml unit). Non significant changes in the TBARs (0.26 ± 0.02 nM of MDA/ μ g of protein) were observed after BBAP-1 treatment. The level of GSH in normal control (1.10 ± 0.06 mg %) was non-significantly decreased in comparison to toxic control (1.04 ± 0.07 mg %). The GSH level was upregulated after the treatment with BBAP-1 (1.4 ± 0.04 mg %). Corresponding to the levels of SOD (0.023 ± 0.002 units of SOD/mg of protein) and catalase (14.40 ± 0.97 nM of H_2O_2 / min/mg of protein) in toxic control; BBAP-1 significantly accompanied to restore the same (i.e. 0.032 ± 0.007 units of SOD/mg of protein and 40.59 ± 0.75 nM of H_2O_2 /mg of protein) comparable to normal control (Table 6).

Table 6: Effect of BBAP-1 and MNU on oxidative stress markers

Groups	TBARs (nM of MDA/ μ g of protein)	GSH (mg%)	SOD (units of SOD/mg of protein)	Catalase (nM of H ₂ O ₂ / min/mg of protein)	PC (nM/ml unit)
Control (0.9% normal saline, p.o)	0.12 \pm 0.03***	1.1 \pm 0.06	0.037 \pm 0.009*	16.2 \pm 1.15	40.43 \pm 5.11***
Toxic control (MNU 8 mg/kg, i.v.)	0.24 \pm 0.007	1.04 \pm 0.07	0.023 \pm 0.002	14.4 \pm 0.97	53.52 \pm 7.88
MNU +BBAP-1 (8 mg/kg i.v. + 56.62 μ g/kg , s.c.)	0.33 \pm 0.01***	1.19 \pm 0.04**	0.027 \pm 0.005	26.75 \pm 5.24***	29.99 \pm 1.57***
MNU + BBAP-1 (8 mg/kg i.v. +113.25 μ g/kg s.c.)	0.26 \pm 0.02	1.4 \pm 0.04***	0.032 \pm 0.007	40.59 \pm 0.75***	31.3 \pm 4.1***

(Values are presented as mean \pm SD). Each group contains eight animals. Comparisons are made on the basis of one-way ANOVA followed by Bonferroni multiple test. All groups are compared to the toxic control group (*p<0.05, **p<0.01, ***p<0.001).

4.6 Measurement of cell death through caspase 3 and caspase 8 assay

Significant upregulation in the caspase 3 and 8 levels was perceived after BBAP-1 treatment in dose dependent manner (Figure 14).

4.7 Western blotting

The expression of the anti-apoptotic protein (Bcl-2 and Bcl-xl) of mitochondria-mediated death apoptosis pathway was increased after MNU administration in the toxic group in comparison with control, which was subsided in BBAP-1 treated groups. Pro-apoptotic protein (BAX) demonstrated elevated expression in treatment groups. Treatment with BBAP-1 perceived downregulation of the downstream apoptotic marker (VDAC, Apaf-1, procaspase 9 and cytochrome c) (Figure 14). Immunoblotting assay affirmed the increased expression of PHD-2 with BBAP-1 treatment, suggesting PHD-2 activation. The same was further confirmed with decreased expression of HIF-1 α , FASN and SREBP-1c after BBAP-1 treatment. UCHL-1 mediated inhibition of NF κ Bp65 expression in BBAP-1 treated group was also evident in a dose-dependent manner (Figure 15).

4.8 qRT-PCR

The immunoblotting assay ascertained mitochondrial-mediated apoptotic death induced by BBAP-1 and the same was subsequently affirmed through the genomic contributors for observed phenotypes using qRT-PCR studies. A significant decrease in the anti-apoptotic genes Bcl-2 and Bcl-xl were recorded after BBAP-1 treatment with vice-versa results for pro-apoptotic BAX. The expression of downstream genes associated with mitochondrial-mediated apoptosis was favorably regulated after the BBAP-1 treatment (Figure 14). Treatment with BBAP-1 favorably upregulated fold change expression of PHD-2 and subsequent diminished fold change expression of

HIF-1 α , FASN, and SREBP-1c. BBAP-1 treatment systematically curtailed down the mRNA expression of UCHL-1 and NF κ Bp65 (Figure 15).

Figure 14: Effect of BBAP-1 treatment on mitochondrial mediated apoptosis

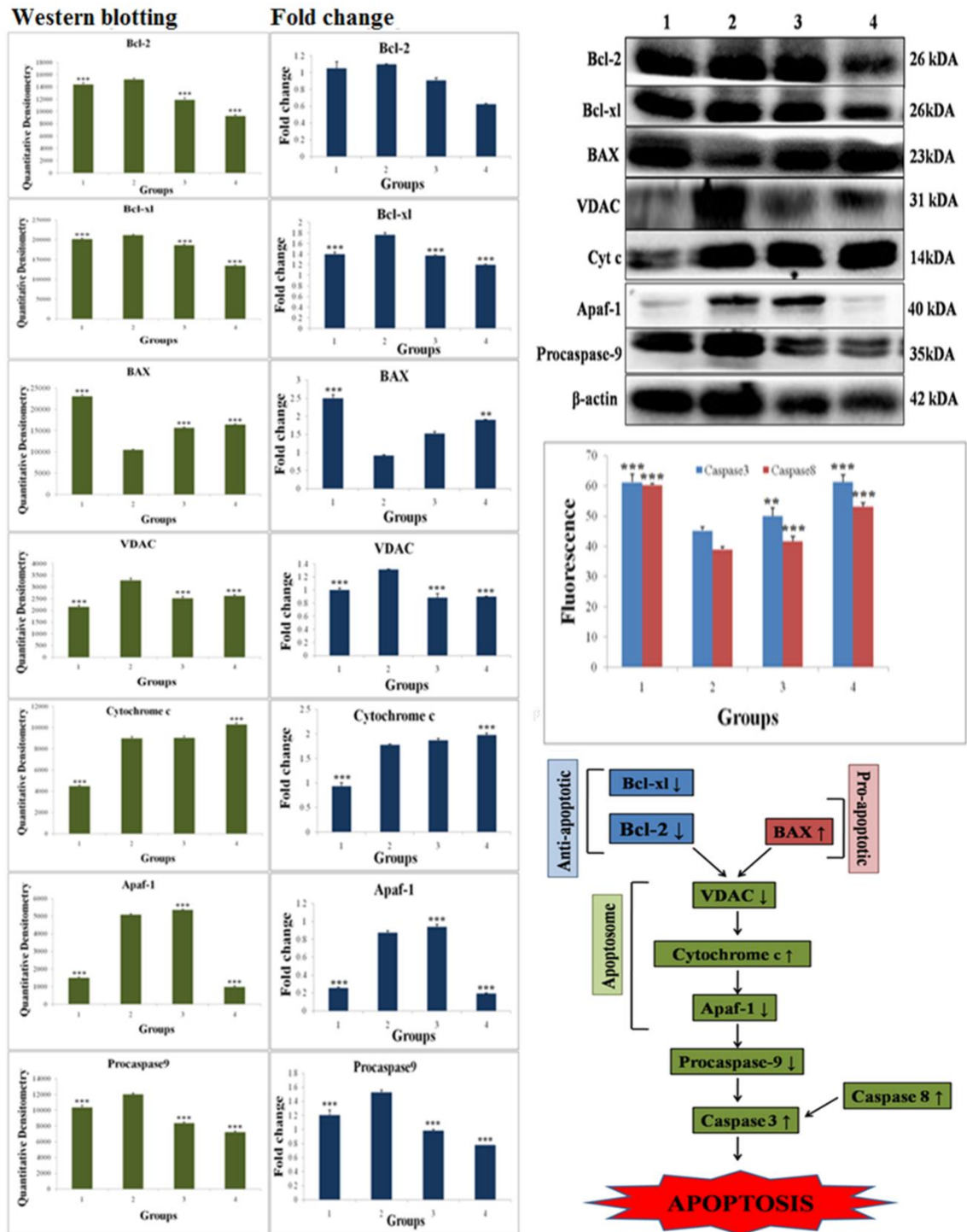
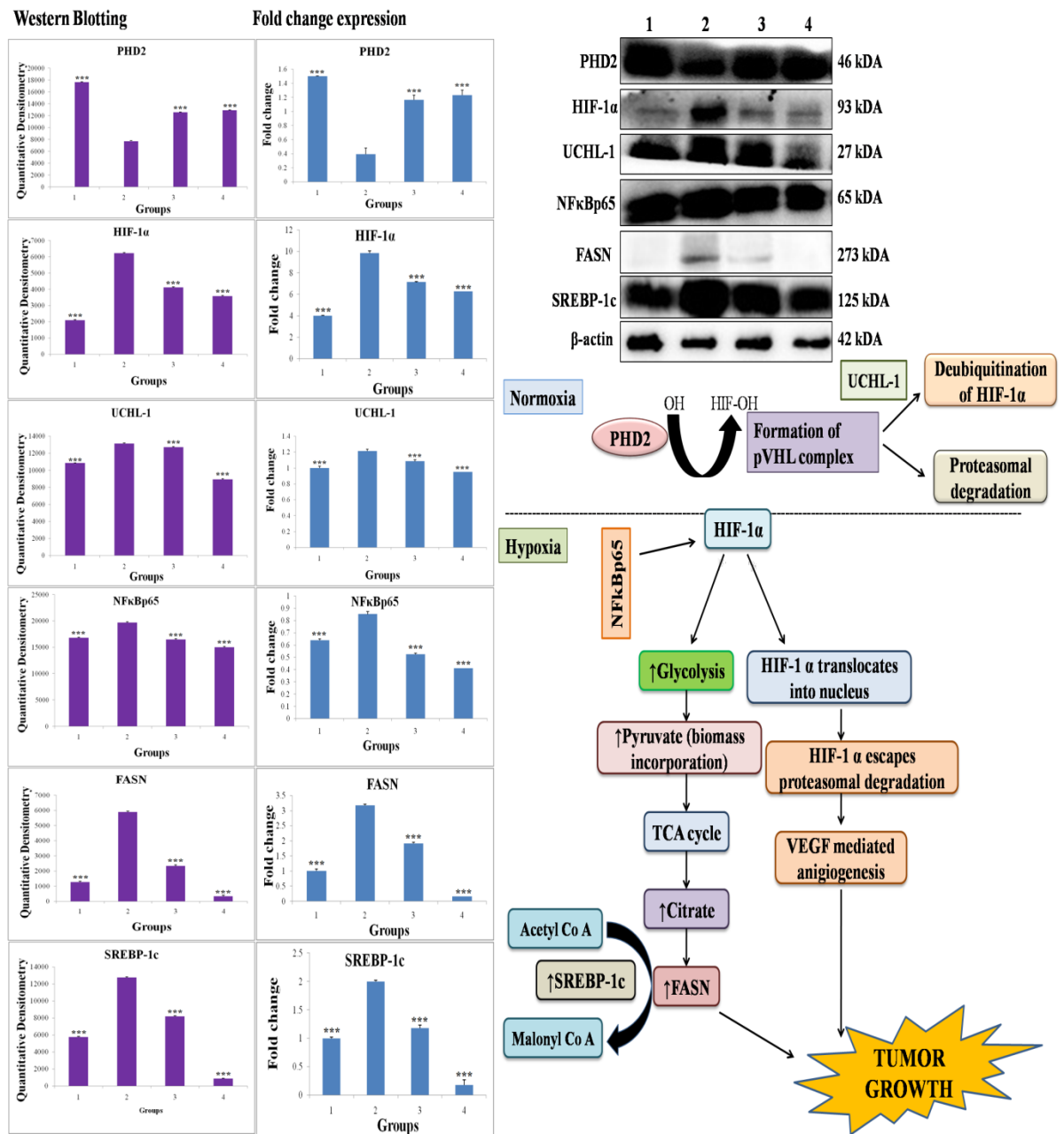


Figure 15: Effect of BBAP-1 treatment on hypoxic pathway in mammary gland cancer



Discussion

In continuation to our previous hypothesis, the present study was undertaken to inquest possible PHD-2 activation with the potential to curtail fastly growing tumor cells [113]. Approximately twenty eight thousand compounds were screened by 50% structure similarity with two known PHD-2 activators (R59949 and KRH102140) through Maestro version 9.3 (Schrödinger). BBAP-1 and BBAP-2 were retrieved through subsequent screening using series of *in silico* tools of drug likeliness and CDRUG server. Subsequently, BBAP-1 and BBAP-2 was recorded to be devoid of any developmental and mutagenic toxicity with sufficiently high oral LD50 prompted us to perform the further evaluation (Figure 6A and B). For BBAP-1, the metabolic profiling revealed CYP450 mediated hydroxylation as the possible mode of metabolism with 6th, 10th, 19th and 20th carbon being most vulnerable positions for hydroxylation whereas the metabolic positions of BBAP-2 revealed that 11th, 12th, 21st and 22nd carbon positions as major site for metabolism through 12 and 22-dealkylation and 11 and 21-ester hydrolysis. CYP3A4 and CYP2D6 were the major cytochrome P450 enzymes involved in their metabolism (Figure 7A and B). Proceeding further, BBAP-1 and BBAP-2 were evaluated for its PHD-2 activation potential using *in vitro* assay. BBAP-1 and BBAP-2 demonstrated significant PHD-2 activation in comparison to control using 2-OG as a substrate (Figure 8A and B). Considering the significant *in vitro* PHD-2 activation by BBAP-1 and BBAP-2, authors considered it further to evaluate the effect of BBAP-1 and BBAP-2 against ER+MCF-7 cells. BBAP-1 demonstrated significant cytotoxic potential against ER+MCF-7 cells in concentration dependent manner. IC 50 dose of BBAP-1 and BBAP-2 were recorded to be lower than the reported IC50 of standard drug (tamoxifen citrate) (Figure 9A and B) [114]. Subsequently, the morphological

changes associated with apoptosis were evaluated through AO/EtBr staining using fluorescence microscopy. The membrane blebbing, chromatin condensation and dotted nuclei were predominant in the BBAP-1 and BBAP-2 treated cells, with the bright orange dot, ensuring apoptosis (Figure 10A and B) [96]. The mitochondrial membrane potential stands a major determinant for evaluating apoptosis and the same was studied using the cationic dye JC-1. JC-1 forms red fluorescent J-aggregates in the mitochondria of the highly permeable apoptotic cells through faster and better penetration due to loss of membrane potential [97]. The experimental outcome indicates that BBAP-1 and BBAP-2 induces mitochondrial depolarization in concentration dependent manner (Figure 11A and B). Eventually, cell cycle analysis was studied through PI to identify the population of cells existing in G₀/G₁, S and G₂/M phase [98]. Treatment with BBAP-1 and BBAP-2 arrested the ER⁺ MCF-7 cells in G₂/M phase of cell cycle represented through the higher number of the cell population in G₀/G₁ phase and an increase in apoptotic cell burden by ten folds at IC₅₀ dose (Figure 12A and B). All in all, BBAP-1 and BBAP-2 demonstrated significant cytotoxic potential against ER⁺MCF-7 cells. The studies further affirmed BBAP-1 and BBAP-2 mediated apoptosis in the ER⁺MCF-7 cell with cell cycle arrest in the G₀/G₁ phase. It would be appropriate to put on records that BBAP-1 and BBAP-2 mediated apoptosis was associated with changes in the mitochondrial membrane permeability, suggesting the participation of mitochondrial-mediated apoptosis in ER⁺MCF-7cells.

The autonomic dysfunction associated with cardiovascular risk in the early breast cancer and breast cancer survivors is a well-reported phenomenon [115]. In fact, autonomic dysfunction has been considered as a marker for long-term efficacy of a chemotherapeutic regime. Henceforth, we found it worth to study the effect of BBAP-

1 upon autonomic control [116]. The reduced autonomic control has been reported to be associated with increased HR along with decreased HRV factors and treatment with MNU was evident for the same [117, 118]. Treatment with BBAP-1 helped to restore the autonomic control and therefore could designate to have good prognostic value in chemoprevention regime proposed through BBAP-1 (Table 3 and 4).

The anticancer efficacy of BBAP-1 was further scrutinized against MNU induced mammary gland carcinoma. Mammary gland whole mount preparations; through carmine staining are used as a suitable method for the examination of small proliferative lesions as represented by an increase in AB count and DF score [119]. The AB represents the largest bulbous structure located at the distal end of the mammary epithelial tree and represents the site for the malignant transformation. The increased in AB number is directly correlated with an increased proliferation [119]. The MNU treatment was evident in the increased in AB count and DF score, which is in corroboration with the previous studies [100]. Treatment with BBAP-1 curtailed the AB count and DF score, suggesting anti-proliferative effect of BBAP-1 (Figure 13A-D and Table 5). The findings through the carmine staining were further endorsed through H&E staining and SEM analysis. Treatment with MNU revealed distorted cellular architecture evident through a scattered pattern of CEC, loss of duct and MC. The LCT and DCT were hard to identify in the MNU treatment and the similar pattern of pathological changes has been reported previously as well [102, 120]. Treatment with BBAP-1 restored the cellular architecture close to control (Figure 13E-H). SEM analysis of the MNU treated group elucidated increased in microvessel formation, loss of intra-arterial cushion and vascular conglomeration as reported in the previous literature [103]. On the contrary, the treatment groups revealed the decreased in microvessel with the profound impression on the branching sites, an indication of

intra-arterial cushions, which regulate the blood flow at the branching sites [104]. Enlarged capillaries, which are the sign of rapidly growing tumors were also absent in BBAP-1 treated groups (Figure 13I-L). All in all, BBAP-1 imparted a significant dose-dependent effect to restore the structural abnormalities but warrants further confirmation to validate its efficacy.

Increased ROS generation and subsequent oxidative stress are linked with carcinogenesis through multiple pathways [121]. Firstly, ROS production promotes redox adaptation leading to activation of cell survival factors and decrease in cell death subsequently causing cancers [122]. Secondly, ROS-mediated oxidative stress helps redox-sensitive kinases, DNA, RNA and protein damage leading to chromosomal abnormalities and finally cancer [123]. Culminating above all, suggests significant association between oxidative stress and cancer progression. MNU treated toxic group revealed up-regulation of biochemical markers of lipid (TBARs) and protein (PC) peroxidation. Noticeable down-regulation of enzymatic defense peroxidation of SOD/catalase/GSH was also evident after MNU treatment. The increase in TBARs and PC could be attributed to the alkylating effect of MNU on cellular membranes [124]. The down-regulated levels of SOD/catalase/GSH as perceived after MNU treatment reflects increased ROS generation. SOD dismutase the $O\bullet$ to O_2 and H_2O_2 . H_2O_2 is further catalyzed by catalase and GSH peroxidase to water [125]. All three works in tandem to curtail ROS ($O\bullet$) and are expected to follow the similar pattern of fold change as perceived in the present experiment. Treatment with BBAP-1 was evident for increased levels of SOD/catalase/GSH and diminished production of TBARs/PC and thereby reflects curtailment of oxidative stress by BBAP-1 (Table 6).

BBAP-1 demonstrated significant protection against MNU induced carcinogenesis when perceived through the markers of apoptosis. BBAP-1 decreased the expression of anti-apoptotic proteins Bcl-2 and Bcl-xl along with positive modulation of BAX expression, a pro-apoptotic member of the Bcl-2 family. It is to be noted that the similar pattern of mRNA induction (BAX) and inhibition (Bcl-2 and Bcl-xl) was observed when quantified through qRT-PCR assay. Under normal conditions, cell loses its specific functions and spontaneously die as a result of apoptosis-modulating the mitochondrial pathway with BAX translocation, cytochrome c release and processing of caspase 9 [126]. The induction of apoptosis was further cross-checked through the decreased expression of VDAC (due to loss of the entire integrity of the channel), suggesting the release of cytochrome c from the mitochondria [127, 128]. The same was endorsed through the increased cytosolic expression of cytochrome c at protein and mRNA level. Increased cytochrome c expression warrants the formation of apoptosome with Apaf-1 and thereby decreases the cytosolic Apaf-1 levels as perceived after the BBAP-1 treatment [129, 130]. Apoptosome formation further cleaves the procaspase 9 to give active caspases 9 and thus reduce the expression of procaspase 9 as observed after the BBAP-1 treatment (Figure 14) [131, 132]. It would be in line to mention that activation of caspases 9, further mediates activation of effector caspases 3 and 8 for execution of apoptosis [133]. Treatment with BBAP-1 up-regulated the levels of both caspases 3 and 8 and thereby accredited apoptosis (Figure 14). From the above line of evidences, one could easily derive that BBAP-1 impart a significant protection against the proliferative and angiogenic effects of MNU by regulating the mitochondrial-mediated apoptosis death pathway.

In pursuance to the hypothesis, we scrutinized the effect of BBAP-1 on PHD-2 mediated degradation of HIF-1 α and other closely related biological markers. Under

hypoxic condition, HIF-1 α escapes proteasomal degradation and promotes tumor growth through up-regulating fatty acid synthesis [134, 135]. The fatty acid synthesis, in the tumor cell, is regulated with the help of FASN (catalyzes the rate-limiting step of acetyl Co-A to malonyl Co-A in fatty acid synthesis) [136]. The conversion of acetyl Co-A to malonyl Co-A by FASN is regulated by SREBP-1c [137]. In the recent past, FASN has gained importance as an oncogenic marker and SREBP-1c modulators as a valid anticancer strategy [138]. BBAP-1 upregulated the expression of PHD-2 and downregulated the expression of HIF-1 α , suggesting its proteasomal degradation. Treatment with BBAP-1 also downregulated the expression of FASN and SREBP-1c and thereby endorses the decreased fatty acid synthesis and lipogenic activity in the mammary gland tissues. The ubiquitination of HIF-1 α (required for proteasomal degradation) was further scrutinized using UCHL-1, as the same participated in deubiquitination of HIF-1 α and thereby promoted the hypoxic microenvironment of the cancerous cells [139]. The expression of UCHL-1 was significantly curtailed after the BBAP-1 treatment, further affirms the proteasomal degradation of HIF-1 α by BBAP-1. Further role of UCHL-1 was validated through its inhibition of NF κ Bp65 subunit in treatment groups, which are in line with our previous experimental outcome against MNU induced mammary gland carcinoma (Figure 15) [140]. With all above, authors would like to conclude that BBAP-1 can activate PHD-2 with subsequent down-regulating effect on HIF-1 α to promote apoptosis through mitochondrial-mediated death pathway.

CHAPTER 5
SUMMARY AND
CONCLUSION

As per our hypothesis, the present study was undertaken for the screening of possible and potential PHD-2 activators for the curtailment of overexpressed HIF-1 α and FASN in mammary gland carcinoma.

In literature, three PHD-2 activators were known but their potential effect upon HIF-1 α and FASN was not elaborated. On the basis of 50% structure similarity, we screened a library of 28000 compounds using Zinc database and Asinex database through Maestro version 9.3 (Schrödinger). After screening the compounds from various filters and CDRUG server, we found only two compounds (BBAP-1 and BBAP-2) which were effective. The *in silico* toxicity profile of both the compounds was estimated using TEST. The *in vitro* PHD-2 assay also confirmed the activation of PHD-2 using 2-OG in the reaction mixture.

After getting confirmed from the *in silico* results, we elaborate the effect of BBAP-1 and BBAP-2 against ER-MCF-7 cells. For the cytotoxicity estimation of the compounds, MTT assay was performed which revealed that the IC₅₀ value of BBAP-1 and BBAP-2 was 15.29 μ M and 16.61 μ M respectively in comparison to control and tamoxifen treated cells. The results revealed that the compounds have better efficacy in comparison to the well known drug tamoxifen. The apoptosis was evaluated using AO/EtBr staining of the cells. It was well known that AO is used for the staining of viable and non-viable cells and it produces green fluorescence when attached with DNA whereas, EtBr stains only dead cells and produced red fluorescence. In the present study, the apoptotic markers were clearly seen after BBAP-1 and BBAP-2 treatment. Subsequently, the mitochondrial depolarization was measured using JC-1 staining of ER+MCF-7 cells. JC-1 is a cationic dye and exhibits as potential dependent accumulation in mitochondria. This accumulation is indicated by fluorescence emission shift from green (~525nm) to orange (~590nm). Mitochondrial depolarization is indicated by an increase in

orange/green fluorescence intensity ratio. BBAP-1 and BBAP-2 were increased the orange/green ratio and produced mitochondrial depolarization. Subsequently, the cell cycle phase distribution was analysed using flow cytometry. PI is a fluorogenic dye and it binds with nucleic acids so that fluorescence emission is proportional to DNA content of the cell. After treatment with BBAP-1 and BBAP-2, the DNA content was high in G0/G1 phase and the cell cycle was arrested in G2/M phase.

Afterwards, the efficacy of BBAP-1 was evaluated against MNU induced mammary gland carcinoma model. It was a well known fact that autonomic dysfunction is associated with breast cancer. In breast cancer patients, the heart rate is increased with decreased in HRV parameters and the similar observations were found after ECG and HRV analysis of the animals treated with BBAP-1. The morphology of the mammary gland tissue was evaluated using carmine staining, H&E staining and SEM analysis. It is a well known fact that ABs, lobules and DF score are the markers of cell proliferation and angiogenesis. In the present study the increased levels of ABs, lobules and DF score were decreased after BBAP-1 treatment. The cell organelles like adipocytes, duct, LCT, DCT, CEC, MEC and lymphocytes were distorted after MNU treatment and BBAP-1 treatment restored all the cell organelles about to normal. The surface architecture of tissues was evaluated using SEM and the results revealed that BBAP-1 treatment reduced the formation of microvessels and intra-arterial cushion. The role of BBAP-1 in antioxidant defence mechanism was evaluated using antioxidants markers like TBARs, SOD, catalase, GSH and PC. BBAP-1 treatment has a pronounced effect upon antioxidant markers. After that we evaluated the markers of apoptosis using caspase 3 and caspase 8 assay. Low dose of BBAP-1 was reduced the level of caspase 3 and caspase 8 in serum samples. The participation of mitochondrial death apoptosis pathway was measured using the immunoblotting and qRT-PCR assay. The protein

expression of fold change gene expression in Bcl-2 family of proteins (Bcl-2, Bcl-xl, BAX, VDAC, Apaf-1, procaspase 9 and cytochrome c) revealed that BBAP-1 produced mitochondrial death apoptosis. The activation of PHD-2 was further screened through immunoblotting and qRT-PCR study of hypoxic pathway. The results revealed that BBAP-1 upregulated the expression and gene fold change of PHD-2 along with decreased protein expression and fold change of HIF-1 α , FASN, SREBP-1c, NF κ Bp65 and UCHL-1.

It was conclude that from the line of evidences derived from the present work that the exogenous chemical activation of PHD-2 can favourably regulate the cellular proliferation through mitochondrial mediated apoptosis. In the same line, BBAP-1 and BBAP-2 are recorded to be the chemical activators of PHD-2 with subsequent down-regulating expression of HIF-1 α and FASN. The present study explicitly endorses the *in vivo* efficacy of BBAP-1 against mammary gland carcinoma and commands the need for clinical validation for exploring its future prospect as an anticancer agent.

1. Fuchs Y and Steller H. Programmed Cell Death in Animal Development and Disease. *Cell*, 147(4), 2011, 742-758.
2. Goodsell DS. The Molecular Perspective: VEGF and Angiogenesis. *The Oncologist*, 7(6), 2002, 569-570.
3. Azevedo SA et al. Metastasis of circulating tumor cells: Favorable soil or suitable biomechanics, or both? *Cell Adh Migr*. 9(5), 2015, 345–356.
4. Assary RS and Curtiss LA. Comparison of Sugar Molecule Decomposition through Glucose and Fructose: A High-Level Quantum Chemical Study. *Energy Fuels* 26 (2), 2012, 1344-1352.
5. Hardie DG. Organismal Carbohydrate and Lipid Homeostasis. *Cold Spring Harb Perspect Biol* 2012; 4:a006031.
6. Liberti MV and Locasale JW. The Warburg Effect: How Does it Benefit Cancer Cells? *Trends Biochem Sci*, 41(3), 2016, 211–218.
7. Kroemer G and Pouyssegu J. Tumor Cell Metabolism: Cancer's Achilles' Heel. *Cancer Cell*, 13 (6), 2008, 472-482.
8. Papanianni M. Advances in citric acid fermentation by *Aspergillus niger*: Biochemical aspects, membrane transport and modelling. *Biotechnology Advances*, 25 (3), 2007, 244-263.
9. Masson N and Ratcliffe PJ. Hypoxia signaling pathways in cancer metabolism: the importance of co-selecting interconnected physiological pathways. *Cancer Metab*. 2014; 2, 3.
10. Eales KL, Hollinshead KER and Tennant DA. Hypoxia and metabolic adaptation of cancer cells. *Oncogenesis*, 2016, 5(1), e190.
11. Burns SJ and Manda G. Metabolic Pathways of the Warburg Effect in Health and Disease: Perspectives of Choice, Chain or Chance. *Int J Mol Sci*. 2017, 18(12), 2755.
12. Semenza GL. Hypoxia-Inducible Factor 1: Regulator of Mitochondrial Metabolism and Mediator of Ischemic Preconditioning. *Biochim Biophys Acta*. 2011, 813(7), 1263–1268.
13. Monaco ME. Fatty acid metabolism in breast cancer subtypes. *Oncotarget*. 2017, 25, 8(17), 29487–29500.
14. Alwarawrah Y et al. Fasnall, a Selective FASN Inhibitor, Shows Potent Anti-tumor Activity in the MMTV-Neu Model of HER2+ Breast Cancer. *Cell Chemical Biology*. 2016, 23 (6), 678-688.

15. Varga T, Czimmerera Z and Nagy L. PPARs are a unique set of fatty acid regulated transcription factors controlling both lipid metabolism and inflammation. *Biochimica et Biophysica Acta (BBA) - Molecular Basis of Disease*, 2011, 1812(8), 1007-1022.
16. Ricoult SJH et al. Oncogenic PI3K and K-Ras stimulate de novo lipid synthesis through mTORC1 and SREBP. *Oncogene*, 2016, 35, 1250–1260.
17. Muz B et al. The role of hypoxia in cancer progression, angiogenesis, metastasis, and resistance to therapy. *Hypoxia (Auckl)*. 2015, 3, 83–92.
18. Heddleston JM et al. Hypoxia inducible factors in cancer stem cells. *Br J Cancer*. 2010, 102(5), 789–795.
19. Prabhakar NR and Semenza GL. Oxygen Sensing and Homeostasis. *Physiology (Bethesda)*. 2015, 30(5), 340–348.
20. Krock BL, Skuli N and Celeste SM. Hypoxia-Induced Angiogenesis: Good and Evil. *Genes Cancer*. 2011, 2(12), 1117–1133.
21. Semenza GL. Defining the Role of Hypoxia-Inducible Factor 1 in Cancer Biology and Therapeutics. *Oncogene*. 2010, 4, 29(5), 625–634.
22. Mole DR et al. Regulation of HIF by the von Hippel-Lindau tumour suppressor: implications for cellular oxygen sensing. *IUBMB Life*. 2001, 52(1-2), 43-7.
23. Masoud GN and Li W. HIF-1 α pathway: role, regulation and intervention for cancer therapy. *Acta Pharmaceutica Sinica B*. 2015, 5 (5), 378-389.
24. Dengler VL, Galbraith M and Espinosa JM. Transcriptional Regulation by Hypoxia Inducible Factors. *Crit Rev Biochem Mol Biol*. 2014, 49(1), 1–15.
25. Freedman SJ et al. Structural basis for recruitment of CBP/p300 by hypoxia-inducible factor-1 α . *Proc Natl Acad Sci U S A*. 2002, 6, 99(8), 5367–5372.
26. Rabinowitz MH. Inhibition of hypoxia-inducible factor prolyl hydroxylase domain oxygen sensors: tricking the body into mounting orchestrated survival and repair responses. *J Med Chem*. 2013, 12; 56(23), 9369-402.
27. Selvaraju V et al. Molecular Mechanisms of Action and Therapeutic Uses of Pharmacological Inhibitors of HIF–Prolyl 4-Hydroxylases for Treatment of Ischemic Diseases. *Antioxid Redox Signal*. 2014, 1, 20(16), 2631–2665.
28. Appelhoff RJ. Differential Function of the Prolyl Hydroxylases PHD1, PHD2, and PHD3 in the Regulation of Hypoxia-inducible Factor. *Journal of Biol Chemi*. 2004, 10, 279, 38458-38465.

29. Gorresa KL and Raines RT. Prolyl 4-hydroxylase. *Crit Rev Biochem Mol Biol.* 2010, 45(2), 106–124.
30. Longbotham JE et al. Structure and Mechanism of a Viral Collagen Prolyl Hydroxylase. *Biochemistry*, 2015, 54 (39), 6093–6105.
31. Yun S et al. Prolyl hydroxylase-2 (PHD2) exerts tumor-suppressive activity in pancreatic cancer. *Cancer*, 2012, 118 (4), 960-972.
32. Chan DA et al. Tumor Vasculature is Regulated by PHD2-mediated Angiogenesis and Bone Marrow-Derived Cell Recruitment. *Cancer Cell.* 2009, 2, 15(6), 527–538.
33. Mazzone M et al. Heterozygous Deficiency of PHD2 Restores Tumor Oxygenation and Inhibits Metastasis via Endothelial Normalization. *Cell*, 2009, 6; 136(5), 839–851.
34. Kuchnio A et al. The Cancer Cell Oxygen Sensor PHD2 Promotes Metastasis via Activation of Cancer-Associated Fibroblasts. *Cell Reports*, 2015, 12(6), 992-1005.
35. Temes E et al. Activation of HIF-prolyl Hydroxylases by R59949, an Inhibitor of the Diacylglycerol Kinase. *Journal of Biol Chem.* 2005, 280, 24238-24244.
36. Nepal M et al. An activator of PHD2, KRH102140, decreases angiogenesis via inhibition of HIF-1 α . *Cell Biochem Funct.* 2011, 29(2), 126-34.
37. Choi et al. Rapid degradation of hypoxia-inducible factor-1 α by KRH102053, a new activator of prolyl hydroxylase 2. *Br J Pharmacol.* 2008, 154(1), 114–125.
38. Chirala SS and Wakil SJ. Structure and function of animal fatty acid synthase.. *Lipids.* 2004, 39(11), 1045-53.
39. Javier AM and Lupu R. Fatty acid synthase and the lipogenic phenotype in cancer pathogenesis. *Nature Reviews Cancer*, 2007, 7, 763–777.
40. Janßen HJ and Steinbüchel A. Fatty acid synthesis in *Escherichia coli* and its applications towards the production of fatty acid based biofuels. *Biotechnology for Biofuels*, 2014:7.
41. Schweizer E and Hofmann J. Microbial Type I Fatty Acid Synthases (FAS): Major Players in a Network of Cellular FAS Systems. *Microbiol Mol Biol Rev.* 2004, 68(3), 501–517.
42. Lucenay KS et al. Cyclin E associates with the lipogenic enzyme ATP-citrate lyase to enable malignant growth of breast cancer cells. *Cancer Res.* 2016, 15, 76(8), 2406–2418.
43. Currie E et al. Cellular Fatty Acid Metabolism and Cancer. *Cell Metab.* 2013, 6, 18(2), 153–161.

44. Flavin R et al. Fatty acid synthase as a potential therapeutic target in cancer. *Future Oncol.* 2010, 6(4), 551–562.
45. Ventura R et al. Inhibition of de novo Palmitate Synthesis by Fatty Acid Synthase Induces Apoptosis in Tumor Cells by Remodeling Cell Membranes, Inhibiting Signaling Pathways, and Reprogramming Gene Expression. *EBioMedicine.* 2015, 2(8), 808–824.
46. Gkretsi V et al. Remodeling Components of the Tumor Microenvironment to Enhance Cancer Therapy. *Front Oncol.* 2015; 5: 214.
47. Impheng H et al. The Selective Target of Capsaicin on FASN Expression and De Novo Fatty Acid Synthesis Mediated through ROS Generation Triggers Apoptosis in HepG2 Cells. *PLoS ONE,* 2014, 9(9): e107842.
48. Furuta E et al. Fatty acid synthase gene is up-regulated by hypoxia via activation of Akt and sterol regulatory element binding protein-1. *Cancer Res.* 2008, 15, 68(4), 1003-11.
49. Wellberg EA et al. Modulation of tumor fatty acids, through overexpression or loss of thyroid hormone responsive protein spot 14 is associated with altered growth and metastasis. *Breast Cancer Res.* 2014, 16, 481.
50. Sahla ME et al. Increased expression of fatty acid synthase and progesterone receptor in early steps of human mammary carcinogenesis. *Int. J. Cancer.* 2006, 120, 224–229.
51. Lu S and Archer MC. Fatty acid synthase is a potential molecular target for the chemoprevention of breast cancer. *Carcinogenesis,* 2005, 26 (1), 153–157.
52. Roy S et al. Alpha-linolenic acid stabilizes HIF-1 α and downregulates FASN to promote mitochondrial apoptosis for mammary gland chemoprevention. *Oncotarget.* 2017, 19, 8(41), 70049–70071.
53. Cheng CS, Wang Z, and Chen J. Targeting FASN in Breast Cancer and the Discovery of Promising Inhibitors from Natural Products Derived from Traditional Chinese Medicine. *Evid Based Complement Alternat Med.* 2014, 2014, 232946.
54. Horiguchi A et al. Fatty acid synthase over expression is an indicator of tumor aggressiveness and poor prognosis in renal cell carcinoma. *J Urol.* 2008, 180(3), 1137-40.
55. Bauerschlag DO et al. Fatty acid synthase overexpression: target for therapy and reversal of chemoresistance in ovarian cancer. *J Transl Med.* 2015, 13, 146.
56. Djefafia SB, Vasseur S and Guillaumond F. Lipid metabolic reprogramming in cancer cells. *Oncogenesis.* 2016, 5, e189.
57. Zhao Y, Butler EB and Tan M. Targeting cellular metabolism to improve cancer therapeutics. *Cell Death Dis.* 2013, 4(3), e532.

58. Yeung TM. Hypoxia and lineage specification of cell line-derived colorectal cancer stem cells. *PNAS*, 201, 108 (11), 4382-4387.
59. Ziello JE, Jovin IS and Huanga Y. Hypoxia-Inducible Factor (HIF)-1 Regulatory Pathway and its Potential for Therapeutic Intervention in Malignancy and Ischemia. *Yale J Biol Med*. 2007, 80(2), 51–60.
60. Chen S et al. HIF-1 α contributes to proliferation and invasiveness of neuroblastoma cells via SHH signaling. *PLoS One*. 2015, 10(3), e0121115.
61. Webster KA. Evolution of the coordinate regulation of glycolytic enzyme genes by hypoxia. *Journal of Experimental Biology* 2003, 206, 2911-2922.
62. Garcia SR et al. Tumor cell metabolism: An integral view. *Cancer Biol Ther*. 2011, 1, 12(11), 939–948.
63. Minamishima YA et al. Somatic inactivation of the PHD2 prolyl hydroxylase causes polycythemia and congestive heart failure. *Blood*. 2008, 15, 111(6), 3236–3244.
64. Jokilehto T and Jaakkola PM. The role of HIF prolyl hydroxylases in tumour growth. *Journal of Cellular and Molecular Medicine*. 2010, 14(4), 758-70.
65. Zhang F and Du G. Dysregulated lipid metabolism in cancer. *World J Biol Chem*. 2012, 26, 3(8), 167–174.
66. Pan MH et al. Tea Polyphenol (–)-Epigallocatechin 3-Gallate Suppresses Heregulin- β 1-Induced Fatty Acid Synthase Expression in Human Breast Cancer Cells by Inhibiting Phosphatidylinositol 3-Kinase/Akt and Mitogen-Activated Protein Kinase Cascade Signaling. *J. Agric. Food Chem*, 2007, 55 (13), 5030–5037.
67. Landree LE et al. C75, a Fatty Acid Synthase Inhibitor, Modulates AMP-activated Protein Kinase to Alter Neuronal Energy Metabolism. *Journal of Biol Chem*, 2004, 279, 3817-3827.
68. Nunomiya A et al. Activation of the hypoxia-inducible factor pathway induced by prolyl hydroxylase domain 2 deficiency enhances the effect of running training in mice. *Acta Physiol (Oxf)*. 2017, 220(1), 99–112.
69. Fan L et al. The Hypoxia-Inducible Factor Pathway, Prolyl Hydroxylase Domain Protein Inhibitors, and Their Roles in Bone Repair and Regeneration. *Biomed Res Int*. 2014, 2014, 239356.
70. Ackerman D and Simon MC. Hypoxia, lipids, and cancer: surviving the harsh tumor microenvironment. *Trends Cell Biol*. 2014, 24(8), 472-8.

71. Yang M et al. Prolyl hydroxylase domain enzymes: important regulators of cancer metabolism. *Hypoxia (Auckl)*. 2014; 2, 127–142.
72. Li P, Tian W and Ma X. Alpha-mangostin inhibits intracellular fatty acid synthase and induces apoptosis in breast cancer cells. *Mol Cancer*. 2014, 13, 138.
73. Gilkes DM and Semenza GL. Role of hypoxia-inducible factors in breast cancer metastasis. *Future Oncol*. 2013, 9(11), 1623–1636.
74. Yoshii Y et al. Fatty Acid Synthase Is a Key Target in Multiple Essential Tumor Functions of Prostate Cancer: Uptake of Radiolabeled Acetate as a Predictor of the Targeted Therapy Outcome. *PLoS ONE*, 2013, 8(5), e64570.
75. Smirnova NA et al. Catalytic mechanism and substrate specificity of HIF prolyl hydroxylases. *Biochemistry (Mosc)*. 2012, 77(10), 1108-19.
76. Chan DA and Giaccia AJ. PHD2 in tumour angiogenesis. *Br J Cancer*. 2010, 103(1): 1–5.
77. Lisy K and Peet DJ. Turn me on: regulating HIF transcriptional activity. *Cell Death Differ*. 2008, 15(4), 642-9.
78. Young CD and Anderson SM. Sugar and fat - that's where it's at: metabolic changes in tumors. *Breast Cancer Res*. 2008, 10(1), 202.
79. Brahimi-Horn MC, Chiche J and Pouyssegur J. Hypoxia and cancer. *J Mol Med (Berl)*. 2007, 85(12), 1301-7.
80. Menendez JA and Lupu R. Fatty acid synthase and the lipogenic phenotype in cancer pathogenesis. *Nat Rev Cancer*. 2007, 7(10), 763-77.
81. Ke Q and Costa M. Hypoxia-inducible factor-1 (HIF-1). *Mol Pharmacol*. 2006, 70(5), 1469-80.
82. Kuhajda FP. Fatty acid synthase and cancer: new application of an old pathway. *Cancer Res*. 2006, 15, 66(12), 5977-80.
83. Zhou J et al. Tumor hypoxia and cancer progression. *Cancer Lett*, 2006, 8, 237(1), 10-21.
84. Menendez JA et al. Does endogenous fatty acid metabolism allow cancer cells to sense hypoxia and mediate hypoxic vasodilatation? Characterization of a novel molecular connection between fatty acid synthase (FAS) and hypoxia-inducible factor-1 α (HIF-1 α) related expression of vascular endothelial growth factor (VEGF) in cancer cells overexpressing her-2/neu oncogene. *J of Cellular Biochemistry*, 2005, 94 (5), 857-863.

85. Zhu et al. Antibody structure determination using a combination of homology modeling, energy-based refinement, and loop prediction. *Proteins*. 2014, 82(8):1646-55.
86. Li and Huang. CDRUG: a web server for predicting anticancer activity of chemical compounds. *Bioinformatics*. 2012, 15, 28(24), 3334-5.
87. Zhang et al. Antitumor Action of a Novel Histone Deacetylase Inhibitor, YF479, in Breast Cancer. *Neoplasia*. 2014, 16(8), 665–677.
88. Mathew et al. Synthesis, ADME studies, toxicity estimation, and exploration of molecular recognition of thiophene based chalcones towards monoamine oxidase-A and B. *Beni-Suef University Journal of Basic and Applied Sciences*, 2016, 5 (4), 396-401.
89. Carlsson et al. Use of historic metabolic biotransformation data as a means of anticipating metabolic sites using MetaPrint2D and Bioclipse. *BMC Bioinformatics*, 2010, 11, 362.
90. Rostkowski, Spjuth and Rydberg P. WhichCyp: prediction of cytochromes P450 inhibition. *Bioinformatics*. 2013, 15, 9(16):2051-2.
91. Richard L. Wurdeman, Kevin M. Church, and Barry Gold. DNA methylation by N-methyl-N-nitrosourea, N-methyl-N'-nitro-N-nitrosoguanidine, N-nitroso(1-acetoxyethyl)methylamine, and diazomethane. The mechanism for the formation of N7-methylguanine in sequence-characterized 5'-[32P]-end-labeled DNA. *J. Am. Chem. Soc.* 1989, 111, 16, 6408-6412.
92. Kuttan R, Parrott D, Kaplan S, Fuller G. Effect of ascorbic acid on prolyl hydroxylase activity, collagen hydroxylation and collagen synthesis in human synovial cells in culture. *Research Communications in Chemical Pathology and Pharmacology*. 1979, 26(2), 337-45.
93. McNeill L et al. A fluorescence-based assay for 2-oxoglutarate-dependent oxygenases. *Analytical Biochemistry*. 2005, 336(1), 125-31.
94. Dey S et al. Anti-carcinogenic activity of *Rubellia tuberosa* L.(Acanthaceae) leaf extract on hepatoma cell line and increased superoxide dismutase activity on macrophage cell lysate. *Int J Pharm Pharm Sci*. 2013, 5, 854-61.
95. Nawata H et al. Estradiol-independent growth of a subline of MCF-7 human breast cancer cells in culture. *Journal of Biol Chem*. 1981, 256(13), 6895-902.
96. Mohankumar K et al. Mechanism of apoptotic induction in human breast cancer cell, MCF-7, by an analog of curcumin in comparison with curcumin—an in vitro and in silico approach. *Chemico-biological interactions*. 2014, 210, 51-63.

97. Yang C et al. Bornyl caffeate induces apoptosis in human breast cancer MCF-7 cells via the ROS-and JNK-mediated pathways. *Acta Pharmacologica Sinica*. 2014, 35(1), 113-23.
98. Riccardi C and Nicoletti I. Analysis of apoptosis by propidium iodide staining and flow cytometry. *Nature Protocols*. 2006, 1(3), 1458-61.
99. Shintaku T et al. Effects of propofol on electrocardiogram measures in mice. *Journal of Pharmacological Sciences*. 2014, 126(4), 351-8.
100. Manral C et al. Effect of β -sitosterol against methyl nitrosourea-induced mammary gland carcinoma in albino rats. *BMC Complementary and Alternative Medicine*. 2016, 16(1), 260.
101. De Assis S et al. Changes in mammary gland morphology and breast cancer risk in rats. *JoVE (Journal of Visualized Experiments)*. 2010, (44), e2260-e.
102. Richert MM et al. An atlas of mouse mammary gland development. *Journal of Mammary Gland Biology and Neoplasia*. 2000, 5(2), 227-41.
103. Yoshida H et al. Induction of mammary dysplasia and mammary carcinoma in neonatally androgenized female rats by 7, 12-dimethylbenz [a] anthracene. *Journal of the National Cancer Institute*. 1980, 64(5), 1105-12.
104. Takumi Y, Kaido T and Uehara Y. Changes in density and architecture of microvessels of the rat mammary gland during pregnancy and lactation. *Archives of Histology and Cytology*. 1989, 52(2), 115-22.
105. Tiwari V et al. Redefining the role of peripheral LPS as a neuroinflammatory agent and evaluating the role of hydrogen sulphide through metformin intervention. *Inflammopharmacology*. 2016, 24(5), 253-64.
106. Kaithwas G, Singh P and Bhatia D. Evaluation of in vitro and in vivo antioxidant potential of polysaccharides from Aloe vera (*Aloe barbadensis* Miller) gel. *Drug and Chemical Toxicology*. 2014, 37(2), 135-43.
107. Devarajan E et al. Down-regulation of caspase 3 in breast cancer: a possible mechanism for chemoresistance. *Oncogene*. 2002, 21(57), 8843-51.
108. Sharma N and Ahmad Y. An effective method for the analysis of human plasma proteome using two-dimensional gel electrophoresis. *Journal of Proteomics & Bioinformatics*. 2011, 2009.
109. Laemmli UK. Cleavage of structural proteins during the assembly of the head of bacteriophage T4. *Nature*. 1970, 22, 680-5.

110. Towbin H, Staehelin T and Gordon J. Electrophoretic transfer of proteins from polyacrylamide gels to nitrocellulose sheets: procedure and some applications. *Proceedings of the National Academy of Sciences*. 1979, 76(9), 4350-4.
111. Giulietti A et al. An overview of real-time quantitative PCR: applications to quantify cytokine gene expression. *Methods*. 2001, 25(4), 386-401.
112. Mishra RK et al. Palonosetron attenuates 1, 2-dimethyl hydrazine induced preneoplastic colon damage through downregulating acetylcholinesterase expression and up-regulating synaptic acetylcholine concentration. *RSC Advances*. 2016, 6(46), 40527-38.
113. Singh et al. Prolyl hydroxylase mediated inhibition of fatty acid synthase to combat tumor growth in mammary gland carcinoma. *Breast Cancer*. 2016, 23, 820–829.
114. Seeger H et al. Inhibition of human breast cancer cell proliferation with estradiol metabolites is as effective as with tamoxifen. *Hormone and metabolic research*. 2004, 36(05), 277-80.
115. Julius S and Nesbitt S. Sympathetic overactivity in hypertension a moving target. *American journal of hypertension*. 1996, 9(S4), 113S-20S.
116. Dropcho EJ. Autoimmune central nervous system paraneoplastic disorders: mechanisms, diagnosis, and therapeutic options. *Annals of neurology*. 1995, 37(S1), 102-13.
117. Low PA, Vernino S and Suarez G. Autonomic dysfunction in peripheral nerve disease. *Muscle & nerve*. 2003, 27(6), 646-61.
118. Yeh ET et al. Cardiovascular complications of cancer therapy diagnosis, pathogenesis, and management. *Circulation*. 2004, 109(25), 3122-31.
119. White SS et al. Effects of perfluorooctanoic acid on mouse mammary gland development and differentiation resulting from cross-foster and restricted gestational exposures. *Reproductive Toxicology*. 2009, 27(3), 289-98.
120. Russo IH, Tewari M and Russo J. Morphology and development of the rat mammary gland. *Integument and Mammary Glands: Springer*; 1989, 233-52.
121. Reuter S et al. Oxidative stress, inflammation, and cancer: how are they linked? *Free Radical Biology and Medicine*. 2010, 49(11), 1603-16.
122. Trachootham D, Alexandre J and Huang P. Targeting cancer cells by ROS-mediated mechanisms: a radical therapeutic approach? *Nature reviews Drug discovery*. 2009, 8(7), 579-91.
123. Valko M et al. Free radicals, metals and antioxidants in oxidative stress-induced cancer. *Chemico-biological interactions*. 2007, 160(1), 1-40.

124. Andrei S et al. Protective Activity of Polyphenon E Against Liver Protein Oxidation in Rats after Mnu IP Administration. *Bulletin of University of Agricultural Sciences and Veterinary Medicine Cluj-Napoca Veterinary Medicine*. 2014, 71(1), 15-8.
125. Halliwell B. Superoxide dismutase, catalase and glutathione peroxidase: solutions to the problems of living with oxygen. *New Phytologist*. 1974, 73(6), 1075-86.
126. Tsuruta F, Masuyama N and Gotoh Y. The phosphatidylinositol 3-kinase (PI3K)-Akt pathway suppresses Bax translocation to mitochondria. *Journal of Biological Chemistry*. 2002, 277(16), 14040-7.
127. Baines CP et al. Voltage-dependent anion channels are dispensable for mitochondrial-dependent cell death. *Nature cell biology*. 2007, 9(5), 50-5.
128. Madesh M and Hajnóczky G. VDAC-dependent permeabilization of the outer mitochondrial membrane by superoxide induces rapid and massive cytochrome c release. *The Journal of cell biology*. 2001, 155(6), 1003-16.
129. Adams JM and Cory S. Life-or-death decisions by the Bcl-2 protein family. *Trends in biochemical sciences*. 2001, 26(1), 61-6.
130. van Loo G et al. The role of mitochondrial factors in apoptosis: a Russian roulette with more than one bullet. *Cell death and differentiation*. 2002, 9(10), 1031-42.
131. Acehan D et al. Three-dimensional structure of the apoptosome: implications for assembly, procaspase-9 binding, and activation. *Molecular cell*. 2002, 9(2), 423-32.
132. Bratton SB and Salvesen GS. Regulation of the Apaf-1–caspase-9 apoptosome. *J Cell Sci*. 2010, 123(19), 3209-14.
133. Budihardjo I et al. Biochemical pathways of caspase activation during apoptosis. *Annual review of cell and developmental biology*. 1999, 15(1), 269-90.
134. Munoz-Pinedo C, El Mjiyad N and Ricci J. Cancer metabolism: current perspectives and future directions. *Cell death & disease*. 2012, 3(1), e248.
135. Soga T. Cancer metabolism: key players in metabolic reprogramming. *Cancer Science*. 2013, 104(3), 275-81.
136. Mansour M et al. Thiazolidinediones/PPAR γ agonists and fatty acid synthase inhibitors as an experimental combination therapy for prostate cancer. *International Journal of Oncology*. 2011, 38(2), 537.
137. Sebastiani V et al. Fatty acid synthase is a marker of increased risk of recurrence in endometrial carcinoma. *Gynecologic Oncology*. 2004, 92(1), 101-5.

References

138. Bovenga F, Sabbà C and Moschetta A. Uncoupling nuclear receptor LXR and cholesterol metabolism in cancer. *Cell Metabolism*. 2015, 21(4), 517-26.
139. Goto Y et al. UCHL1 provides diagnostic and antimetastatic strategies due to its deubiquitinating effect on HIF-1 α . *Nature Communications*. 2015, 6.
140. Rani A et al. α -Chymotrypsin regulates free fatty acids and UCHL-1 to ameliorate N-methyl nitrosourea induced mammary gland carcinoma in albino wistar rats. *Inflammopharmacology*. 2016, 24(5), 277-86.

APPENDIX-I
ANIMAL APPROVAL
CERTIFICATE



INSTITUTIONAL ANIMAL ETHICAL COMMITTEE (IAEC)

REG. No. - 1451/PO/a/11/CPCSEA Dated 02/08/2011 UNDER RULE 13 OF THE "BREEDING OF
AND EXPERIMENTS ON ANIMALS (CONTROL AND SUPERVISION) RULES 1998"

UPIAEC/2014/FEB./16

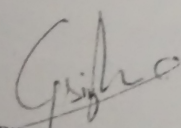
DATE: 08/02/2014

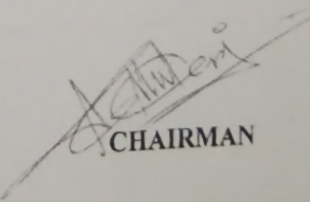
APPENDIX-II

CERTIFICATE

PLAGIARISM

This is to certify that Mr./Ms/Mrs Manjari Singh a student of M.Pharm. / Ph.D. is permitted /
not permitted to carry out experiments for the dissertation / thesis work entitled "Modulating
prohyl hydroxylase (PHD2) activity to alter glycolytic pathway and fatty acid synthase
expression in tumor cells" as per the details mentioned and after observing the usual formalities
laid down by IAEC as per the provisions made by CPCSEA.


MEMBER SECRETARY


CHAIRMAN

APPENDIX-II

PLAGIARISM

REPORT

Urkund Analysis Result

Analysed Document: Manjari Singh.pdf (D37177659)
Submitted: 4/3/2018 3:56:00 PM
Submitted By: shodhganga.bbau@gmail.com
Significance: 9 %

Sources included in the report:

lakhveer.docx (D30973721)
<http://diposit.ub.edu/dspace/handle/2445/61729>
<https://www.duo.uio.no/handle/10852/36039>
<https://www.duo.uio.no/handle/10852/59079>
<http://doras.dcu.ie/18175/>
<http://www.cancerindex.org/geneweb/FASN.htm>
<https://www.ncbi.nlm.nih.gov/pmc/articles/PMC3669310/>
http://cancerres.aacrjournals.org/content/74/19_Supplement/4332
<http://www.jbc.org/content/283/43/29341.full>
<http://nomuraresearchgroup.com/wp-content/uploads/2015/01/Benjaminetal2015ACSCB.pdf>
<https://translational-medicine.biomedcentral.com/articles/10.1186/s12967-015-0732-5>
https://scholarworks.iupui.edu/bitstream/handle/1805/1863/PHD%20thesis_Hailan%20Liu.pdf;sequence=1
<http://onlinelibrary.wiley.com/doi/10.1002/icl3.1039/full>
<https://www.sciencedirect.com/science/article/pii/S2211124715007500>
<http://genesdev.cshlp.org/content/17/21/2614.full.html>
<https://link.springer.com/article/10.1007%252Fs10495-017-1366-2>
http://www.3vbio.com/wp-content/uploads/2015/07/2015_VenturaHeuer_TV3166SingleAgentOncologyPreclinical_EBIOM.pdf
<https://www.scbt.com/scbt/product/sreb-1-antibody-2a4/>
<http://europepmc.org/articles/PMC3197858>
<https://www.ncbi.nlm.nih.gov/pubmed/15669079>
<https://www.ncbi.nlm.nih.gov/pmc/articles/PMC5412909/>
<http://journals.plos.org/plosone/article?id=10.1371/journal.pone.0064570>
<https://worldwidescience.org/topicpages/r/rag2+phd+domain.html>
<https://worldwidescience.org/topicpages/t/targeted+tumor+therapy.html>
<https://link.springer.com/article/10.1007/s10787-016-0280-5>
<https://www.ncbi.nlm.nih.gov/pmc/articles/PMC4966711/>

Instances where selected sources appear:

APPENDIX-III
PUBLICATIONS

Prolyl hydroxylase mediated inhibition of fatty acid synthase to combat tumor growth in mammary gland carcinoma

Manjari Singh¹ · Uma Devi² · Subhadeep Roy¹ · Pushpraj S. Gupta² · Shubhini A. Saraf¹ · Gaurav Kaithwas¹

Received: 1 December 2015 / Accepted: 24 February 2016
© The Japanese Breast Cancer Society 2016

Abstract Cancer is a group of cells which grow in an uncontrolled manner and invades to the adjacent organs to form malignant tumors. Tumor hypoxia results due to contrast between the cellular oxygen expenditure and oxygen supply to the cells. Hypoxia inducible factor (HIF) is a heterodimeric transcription factor encompass of oxygen sensitive α subunit and constitutively expressed β subunit both of which are basic helix-loop-helix protein. The stability of HIF is primarily regulated by post translational prolyl hydroxylation, catalyzed by prolyl hydroxylase 2 (Phd-2). Phd-2 is a group of enzymes that acts as an oxygen sensor. Cancer cells have altered metabolism as they fulfil their energy needs through glycolysis and lipid biogenesis. HIF-1 α is known to upregulate glycolysis by activating the transcription of enzymes on the glycolytic pathway and through lipogenesis. Cancer cells have over expressed fatty acid synthase owing to altered glycolytic pathway. Considering the above, it is hypothesized that chemical activation of Phd-2 can curtail down HIF-1 α and subsequently fatty acid synthase expression.

Keywords Fatty acid synthase · Hypoxia inducible factor · Hypoxia · Normoxia · Prolyl hydroxylase

Abbreviations

ATP	Adenosine tri phosphate
NADPH	Nicotinamide adenine di phosphate
HIF	Hypoxia inducible factor
pVHL	Von Hippel Lindau tumor suppressor protein
FASN	Fatty acid synthase
VEGF	Vascular Endothelial Growth Factor
HRE	Hypoxia response element
Phd-2	Prolyl hydroxylase 2
2OG	2-oxoglutarate
EGCG	Epigallocatechin-3-gallate
SREBP	Sterol regulatory element binding protein

Introduction

A body is made up of many living cells, which grow, multiply and generate new cells and die after some time in an accordingly manner called apoptosis. In case of cancer, body cells start growing out of control. They cannot die and grow deliberately to form new cells and form their own blood vessels through angiogenesis. Subsequently, cancer cells metastasise into the nearby organs, when their growth is not diversified or arrested. At this stage, cancer cells replace normal tissues and form new mass termed as tumor. There are eight endorsements of cancer participating in the physiology of cancer: self sufficient pro growth signalling, loss of sensitivity to antigrowth signals, resistance to cell death, replicating without limit, angiogenesis, invasion and metastasis, reprogrammed metabolism and evading immune surveillance [1, 2].

Manjari Singh and Uma Devi have contributed equally.

SHIATS-Deemed to be University is formerly Allahabad Agricultural Institute.

✉ Gaurav Kaithwas
gauravpharm@gmail.com; gauravpharm@hotmail.com

¹ Department of Pharmaceutical Sciences, School of Biosciences and Biotechnology, Babasaheb Bhimrao Ambedkar University (A Central University), Vidya Vihar, Raebareli Road, Lucknow 226025, India

² Department of Pharmaceutical Sciences, Faculty of Health Medical Sciences Indigenous and Alternative Medicine, SHIATS-Deemed to be University, Naini, Allahabad, Uttar Pradesh, India



Cite this: *RSC Adv.*, 2018, 8, 12848

Chemical activation of prolyl hydroxylase-2 by BBAP-1 down regulates hypoxia inducible factor-1 α and fatty acid synthase for mammary gland chemoprevention†

Manjari Singh,^{‡a} Uma Devi,^{‡b} Subhadeep Roy,^a Pushpraj S. Gupta^a and Gaurav Kaithwas^{ib*^a}

(4-[7-(Acetyloxy)-2-ethyl-2*H*-chromen-3-yl] phenyl acetate) (BBAP-1) was identified as a potential prolyl hydroxylase-2 activator and tested for this activity using the 2-oxoglutarate dependent *in vitro* assay. BBAP-1 was evaluated for its cytotoxic potential against ER + MCF-7 cells, and *N*-methyl-*N*-nitrosourea induced estrogen positive mammary gland carcinoma model. The effect of BBAP-1 on cellular morphology was evaluated using *in vitro* acridine orange/ethidium bromide and JC-1 staining. The morphological symptoms of apoptosis were evident after BBAP-1 treatment when studied through cell staining using acridine orange/ethidium bromide and JC-1 dye. Flow cytometric analysis revealed that BBAP-1 treatment arrested the cell cycle in the G2/M phase. *In vivo* study revealed the morphological changes of mammary gland tissue when scrutinized using carmine staining, hematoxylin and eosin staining and scanning electron microscopy. BBAP-1 treatment produced a marked effect on histopathological and morphological features when scrutinized against *N*-methyl-*N*-nitrosourea induced mammary gland carcinoma. Treatment with BBAP-1 also attenuated the deleterious effects of *N*-methyl-*N*-nitrosourea as measured on the basis of oxidative stress markers. Immunoblotting and qRT-PCR analysis revealed the participation of BBAP-1 in the mitochondrial mediated death apoptosis pathway and BBAP-1 also downregulated the hypoxic pathway through activation of prolyl hydroxylase-2. It was concluded that BBAP-1 activated the prolyl hydroxylase-2 enzyme and curtailed the over expression of hypoxia inducible factor-1 α and fatty acid synthase along with the mitochondrial mediated death apoptosis pathway.

Received 8th February 2018
Accepted 19th March 2018

DOI: 10.1039/c8ra01239c

rsc.li/rsc-advances

Introduction

Tumor hypoxia is a condition where solid tumors have insufficient oxygen supply, leading to an imbalance in their consumption of oxygen. Thus, hypoxia alters the cellular energy production mechanism, with the anaerobic mode prevailing over aerobic respiration.¹ In the hypoxic state, an imbalance is developed between the supply and consumption of oxygen.^{2,3} Importantly, hypoxia distress in cancer cells leads to an alteration in their metabolite signaling, consequently promoting

glycolysis and lipid biogenesis (Warburg effect) over the tri-carboxylic acid (TCA) cycle and beta-oxidation.⁴

The hypoxic microenvironment triggers hypoxic signaling pathways in which hypoxia inducible factor (HIF) is the most clearly understood transcription factor.⁵ The structure of HIF is a basic helix-loop-helix PAS (Per, Arnt, Sim) domain, which consists of two subunits HIF-1 α and HIF-1 β .⁶ HIF-1 α is found to be overexpressed in all types of cancer and enables tumor cells to grow under hypoxic conditions.⁷ It would be appropriate to note that increased glycolysis and lipogenic activity is one of the major methods by which the tumor cells meet their high energy and lipid requirements.⁸ In addition to the above, HIF-1 α regulates the process of angiogenesis through binding with vascular endothelial growth factor (VEGF).⁹

During normoxia, HIF-1 α goes through proteasomal degradation, which is regulated by prolyl hydroxylases (PHDs), followed by binding with von Hippel-Lindau (pVHL) suppresser protein.¹⁰ PHDs include the iron and 2-oxoglutarate (2-OG) dependent dioxygenase and are responsible for the hydroxylation of HIF-1 α .¹¹ In mammals, three isoforms of PHDs (PHD-1,

^aDepartment of Pharmaceutical Sciences, Babasaheb Bhimrao Ambedkar University (A Central University), Vidya Vihar, Raebareli Road, Lucknow-226025, UP, India. E-mail: gauravpharm@hotmail.com; gauravk@bbau.ac.in; Tel: +91 9670204349

^bDepartment of Pharmaceutical Sciences, Faculty of Health and Medical Sciences, Sam Higginbottom University of Agricultural Sciences and Technology, Naini, Allahabad, UP, India

† Electronic supplementary information (ESI) available. See DOI: 10.1039/c8ra01239c

‡ Both authors have contributed equally.

Publications from the present research work

- ✓ **Manjari Singh**...Gaurav Kaithwas. “Chemical activation of prolyl hydroxylase-2 by BBAP1 down regulates hypoxia inducible factor-1 α and fatty acid synthase for mammary gland chemoprevention”. RSC Advances (Accepted for publication). (IF-3.1).
- ✓ **Manjari Singh**...Gaurav Kaithwas. “Prolyl hydroxylase mediated inhibition of fatty acid synthase to combat tumor growth in mammary gland carcinoma”, Breast Cancer. 2016 Nov; 23(6):820-829 (IF 1.572).

Publications related to research work

- ✓ Swetlana Gautam..., **Manjari Singh**...Gaurav Kaithwas. “DuCLOX-2/5 Inhibition Attenuates Inflammatory Response and Induces Mitochondrial Apoptosis for Mammary Gland Chemoprevention” Front. Pharmacol., 06 April 2018 | <https://doi.org/10.3389/fphar.2018.00314> (IF-4.4).
- ✓ Subhadeep Roy, **Manjari Singh**...Gaurav Kaithwas. “GLA supplementation regulates PHD2 mediated hypoxia and mitochondrial apoptosis in DMBA induced mammary gland carcinoma”. Int J Biochem Cell Biol. 2018 Jan 17. pii: S1357-2725(18)30017-7. doi: 10.1016/j.biocel.2018.01.011 (IF-3.5).
- ✓ Rajnish Kumar Yadav, **Manjari Singh**...Gaurav Kaithwas. “Modulation of oxidative stress response by flaxseed oil: Role of lipid peroxidation and underlying mechanisms” Prostaglandins and Other Lipid Mediators 135 (2018) 21–26. (IF-2.6)
- ✓ Swetlana Gautam...**Manjari Singh**...Gaurav Kaithwas. “Rifaximin, a pregnane X receptor (PXR) activator regulates apoptosis in a murine model of breast cancer”. RSC Adv., 2018, 8, 3512–3521 (IF-3.1).
- ✓ Abdulaziz S. Saeedan...**Manjari Singh**...Gaurav Kaithwas. “Effect of early natal supplementation of paracetamol on attenuation of exotoxin/endotoxin induced pyrexia and precipitation of autistic like features in albino rats”. Inflammopharmacology, <https://doi.org/10.1007/s10787-017-0440-2>. (IF-2.590).
- ✓ Vidhata Rani...**Manjari Singh**...Gaurav Kaithwas. “Effects of minocycline and doxycycline against terbutaline induced early postnatal autistic changes in albino rats”. Physiology & Behavior 183 (2018) 49–56 (IF-2.341).
- ✓ Rani A...**Singh M**...Kaithwas G. “ α -Chymotrypsin regulates free fatty acids and UCHL-1 to ameliorate N-methyl nitrosourea induced mammary gland carcinoma in albino wistar rats”. Inflammopharmacology. 2016 Oct; 24(5):277-286. Epub 2016 Sep 26. (IF- 2.590).
- ✓ Shreesh Raj Sammi...**Manjari Singh**...Gaurav Kaithwas. “Galantamine attenuates N,N-dimethyl hydrazine induced neoplastic colon damage by inhibiting acetylcholinesterase and bimodal regulation of nicotinic cholinergic neurotransmission”. European Journal of Pharmacology 818 (2018) 174–183 (2.896).
- ✓ Subhadeep Roy...**Manjari Singh**...Gaurav Kaithwas. “Alpha-linolenic acid arbitrates mitochondrial apoptosis, curbs the hypoxic microenvironment and de novo fatty acid synthesis to impart anticancer effects”. Oncotarget (IF-5.168).

- ✓ Rakesh K. Mishra...**Manjari Singh**...Gaurav Kaithwas. “Palonosetron attenuates 1, 2-dimethyl hydrazine induced preneoplastic colon damage through downregulating acetylcholinesterase expression and up-regulating synaptic acetylcholine concentration”, RSC Adv., 2016,6,40527 (IF-3.108).
- ✓ Chetan Manral...**Manjari Singh**...Gaurav Kaithwas, “Effect of β -sitosterol against methyl nitrosourea-induced mammary gland carcinoma in albino rats.” BMC Complementary and Alternative Medicine, 2016; 16: 260 (IF- 2.28).
- ✓ Virendra Tiwari, **Manjari Singh**...Gaurav Kaithwas. “Redefining the role of peripheral LPS as a neuroinflammatory agent and evaluating the role of hydrogen sulphide through metformin intervention”. Inflammopharmacology. 2016 Oct; 24(5):253-264 (IF 2.590).
- ✓ Uma Devi...**Manjari Singh**...Gaurav Kaithwas. “Experimental Models for Autistic Spectrum Disorder-Follow Up For the Validity”, Review Journal of Autism and Developmental Disorders, 2016, 3(4), 358–376.
- ✓ Yadav S...**Singh M**...Kaithwas G. “Comparative efficacy of alphinolenic acid and gamma-linolenic acid to attenuate valproic acid-induced autism-like features”. J Physiol 2017 May; 73(2):187-198 (IF- 2.444).
- ✓ Raju Gautam, **Manjari Singh**...Gaurav Kaithwas. “Rutin attenuates intestinal toxicity induced by Methotrexate linked with anti-oxidative and anti-inflammatory effects”. BMC Complementary and Alternative Medicine, (2016) 16:99. (IF- 2.28).
- ✓ Arvind Kumar Giri...**Manjari Singh**...Gaurav Kaithwas. “Effect of Lycopene against Gastroesophageal reflux disease in experimental animals”. BMC complimentery and alternative medicine, 2015 (IF- 2.28).
- ✓ Gaurav Kaithwas...**Manjari Singh** “Preclinical Appraisal of Terbutaline Kinfolks in Precipitation of Autistic Spectrum Disorder”. RSC Advances 04/2015; DOI: 10.1039/C5RA04213E (IF-3.108).
- ✓ Arun Kumar, **Manjari Singh**...Gaurav Kaithwas. “Effect of palonosetron (5HT-3 antagonist) and pantoprazole (PPI) against surgical esophagitis induced by forestomach and pylorus ligation in albino rats”. Human and Experimental Toxicology, 2015 (IF- 1.74).
- ✓ Sukesh K Gupta...**Manjari Singh**...Gaurav Kaithwas. “Efficacy of variable dosage of aspirin in combating methotrexate-induced intestinal toxicity”. RSC Advances 01/2015; 5(13):9354-9360. (IF-3.108).
- ✓ Gaurav Kaithwas...**Manjari Singh** “Effect of Enteral Administration of α – Linolenic Acid and Linoleic Acid against Methotrexate Induced Intestinal Toxicity in Albino Rats”. RSC Advances 10/2014. (IF-3.108).
- ✓ Sanjit Kumar, **Manjari Singh**...Gaurav Kaithwas. “Effect of rutin against gastric esophageal reflux in experimental animals”. Toxicology mechanisms and methods 09/2014 (IF-1.548).

Presentations/conferences attended

- ✓ Presented poster in IHPA Golden Jubilee Conference, 2014 under the theme “Restructuring Pharmacy Curricula: Need of Health Sector”.
- ✓ Presented poster in 2nd Lucknow Science Congress organized by Babasaheb Bhimrao Ambedkar University, Lucknow.
- ✓ Presented oral presentation in International Conference in Babasaheb Bhimrao Ambedkar University Lucknow 2015 under the theme “Nanoformulations and Translational Research: Small getting Bigger”.
- ✓ Presented oral presentation in International Conference in Babasaheb Bhimrao Ambedkar University Lucknow 2017 under the theme “International conference on Updated in Cancer Prevention and research”.
- ✓ Two days workshop organized by BBD, Lucknow & conducted by IIPTA, Delhi on “Role of IPR in Pharmaceutical Industry”.
- ✓ One day workshop organized by BBAU, Lucknow on “Placements & Employments Prospects in Indian Patent Prospects in Indian Patent offices and Hands on Training for Patenting the Research Work.”
- ✓ Attended three days workshop on “Cheminformatics: Applications in Drug Designing” held on Biotech Park, Lucknow.
- ✓ Participated in workshop on “NMR/MRI from molecules to human behavior” Sponsored by DST-India